THE IMPACT OF PRENATAL TESTOSTERONE ON ADULT CRANIAL FLUCTUATING ASYMMETRY IN PRIMATES: DEVELOPMENTAL STRESS WITHIN THE SAME INDIVIDUAL

by

SKYE GRUBB

A THESIS

Presented to the Department of Anthropology
and the Robert D. Clark Honors College
in partial fulfillment of the requirements for the degree of
Bachelor of Science

May 2025

An Abstract of the Thesis of

Skye Grubb for the degree of Bachelor of Science
in the Department of Anthropology to be taken June 2025

Title: The Impact of Prenatal Testosterone on Adult Cranial Fluctuating Asymmetry in Primates: Developmental Stress Within the Same Individuals

Approved: *Frances White, Ph.D.*
Primary Thesis Advisor

Fluctuating asymmetry has long been studied in the crania of primates, but research connecting fluctuating asymmetry with other measures of anatomical stress across the body of individuals is extremely limited. The degree of cranial asymmetry has been shown to reflect the degree of genetic and/or environmental stress an individual experiences during development. In contrast, the ratio of the second to fourth digit reflects levels of prenatal testosterone exposure, with low ratios (i.e., a longer fourth digit) reflecting higher testosterone levels during an individual's development. This study seeks to investigate the connection of cranial asymmetry to postcranial asymmetry in a range of individual primate specimens. I examined 17 total specimens from a range of primate species, which were selected for having both proximal phalanges with present epiphyses and primarily intact skulls suitable for symmetry analyses. Skulls were analyzed through landmarking a collection of midpoints and bilateral morphological traits. The second and fourth proximal phalanges' lengths were measured to establish individual specimens' second to fourth digit (2D:4D) ratios. The results suggest that there was a significant regression of fluctuating asymmetry on 2D:4D that explained 32% of the variation. Individuals with higher testosterone measures had higher levels of asymmetry in both males and females. As the first study that compares these two morphological measures in the same individual, this study shows a direct relationship between morphological measures of developmental stress and prenatal testosterone levels as a whole-body phenomenon in primates.

Acknowledgements

I would like to thank Dr. Frances White for serving as my primary thesis advisor and the many hours of invaluable guidance she provided me with over the course of this now three-year long project. I am particularly grateful for her ability to convince the lab microscribe to cooperate with the landmarking process, as it certainly didn't listen to me! I am also incredibly thankful for her willingness to mentor my research in my very first year of university, when I hardly had any idea of what research could look like, and for every year I got to work with her after that. I would also like to thank Dr. Marisa King for serving on my committee as my CHC representative and for her interest and willingness to leap onto this project at its most important stages. Her excellent advice on my project and the editing process was an absolutely invaluable resource and majorly appreciated.

I am grateful as well for Dr. Stephen Frost's guidance on sorting the digits and for inspiring my confidence on the more challenging portions of my project, as sorting felt impossible at times. I would like to thank Dr. Larry Ulibarri for being the first person to believe in my ability to conduct research and for introducing me to the Primate Osteology Lab in the first place. I can't imagine how different my path at university would have been without his guidance.

I would like to extend a very special thank you to Simon Apollo, without whom I could not have completed this project. I am grateful for the long hours in the lab spent problem-solving equipment, hunting through the collection for specimens, and encouraging me along the way.

Finally, I would like to thank Jackie, Dana, and Rita for the many hours of listening to my ramblings as I put this project together and allowing me to spend every moment from dawn to dusk in the office working to pull this thesis together.

Table of Contents

List of Figures

List of Tables

Introduction

Fluctuating asymmetry specifically refers to the degree of difference between homologous traits that occur on bilateral sides of the body, meaning regular traits that appear on the right and left sides (Klingenberg et al. 2002; Klingenberg 2015). While this is not the only type of symmetry that can be investigated, as life across all taxa displays symmetry in some manner, bilateral symmetry is the most common form of symmetry across the animal and plant kingdoms.

Fluctuating asymmetry has been utilized across a variety of disciplines, including numerous fields of biology, medicine, agriculture, and more (Graham et al. 2010). It has been particularly studied in biological anthropology in both human (Graham et al. 2010; Klingenberg 2015; Little et al. 2008) and nonhuman primate contexts (Frost et al. 2003; Little et al. 2008; Tallman et al. 2014), ranging from fossil hominids and primates to historical humans to modern humans and primates. Fluctuating asymmetry and other symmetry measures of the body can be applied in a variety of ways depending on the subject of study, as this topic has been broadly applied to bacteria, viruses, plants, and animals for differing applications (Graham et al. 2010). Previous work investigating fluctuating asymmetry in primates has investigated two and three dimensions in both cranial materials, including skulls, mandibles, and teeth, and postcranial materials, such as limb lengths, and has been used as a measure of developmental and/or physiological stress, such as disease load, with highly stressed individuals showing more asymmetry (Little et al. 2008). Low asymmetry, in contrast, is characteristic of individuals who have either experienced less stress or are strongly buffered against stress due to higher genetic fitness and resistance to disease (Little et al. 2008). The degree of asymmetry is a common trait in attractiveness in human (Klingenberg 2015; Little et al. 2008) and non-human primates (Little

et al. 2008) such that highly symmetrical individuals are found to be more attractive to the opposite sex, as low asymmetry functions as an honest signal of genetic health and resources (Hallgrímsson 1998).

During development, individuals may also be stressed by hormone loading, especially testosterone (Nelson and Shultz 2010). However, individuals with high testosterone often show anatomical signals that may also function as honest signals of an individual's health and access to resources (McGlothlin et al. 2008). Interestingly, a more subtle signal of testosterone loading is observed in the hands: the ratio between the lengths of the second to the fourth digit, or the 2D:4D ratio (Manning 2002). The 2D:4D ratio reflects the amount of testosterone experienced in utero, with individuals exposed to higher testosterone levels having relatively longer fourth digits and a lower 2D:4D ratio (Nelson and Shultz 2010). This ratio has been used to understand a wide range of testosterone-related traits including intraspecific competition, aggression, and promiscuity across different human (Little et al. 2008) and non-human primate species (Little et al. 2008) and is useful to investigate the hormonal markers of development in primates and their association with social structure categories experienced by individuals of different species (Manning 2002, Nelson and Shultz 2010).

While cranial asymmetry and 2D:4D have been measured in a wide range of species (e.g., Frost et al. 2003; Howlett 2019; Manning 2002; Nelson and Shultz 2010), this is the first study to examine cranial asymmetry and 2D:4D in the same individuals in order to understand how these two factors interact. To investigate this, I analyzed the skulls and digit ratios of 17 specimens from the University of Oregon Museum of Natural and Cultural History's Comparative Primate Collection. Cranial symmetry measurements of the skulls are useful to

investigate the traits most relevant to sexual selection, as it indexes the stability of a primate's growth during its development.

Through comparing these two measures in individuals from a variety of species, it was possible for me to investigate both how stress impacts development as a whole-body phenomenon, and if stress is experienced or recorded in differing degrees within the body according to sex. Importantly, this study investigates the 2D:4D ratio as a driver of asymmetry in primates and the connection between differing anatomical measures of stress that are recorded in the expressed physical traits of the body during development.

Background

2D:4D Ratio

The ratio between the second and fourth digits in the hands of primates, referred to as the 2D:4D ratio, has been well studied in primates. In particular, the 2D:4D ratio has been linked in both males and females to a range of sexual social behaviors and traits, including competitiveness, sexual dimorphism, promiscuity, dominance, mate-attracting behaviors, increased intrasexual competition, and aggression, among others (Nelson et al. 2010; Nelson and Shultz 2010).

The 2D:4D ratio is associated with the intensity of prenatal androgen effects in primates, as the fourth digit is highly sensitive to prenatal androgens, causing a longer fourth digit as compared to their second digit, and therefore a lower 2D:4D ratio, to develop (Nelson and Shultz 2010). The primary effect of prenatal androgens is the organization of the brain and body tissues according to the specific pattern determined by the sex of a primate, particularly important in regards to developing ideal male phenotypes (Nelson et al. 2010; Nelson and Shultz 2010).

Typically, the 2D:4D ratio is lower in males than females of their species, reflecting the effect of testosterone, a prenatal androgen, as a significant influence on development (Nelson and Shultz 2010). 2D:4D ratios also reflect the social structure of species' mating systems and the social behaviors preferential for success in those mating systems (Howlett 2019; Nelson and Shultz 2010). Primates in monogamous (males and females mating exclusively with one individual, also referred to as pair-bonded) mating systems with low frequency and low intensity of male intrasexual competition showed the highest 2D:4D ratios, and as such the smallest impact from prenatal androgen effects, while primates with polygynous (one male mating with multiple females) or polygynandrous (males and females both mating with multiple individuals)

mating systems with high frequency and high intensity of male intrasexual competition showed the lowest 2D:4D ratios, and were most impacted by prenatal androgen effects (Nelson and Shultz 2010). For example, despite being closely related species, chimpanzees (*Pan troglodytes)*, who have competitive mating systems, had low 2D:4D ratios, while bonobos (*Pan paniscus)*, who have more tolerant and less competitive mating systems, had high 2D:4D ratios (Nelson and Shultz 2010).

These general trends applied consistently within and between taxonomic groups, suggesting prenatal androgen effects can potentially provide an explanation for the development of beneficial sexual and social behaviors according to each species (Nelson and Shultz 2010). Importantly, this relationship remains consistent across both sexes. Female primates across taxonomic groups mirror the general trends of their male counterparts, where intense and frequent competition in mating systems resulted in low 2D:4D ratios and limited competition in mating systems resulted in high 2D:4D ratios (Howlett 2019; Nelson and Shultz 2010).

Within species, it is expected that males will have lower 2D:4D ratios than their female counterparts, on account of sexual dimorphism and the importance of testosterone in the development of male traits important for sexual selection (Nelson and Shultz 2010). Studies such as Nelson and Shultz (2010) have found near-significance in differences within the 2D:4D ratios of a species by sex, particularly in primates of highly competitive mating systems. Pair-bonded species do not show this same significance, and males and females of low competition mating systems have no sex difference in their 2D:4D ratios (Nelson and Shultz 2010).

2D:4D has also been shown to have a relationship with the maintenance of dominance in highly competitive environments, though results have been mixed (Howlett 2019; Nelson et al. 2010). Lower 2D:4D ratios were associated with higher ranks for female rhesus macaques

(*Macaca mulatta*) compared to other females in their matriline. Similar results have been found in other species, particularly species characterized by female dominance, but traits important to male intrasexual competition, such as canine crown height and dimorphism were not found to be significant in relation to their 2D:4D ratios within their species (Howlett 2019; Nelson et al. 2010; Plavcan 2004). Overall, prenatal androgens provide similar benefits to both males and females in competitive environments and may act as a mechanism for the development and appropriate expression of competitively beneficial behaviors that improve fitness in competitive environments, but the variation in behavior is complex (Howlett 2019). Varying levels of prenatal androgens may provide a competitive advantage through the development of appropriate cooperative and competitive behaviors in primates of both sexes depending on the competitiveness of their mating system and the strength of selection for particular types of behavior (Howlett 2019). For example, males in highly competitive environments may experience less selection for cooperative behaviors and greater selection for dominance and aggression, facilitated by selection for prenatal androgen effects, allowing them to be the most adaptive to their highly competitive environments and lowering their 2D:4D ratio (Nelson et al. 2010).

Social rank is also important to primates in regard to access to resources, as competition for resources is prevalent to all primates, regardless of social structure or mating system. This competition for resources can lead to nutritional deprivation and stress that can impact fetal development in lower ranks (Nelson et al. 2010). Rank can determine the number of stressful events that occur throughout an individual's development (Nelson et al. 2010). While it is not fully known whether prenatal androgen effects are derived directly from the maternal individual or the fetus, genetic studies have shown moderate to high heritability in both humans and rhesus

macaques (Nelson et al. 2010; Nelson and Shultz 2010). Given the aforementioned link between prenatal androgen effects and the development and appropriate expression of competitively beneficial behaviors, it is possible that the impacts of prenatal androgen effects are reflected in the potential to develop certain behaviors over others or reduce the ability for the beneficial behavior to emerge at all for a primate to express the appropriate behavior for their rank (Nelson et al. 2010; Nelson and Shultz).

2D:4D is complicated as well by the nature of sex-linked social behaviors being influenced by experienced social contexts and learning for appropriate expression, as well as the issue of some differences in 2D:4D ratios between species possibly being attributable to locomotive adaptations (Nelson et al. 2010; Nelson and Shultz 2010). However, Nelson and Schultz (2010) controlled for arboreality versus terrestriality for its effect on the expression of 2D:4D, and the relationship between 2D:4D and mating systems remained. In terms of genetic expression, the distal limb buds and genital buds are both controlled by the same *HOX* genes, which are sensitive to sex hormones, providing a developmental commonality that supports the link between 2D:4D and sex-linked social behaviors (Nelson et al. 2010).

The complexity in the expression of traits is not unique to 2D:4D or other morphological body measures when investigating the impacts of stress on different developmental processes. In the postcrania, 2D:4D ratios are only a single method adjacent to the analysis of stress. Other postcranial measures, such as the symmetry of limb lengths, have been studied to investigate the overlap of the expression of behavior from morphological measures (Willmore et al. 2005). However, other postcranial measures are influenced in similar ways by their importance as a functional structure for locomotion (Willmore et al. 2005).

Development and Symmetry

Each individual primate has a collection of genes that code for specific functional and sexually selected traits for expression in the individual (Graham et al. 2010). This collection of genes, referred to as an individual's genotype, codes for the target phenotype, or expression of an idealized trait, throughout the growth and development of the individual, with selection favoring the maintenance of an idealized developmental trajectory (Graham et al. 2010; Klingenberg 2019). The idealized trajectory would ensure an adult individual possessed all of the ideal traits for its environment, signaling an individual's fitness through the physical expression of a collection of its idealized traits, or phenotype (Graham et al. 2010).

During development, individuals inevitably experience stressors, referred to here as perturbations, that impact their ability to maintain an idealized developmental trajectory (Graham et al. 2010; Hallgrímsson et al. 2002). Stress can refer to any kind of perturbation that directs energy away from processes of growth and development, which includes both internal, genetic perturbations and external, environmental perturbations that result in the deviation of development from its idealized trajectory (Graham et al. 2010; Hallgrímsson et al. 2002). The process of expressing genes is regarded as inherently noisy and can impact development and prevent an individual from reaching the ideal target phenotype (Hallgrímsson 1998; Hallgrímsson et al. 2002). This "noisiness" within the expression of an individual genotype leads to random deviations away from the target phenotype (Hallgrímsson et al. 2002). However, it is because of these perturbations that a single genotype within an individual can produce numerous different phenotypes depending on the frequency and severity of the perturbations they experience during their development, as well as the buffering strategies utilized to reduce the impact of these perturbations (Hallgrímsson et al. 2002). The effects experienced by individuals

from their internal buffering strategies is referred to as canalization, which is the suppression of variation in the phenotype, returning an individual's development closer to the target phenotype (Graham et al. 2010; Hallgrímsson et al. 2002). The more effective an individual's buffering strategies are, the greater the minimization of the perturbation, ensuring the traits of an individual are impacted as mildly as possible (Graham et al. 2010; Hallgrímsson et al. 2002). Any diversion from the target phenotype may impact the fitness of individuals, such as their mating success (Graham et al. 2010; Hallgrímsson 1998).

The process of canalization reflects all processes that result in the buffering of environmental and genetic perturbations, but internal strategies also exist to buffer the "noisiness" of gene expression, which is referred to as developmental stability (Hallgrímsson et al. 2002; Willmore et al. 2005). Both developmental stability and canalization contribute to the idealized trajectory of phenotypic expression in individuals (Willmore et al. 2005). It is likely that many of these processes overlap with one another in the developmental trajectory, showing greater redundancy on particular traits and buffering all perturbations to maintain these particular traits as closely to the phenotypic ideal as possible (Hallgrímsson 1998; Hallgrímsson et al. 2002; Willmore et al. 2005). The fewer genetic determinants and other internal buffering strategies an individual has for a particular trait, the further from the target phenotype the trait becomes when developed (Hallgrímsson 1998). It is possible this reflects the nature of a trait as of either functional or sexually selected importance to individuals, as long bones show greater insensitivity to stress than cranial elements that are of importance to sexual selection (Hallgrímsson 1998). This is significant in connection to the 2D:4D ratio, as the redundancy of many overlapping processes on functional and sexually selected traits suggests that structures will be similarly impacted despite their differences, such as the genetic overlap in control of the

development of both the limb buds and genital buds (Hallgrímsson et al. 2002). More overlapping processes on a single structure in development can both help and hinder buffering perturbations as well. It is possible that interdependent processes can also serve to amplify errors in the case of particular perturbations or multiple failures (Willmore et al. 2005). It is also possible these processes extend further, but studies investigating the patterns of variability between cranial and postcranial elements are extremely limited (Willmore et al. 2005).

This reflects again on the amount of energy available to allocate to developing as close to the target phenotype as possible versus supporting the growth of functional elements in the body (Hallgrímsson 1998). Studies have shown that greater deviance from the target phenotype is associated with reduced overall size in individuals, similarly reflecting the relationship between the allocation of finite energy resources and developmental processes (Hallgrímsson 1998; Little et al. 2008). Ultimately, phenotypic traits require energy to produce during development, and an individual must be able to afford such a trait, especially a nonfunctional trait specifically for sexual selection, in order to reach their target phenotype to present to potential mates (Little et al. 2008).

The development of idealized phenotypic traits or the lack thereof cannot be faked by individuals, as these traits require an energetic input to exist in line with the target phenotype (Little et al. 2008). This means that nonfunctional traits developed from sexual selection are honest signals of mate quality, indicating individuals are of high quality because they could maintain the development of their sexually selected traits due to better buffering strategies or reduced genetic sensitivity to stressors (Hallgrímsson 1998, Little et al. 2008). Sexually dimorphic traits are highly associated with prenatal androgens such as testosterone and oestrogen, which have been shown to reduce resistance to disease and parasites (Little et al.

2008). Because of this, traits that rely on high amounts of prenatal androgens are indicators of individuals with strong immune systems, as the individual would not have had to allocate energy away from the development of sexually dimorphic traits to combat illness (Little et al. 2008). In many species, the traits themselves that are displayed often overlap to signal the same factor of mate quality, much in the same way that genetics and buffering strategies seek a certain measure of redundancy in order to reach the target phenotype (Hallgrímsson 1998; Little et al. 2008; Willmore et al. 2005). This allows individuals more opportunities to signal their quality and improves the accuracy of signaling, but risks displaying multiple measures of low quality as well (Little et al. 2008).

Despite canalization and the other processes of developmental stability that seek to maintain an idealized target phenotype, individuals still show variation among many structures, both functional traits and nonfunctional traits relating to sexual selection, which results from both the "noisiness" of gene expression as well as the general imprecision of the developmental process and the buffering strategies themselves (Hallgrímsson 1998; Klingenberg 2015, Willmore et al. 2005). While these deviations from the idealized development trajectory can appear in a variety of ways, one method for quantifying these differences is that of fluctuating asymmetry, which can be utilized to index the stability of an individual's development during its growth and development and the stressors it experienced therein (Graham et al. 2010; Hallgrímsson 1998; Hallgrímsson et al. 2002; Klingenberg 2015; Little et al. 2008).

Fluctuating Asymmetry

All lifeforms have symmetry of some kind (Graham et al. 2010). Bilateral symmetry, referring to symmetry of the left and right sides of the body, is the most common type of

symmetry found in animals (Graham et al. 2010). Fluctuating asymmetry denotes small differences between traits found bilaterally on the body, occurring equally on the right and left sides, due to the random deviations from the target phenotype, reflecting the ability of an individual to maintain their idealized developmental trajectory under the environmental conditions they experience (Klingenberg 2015; Little et al. 2008). In the theoretical case of perfectly reaching the target phenotype, an individual's right and left sides would be exact mirror images of the other where bilateral symmetry controls the development of the structure (Klingenberg et al. 2002; Klingenberg 2015; Klingenberg 2019). In reality, the right and left sides of individuals vary from both each other and the target phenotype in differing ways (Klingenberg 2015). Despite both sides of an individual experiencing nearly the same environment, including experiencing the same genetic and environmental stressors, the sides will still differ from one another as they develop separately, and are therefore likely to produce different deviations from the target phenotype per side (Klingenberg 2015). However, these differences between bilaterally occurring traits are often very subtle due to the canalization of these traits (Hallgrímsson et al. 2002; Klingenberg 2015).

As discussed above, a variety of genetic and environmental perturbations can impact symmetry, as perfect symmetry is the target phenotype of the individual (Graham et al. 2010; Klingenberg 2019). Fluctuating asymmetry is of particular interest because it is not adaptive to an individual's environment in the same way that, for example, locomotion would favor symmetrical overall limb lengths, and is instead reflective of an individual's ability to buffer its environment and canalize its traits in order to maintain a stable development of their idealized target phenotype (Graham et al. 2010; Klingenberg 2019; Little et al. 2008). An individual expending more energy towards its symmetry does not reflect the development of a specific

adaptation to the environment, as the symmetry in and of itself does not offer a modification capable of buffering particular perturbations, it simply reflects the efficacy of an individual's pre-existing strategies (Graham et al. 2010). In other words, symmetry itself does not increase the resilience of an individual against perturbations, but it does reflect how adaptive its buffering strategies are to the environment it is developing in.

Functional structures are impacted by fluctuating asymmetry during development to an extent (Willmore et al. 2005). In relation to one another, the successful development of a functional structure is partially dependent on the successful development of structures that are associated with it, such as muscular growth and usage throughout an individual's development impacting the development of that individual's bones (Willmore et al. 2005). Prior work has shown increased variation from the target phenotype is connected to increased strain from muscular growth and usage, especially regarding individuals with asymmetrical muscular development that preferentially stresses one side of the body (Hallgrímsson 1998; Willmore et al. 2005). Because of this interdependence of structures, the canalization of traits to the target phenotype improves over developmental time, where more highly developed structures are more able to resist the perturbations enacted by their associated structures (Willmore et al. 2005). This predicts that skeletal elements that form particularly early in development are more susceptible to variation, therefore showing greater deviation from the target phenotype (Willmore et al. 2005). Skeletal elements that take a longer time to fully develop overall are also more susceptible to variation, as the number of perturbations experienced and recorded in an individual's asymmetry increases with greater developmental time (Hallgrímsson 1998).

Fluctuating asymmetry is a particularly useful method to investigate the impact of stress on nonfunctional, sexually selected traits that are, at large, more susceptible to the impacts of

stress than their functional counterparts that are prioritized in energy allocation (Graham et al. 2010; Little et al. 2008; Willmore et al. 2005). This is what leads to the importance of fluctuating asymmetry in honestly signaling mate quality, as the stress experienced by an individual will be recorded in the phenotypic expression of fluctuating asymmetry and honestly signaled to potential mates (Graham et al. 2010; Little et al. 2008). If an individual developed in a stable environment or had particularly effective buffering strategies, the amount of fluctuating asymmetry in the individual will be minimal, acting as an honest signal of its high quality to potential mates (Graham et al. 2010). This is true of the opposite as well, where an individual who developed in an unstable, poorly-buffered environment will retain a high degree of fluctuating asymmetry, which acts as an honest signal of its lower quality to potential mates (Graham et al. 2010).

Previous work regarding fluctuating asymmetry has shown a correlation with fitness, intensity of sexual selection, and stress (Hallgrímsson et al. 2002). Fluctuating asymmetry has also been connected to developmental noise, growth rates, fecundity, fertility, survivability, sexual dimorphism, and the facilitation of development by sex hormones (Hallgrímsson et al. 2002; Little et al. 2008). Prior studies regarding fluctuating asymmetry have shown it to be a useful measure across numerous structures in the body throughout both prenatal and postnatal developmental, including both functional and nonfunctional, sexually selected structures such as skulls, teeth, long bones, sexual selection ornaments, and more (Hallgrímsson 1998; Little et al. 2008). However, little has been done to connect the variability or association of these methods across the body, as each study maintains its method of analysis to an isolated structure, citing that the main mechanisms for fluctuating asymmetry will differ according to differing developmental patterns, as there is no strong evidence suggesting fluctuating asymmetry affects

the whole body in the same ways (Hallgrímsson 1998; Klingenberg 2015; Willmore et al. 2005). These studies also primarily rely on and recommend study towards populations and species-wide measures for study, neglecting individual measures across the body within the same individuals (Klingenberg 2015; Nelson and Shultz 2010). Through the analysis of both cranial and postcranial elements from the same individuals, it is possible for me to investigate the connection between sexual selection, fitness, and stress in primates as a whole body phenomenon.

Methods

Specimen Selection

A total of 17 specimens were selected for this study from the University of Oregon's Comparative Primate Collection of the Museum of Natural and Cultural History. The Comparative Primate Collection houses over 700 primates, including both captive specimens from the Oregon National Primate Research Center and wild-caught specimens. Because of the varied origins of collected specimens, there are a range of conditions and skeletal elements present in each specimen. While care was taken in selecting specimens for analysis that were most intact and in the greatest possible conditions, not all specimens included all morphological traits preferred for cranial landmarking or fully intact and digit-ray coded phalanges, leading to adjustments to data collection being made on a specimen-by-specimen basis.

Selection encompassed African, Asian, and South American monkeys and apes from primarily polygynous and polygynandrous social structures, and a small number of specimens from monogamous social structures. Both male, female, adult, and subadult individuals were included in this analysis. Strepsirrhines were excluded from this analysis due to their significant and unusual sexual dimorphism and social structures as compared to other primate groups. Particular species, ages, and sexes are reported in Table 1.

Given the range of conditions represented within the collection, the sample size for this study is smaller than ideal and is best representative of adult primates from polygynous and polygynandrous social structures. Further study of a broader range of specimens from differing social structures is needed to determine larger trends of fluctuating symmetry to connect individual primates to more typically studied larger population or species trends. Apes are also underrepresented in the current collection of specimens and merit a greater focus for future work.

In contrast, macaques (*Macaca spp.*) are well-represented in this overall sample size. Subadults also represent only a small portion of this sample, and merit greater study. Subadult specimens were difficult to include due to the lack of epiphysis presence on the proximal phalanges, preventing a comparison with intact adult specimens.

Table 1. Specimen information and social system ranking *(Nelson and Shultz 2010).

Specimen ID	Species	Sex	Age	Type	Social Structure*	Competition*
342-2392	Cercopithecus mitis	UK	A	African	Polygynandrous	3
343-6000	Miopithecus talapoin	F	A	African	Polygynandrous	4
195-7337	Macaca fascicularis	F	A	Asian	Polygynandrous	4
195-7613	Macaca fascicularis	F	A	Asian	Polygynandrous	4
291-06069	Macaca fuscata	F	SA	Asian	Polygynandrous	4
305-2413	Macaca mulatta	UK	UK	Asian	Polygynandrous	4
305-2412	Macaca mulatta	F	A	Asian	Polygynandrous	4
305-10004	Macaca mulatta	F	SA	Asian	Polygynandrous	4
305-10433	Macaca mulatta	M	A	Asian	Polygynandrous	4
300-673	Macaca nemestrina	M	A	Asian	Polygynandrous	4
300-2512	Macaca nemestrina	F	A	Asian	Polygynandrous	4
244-2415	Hylobates syndactylus	UK	UK	Asian	Monogamous	1
137-2112	Alouatta caraya	M	A	South American	Polygynandrous	4
170-2414	Cacajao rubicundus	UK	UK	South American	Polygynandrous	3
079-3924	Callimico goeldii	UK	A	South American	Monogamous	1
127-1791	Cebus albifrons	M	A	South American	Polygynandrous	4
127-23107	Cebus albifrons	M	UK	South American	Polygynandrous	4

Sex Identification

In total, 4 specimens included in this study were initially of unknown sex. *Callimico goeldii* and *Hylobates syndactylus* were unable to be sexed due to the lack of sexual dimorphism in primates of typically monogamous social structures (Nelson and Shultz 2010). *Cacajao calvus rubicundus* was unable to be sexed as well, as very little is known of the species (Robinson et al. 1987). While we would expect to see significant sexual dimorphism in *Cacajao calvus rubicundus* due to their typically polygynous social structures, there is simply not enough information to confidently assign sex to the skeletal remains in this study (Robinson et al. 1987). However, it was possible to identify the sex of the *Macaca mulatta* specimen that was previously unknown. Following the methods of Wang et al. (2012), this specimen was identified as a female due to the complete eruption of the dentition but a lack of closure in facial sutures, as is typical of female rhesus macaques.

Measuring Cranial Symmetry

Three-dimensional analysis of cranial symmetry was taken via a Microscribe-3DLX (Immersion Corp., San Jose, CA) through set landmarking points for a total of 31 landmarks per skull in the case of completely undamaged specimens. Landmarks in this study refer to a series of x, y, z coordinates describing a three-dimensional shape in space, taken on unambiguous traits that occur bilaterally on the skull (Klingenberg et al. 2002; Tallman et al. 2014). This procedure was developed from Frost et al. (2003) and includes 7 unpaired landmarks defining the midline and 24 paired landmarks defining the position of matching bilateral traits analyzed for symmetry, reported in Table 2.

Table 2. Skull landmarks used in the measurement of cranial asymmetry *(Frost 2003 and Tallman 2014).

Number	Landmark	Type	Definition*
1	Inion	Unpaired	Most posterior point of the cranium when viewed in Frankfurt horizontal
2	Bregma	Unpaired	Junction of coronal and sagittal sutures
3	Glabella	Unpaired	Most anterior point of the frontal when viewed in Frankfurt horizontal
4	Nasion	Unpaired	Fronto-nasal suture in the midline
5	Rhinion	Unpaired	Most anterior point in the midline on the nasals
6	Nasospinale	Unpaired	Most inferior midline point of the piriform aperture
7	Prosthion	Unpaired	Most anteroinferior point on the projection of the premaxilla between the central incisors
8/20	Prosthion 2	Paired	Most anteroinferior point on the premaxilla between the central and lateral incisors
9/21	Premax-max superior	Paired	The point of meeting between the premaxillary suture and the nasal bone or aperture depending on the continuance of the suture to the nasal bone
10/22	Zygo-max inferior	Paired	Anteroinferior point of the zygomaticomaxillary suture in the antero-lateral view
11/23	Zygo-max superior	Paired	Anteroinferior point of the zygomaticomaxillary suture taken at the orbit rim
12/24	Dacryon	Paired	Junction of frontal, lacrimal, and maxilla
13/25	Mid-torus inferior	Paired	Point on inferior margin of supraorbital torus in the middle of the orbit
14/26	Mid-torus superior	Paired	Point superior to the mid-torus inferior on the most superior point of the supraorbital torus when viewed in Frankfurt horizontal
15/27	Frontomalare orbitale	Paired	The point of crossing between the frontozygomatic suture and the inner orbital rim
16/28	Frontomalare temporale	Paired	The point of crossing between the frontozygomatic suture and the lateral edge of the zygoma
17/29	Porion	Paired	The top of the auditory meatus when viewed in Frankfurt horizontal
18/30	Zygo-temp superior	Paired	Superior point of the zygomatico-temporal suture on the lateral face of the zygomatic arch
19/31	Zygo-temp inferior	Paired	Inferior point of the zygomatico-temporal suture on the lateral face of the zygomatic arch

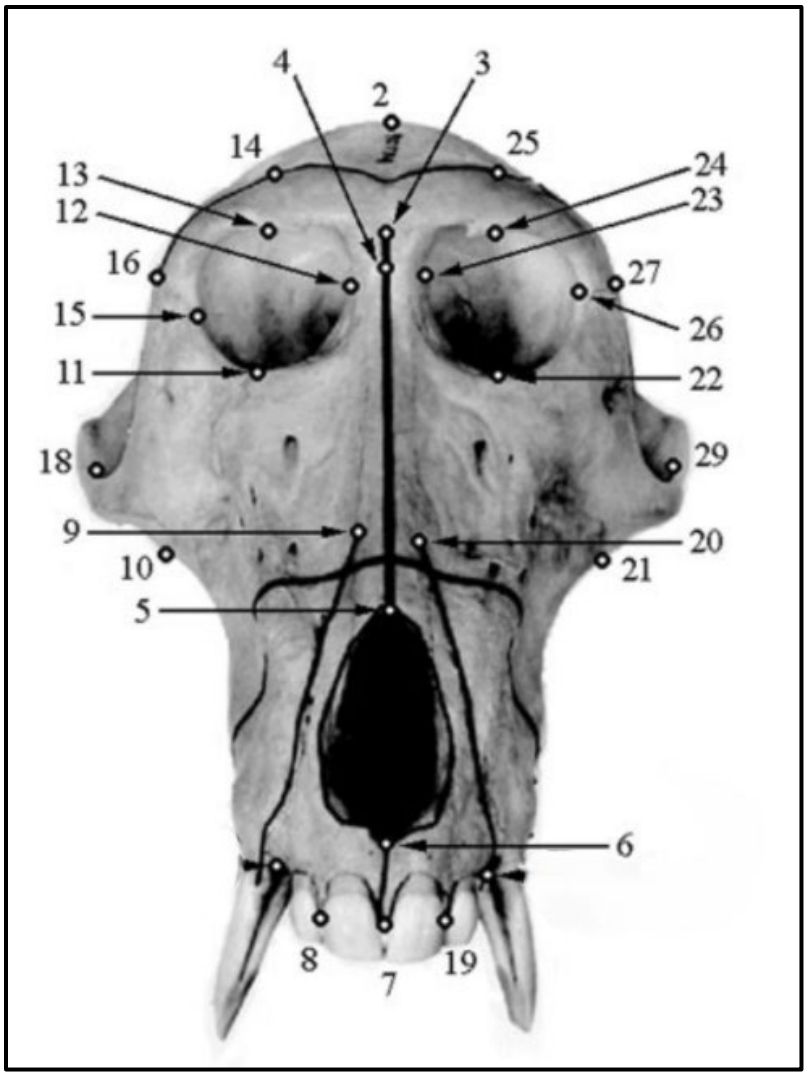

Figure 1. Example of cranial landmarks for analysis of fluctuating asymmetry (Frost 2003).

Specific landmarks were excluded from each skull on a specimen-by-specimen basis in the case of existing damage. 7 specimens had reduced landmarking points taken to calculate their symmetry based on the particular damage they sustained, reduced to the values reported in Table 3. Each specimen was scanned for all available landmarks 5 total times to ensure consistency and accuracy of the points utilized to calculate asymmetry. Each of the specimens' skulls were mounted with clay to a fixed apparatus to which the Microscribe-3DLX (Immersion Corp., San Jose, CA) was also secured and were not moved until all points were collected for analysis.

Table 3. Number of landmarks present and measurable in each cranial specimen.

Specimen ID	Number of Landmarks	Landmarks Removed
342-2392	29	Inion, bregma
343-6000	31	None
195-7337	29	Prosthion 2
195-7613	31	None (scan 5 was reduced by an additional unpaired point, the bregma)
291-06069	31	None
305-2413	31	None
305-2412	31	None
305-10004	27	Mid-torus inferior, mid-torus superior
305-10433	31	None (scan 5 was reduced by an additional paired set, the prosthion 2)
300-673	28	Prosthion, prosthion 2 (scan 5 was reduced by an additional paired set, the premax-max superiors)
300-2512	31	None (scan 5 was reduced by an additional paired set, the zygo-max superiors)
244-2415	31	None
137-2112	31	None
170-2414	31	None (scan 3 was reduced by an additional paired set, the zygo-temp superiors)
079-3924	30	Rhinion
127-1791	28	Prosthion, prosthion 2
127-23107	23	Zygo-max inferior, zygo-max superior, zygo-temp superior, zygo-temp inferior

The landmark data was then transferred to RStudio (Rstudio Team 2020) and three-dimensionally modeled to ensure the accuracy of the landmarks through the packages geomorph and facefuns. Once the input from the Microscribe-3DLX (Immersion Corp., San Jose, CA) was verified for accuracy, the data was transferred again to MorphoJ (Klingenberg 2011) to complete analysis of the symmetric and asymmetric components of the skulls. This was accomplished through Procrustes form fits and vector-based symmetry analyses to quantify the overall symmetry for each skull, conducted within MorphoJ (Klingenberg 2011). Finally, all skulls were

two-dimensionally modeled and displayed against the mirror-image reflection of their bilateral points, displaying the difference between the actual landmark position and the target phenotype (Klingenberg 2011; Klingenberg 2019).

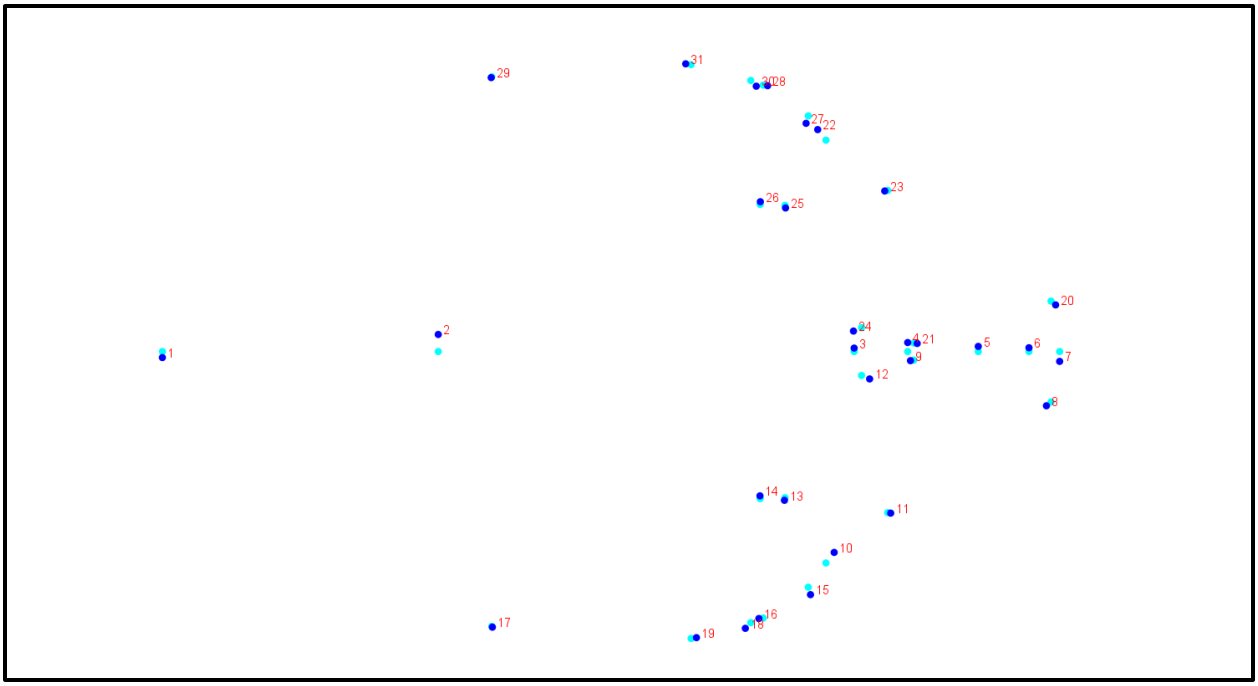

Figure 2. Example MorphoJ analysis plot showing original and reflected points used to calculate asymmetry.

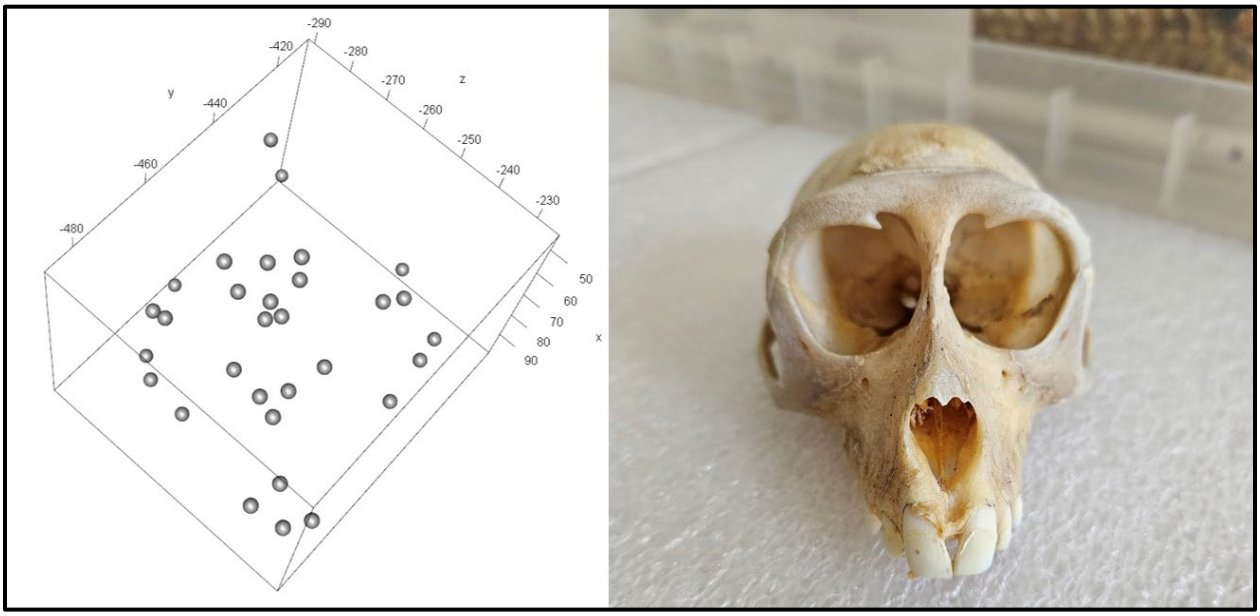

Figure 3. Example skull and three-dimensional plot of microscribe measurement of landmarks, plotted in Rstudio.

Measuring Postcranial Symmetry

The ratio between the second and fourth phalanges was utilized to establish the presentation of symmetry in the postcrania. In order to test the variability and accuracy of measurements taken on the specimens of this study, a brief experiment was performed on each possible stage of remains present in the lab. First, a fully fleshed hand was processed down to exclusively skeletal remains and measured extensively via a digital caliper at both stages for its 2D:4D ratio across several days. Next, a defleshed, articulated hand was extensively measured across several days before being disarticulated and measured again for its 2D:4D ratio. Ultimately, these results indicated that the most consistent and accurate measurements of the 2D:4D ratio were taken on fully disarticulated bone. As such, only fully disarticulated phalanges were used in this study.

Disarticulated phalanges were measured in millimeters using a digital caliper in order to attain the least variable and most accurate 2D:4D ratios. To this end, all specimens with articulated phalanges were processed, cleaned of flesh, and disarticulated before measurements were taken. Specimens that were previously disarticulated but marked through digit-ray coding to specify the order of the phalanges were directly measured. Specimens that were previously disarticulated but not digit-ray coded were sorted according to length, width, robusticity, and degree of fit with sorted metacarpals. Images of all sorted specimens are reported in appendix 1. Due to the nature of the remains, some specimens did not possess entire phalanges for measurement, and unsorted intermediate and distal phalanges were too uncertain to be properly attributed to a particular ordering, proximal phalanges were exclusively measured to approximate the 2D:4D ratio and standardize the measurement across all specimens within the sample.

Statistics

Shape is described as the relative proportion of objects and does not include the exact length measurements themselves, meaning that the size of objects can be statistically removed and shape can be quantified as a vector of ratios and standardizes the measurements for comparison across all objects in the sample (Klingenberg 2016). This is particularly relevant to studies that utilize multiple species in analysis, as the size variation can be quite significant across different primate species.

To this end, fluctuating asymmetry of the crania is calculated through Procrustes form fits, also referred to as Procrustes superimpositions, which removes size and returns only differences in shape (Klingenberg et al. 2002). Essentially, Procrustes superimpositions mirror and reflect all bilateral points across the midline, creating a perfectly symmetrical configuration representing the target phenotype, and layers that mirror image with the actual landmarks taken on those points (Klingenberg et al. 2002; Klingenberg 2019). The difference between the mirror image and the actual landmarks taken is the asymmetric component of the shape (Klingenberg et al. 2002). Next, the data is processed through a Procrustes ANOVA, which assumes an equal amount of variation around each landmark and distributes that variation, removing the direction of the vectors from asymmetry and allowing a generalized measurement to approximate the asymmetry across the whole skull (Klingenberg et al. 2002; Willmore et al. 2005). This means that some traits will be more asymmetrical than others, but that larger asymmetry of those specific traits will be distributed out across all traits in order to make an overall measurement of asymmetry that considers all traits. Procrustes analyses were conducted through MorphoJ (Klingenberg 2011) to establish the asymmetric component of each skull and return the generalized fluctuating asymmetry measurement.

All variables were tested for normality using the Kolmogorov-Smirnov Goodness of Fit tests to a normal distribution and the assumptions of parametric ANOVAs and regression (Sokal and Rohlf 1995). If the variable was found to be normally distributed, it was used in its original form. Non-normally distributed variables were transformed using standard transformation (e.g. Log10 and natural log) and retested for normality. If the variable could not be transformed to normality, then the variable was ranked, re-tested for normality, and the ranked data was then used in the analyses. ANOVAs were used to compare samples for differences in average values, a robust regression was used to detect if there were data outliers, and a regression was used to test for a significant relationship between fluctuating cranial asymmetry and 2D:4D ratio. These statistical analyses were conducted in *SAS*© 9.4 (*SAS* Institute, Cary NC). Each species was classified according to its mating system with 1 having low male-male competition and 4 having the highest male-male competition. The 2D:4D ratio and ranked fluctuating asymmetry data were compared to the mating system and body weight and canine tooth dimorphism (Plavcan 2004). to represent sexual dimorphism using a non-parametric Spearman rank correlation.

Table 4. Summary of final data analyzed showing averages of replicates of asymmetry and 2D:4D measured (see appendices for original full data sets).

Specimen ID	average asym	2D:4D ratio
079-3924	0.000478298	0.897504445
127-1791	0.00084124	0.846831857
127-23107	0.000446945	0.997876633
137-2112	0.001076407	0.932330459
170-2414	0.000536439	0.864128267
195-7337	0.00045866	0.876713788
195-7613	0.000303611	0.980579465
244-2415	0.000536175	1.00900393
291-06069	0.002838014	0.92238817
300-673	0.000249477	1.023694569
300-2512	0.000394706	0.884584274
305-2413	0.000467506	0.960670004
305-2412	0.00072143	0.873783207
305-10004	0.001056801	0.850244383
305-10433	0.000687704	1.037614489
342-2392	0.000263271	0.998958827
343-6000	0.000618405	0.872416159

Results

The complete samples of 2D:4D were not significantly different to normally distributed (Kolmogorov-Smirnov D= 0.1615, $p>0.15$, not significant) and so were not transformed. The sample of fluctuating asymmetry data, however, was significantly different to normal (Kolmogorov-Smirnov D= 0.2534, $p<0.01$, significantly different to normal) and continued to be non-normal when log transformed (Kolmogorov-Smirnov D= 0.2533, $p<0.01$, significantly different to normal), so the data was ranked. The ranked data was then found to be not significantly different to normal (Kolmogorov-Smirnov D= 0.0800, $p>0.015$, not significantly different to normal). Therefore, the original 2D:4D ratios were used with the ranked data from fluctuating asymmetry.

Outlier detection was conducted using a Robust Regression, and no significant outliers or high leverage points were detected, so all the data was included in the subsequent analyses.

Table 5. Results of a Robust Regression Analysis to detect outliers and points with high leverage conducted in SAS©. No outliers or high leverage points were detected.

Number of Observations Read	17
Number of Observations Used	17

Parameter Information	
Parameter	Effect
Intercept	Intercept
twoDfourD	twoDfourD

Summary Statistics						
Variable	Q1	Median	Q3	Mean	Standard Deviation	MAD
twoDfourD	0.8731	0.9224	0.9867	0.9247	0.0595	0.0741
asym	4.5000	9.0000	13.5000	9.0000	5.0498	5.9304

Parameter Estimates							
Parameter	DF	Estimate	Standard Error	95% Confidence Limits		Chi-Square	Pr > ChiSq
Intercept	1	55.1693	17.7273	20.4243	89.9142	9.69	0.0019
twoDfourD	1	-50.0712	19.1338	-87.5727	-12.5697	6.85	0.0089
Scale	1	4.3168					

Diagnostics Summary		
Observation Type	Proportion	Cutoff
Outlier	0.0000	3.0000
Leverage	0.0000	2.2414

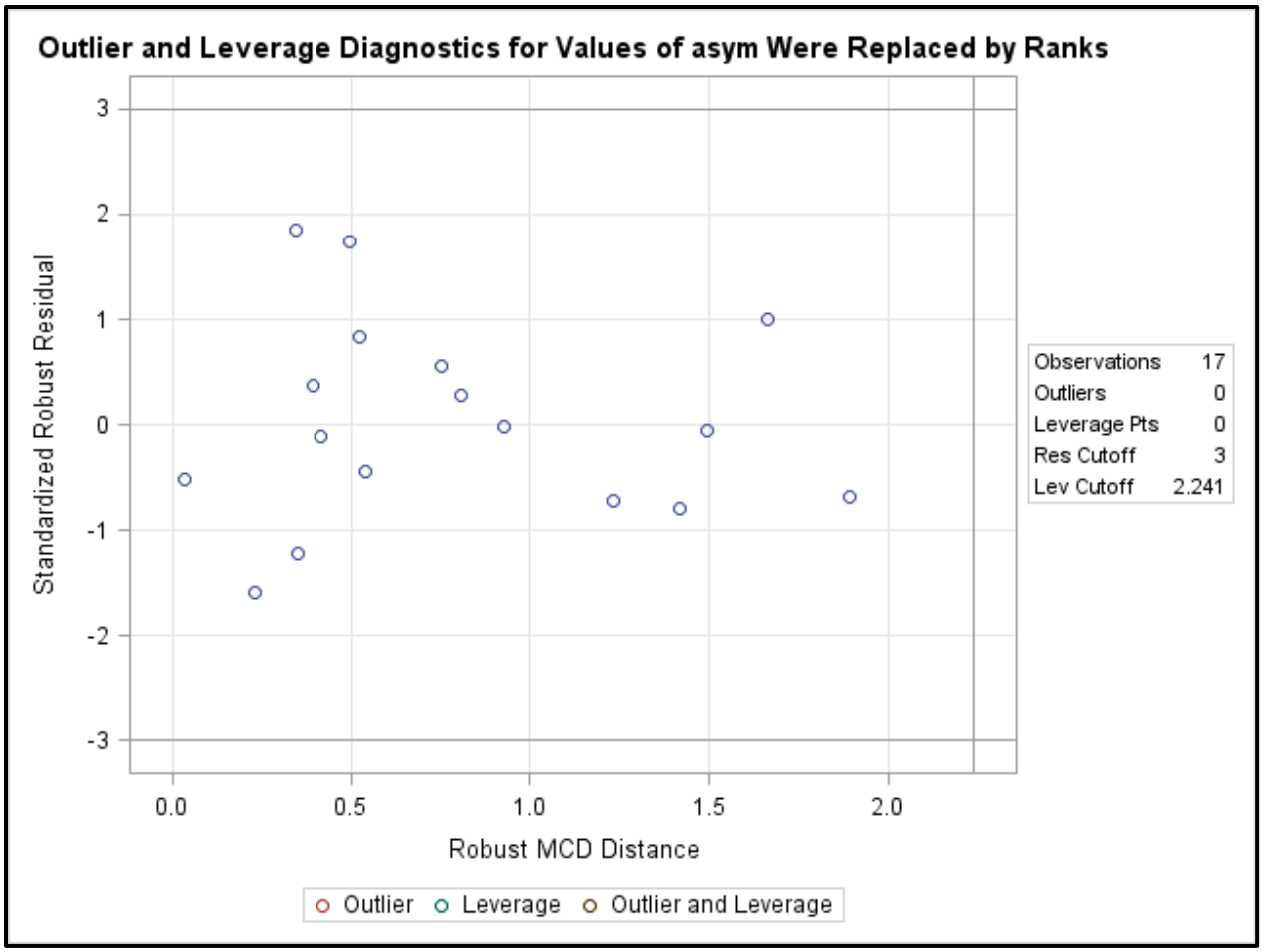

Figure 4. Plot of Outlier and Leverage Diagnostics from a Robust Regression analysis conducted in SAS©.

The ANOVAs showed that there were no significant differences between males, females, and unknown in 2D:4D ratio (F=1.05, df=2,14, p=0.3754, not significant)

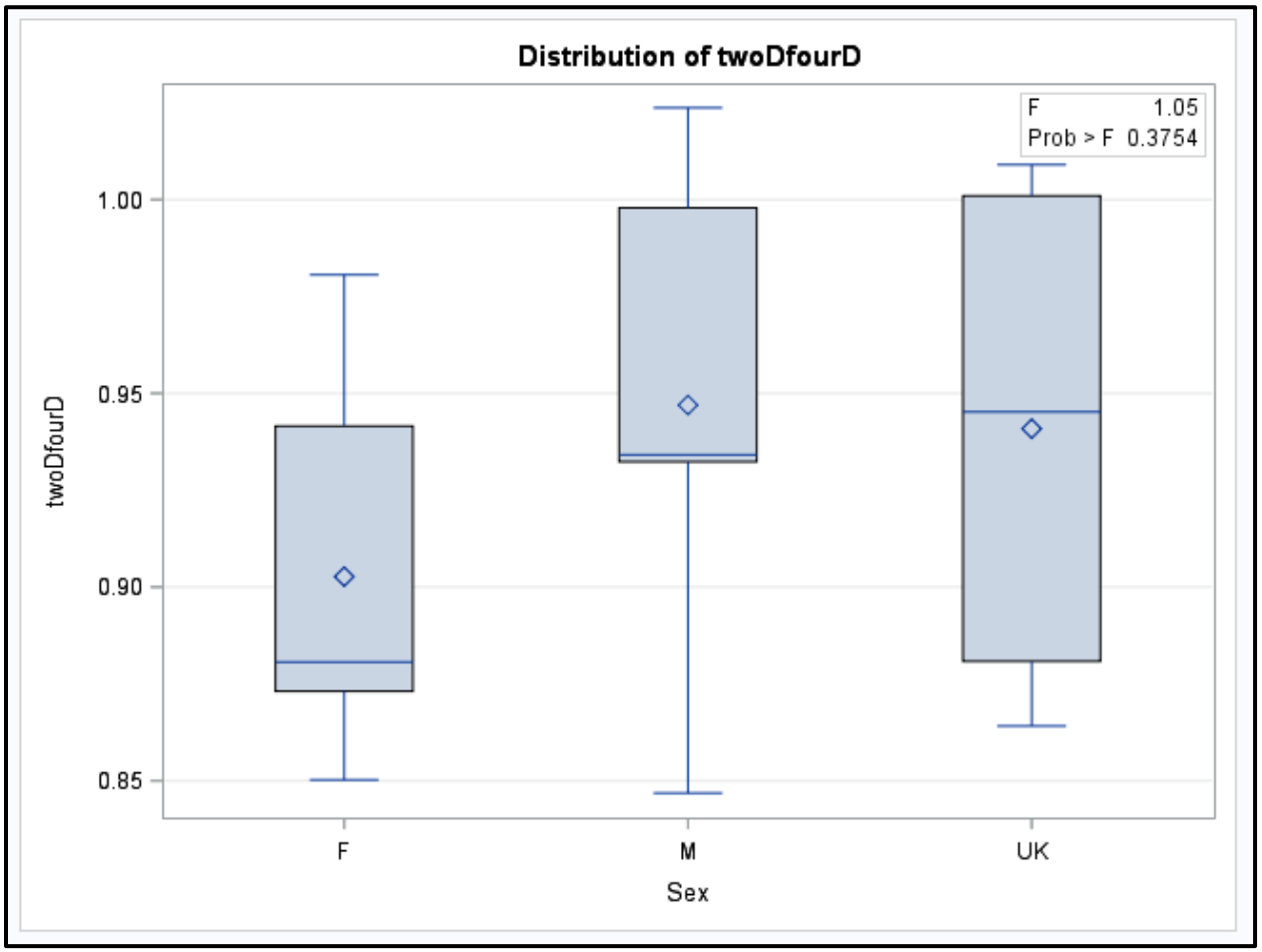

Figure 5. Plot of mean (diamond), median (line) and range (whiskers) from ANOVA comparing male, female and unknown sex 2D:4D finger ratios.

There were no significant differences between males, females, and unknowns in fluctuating asymmetry (F=0.29, df=2,14, p=0.7551, not significant).

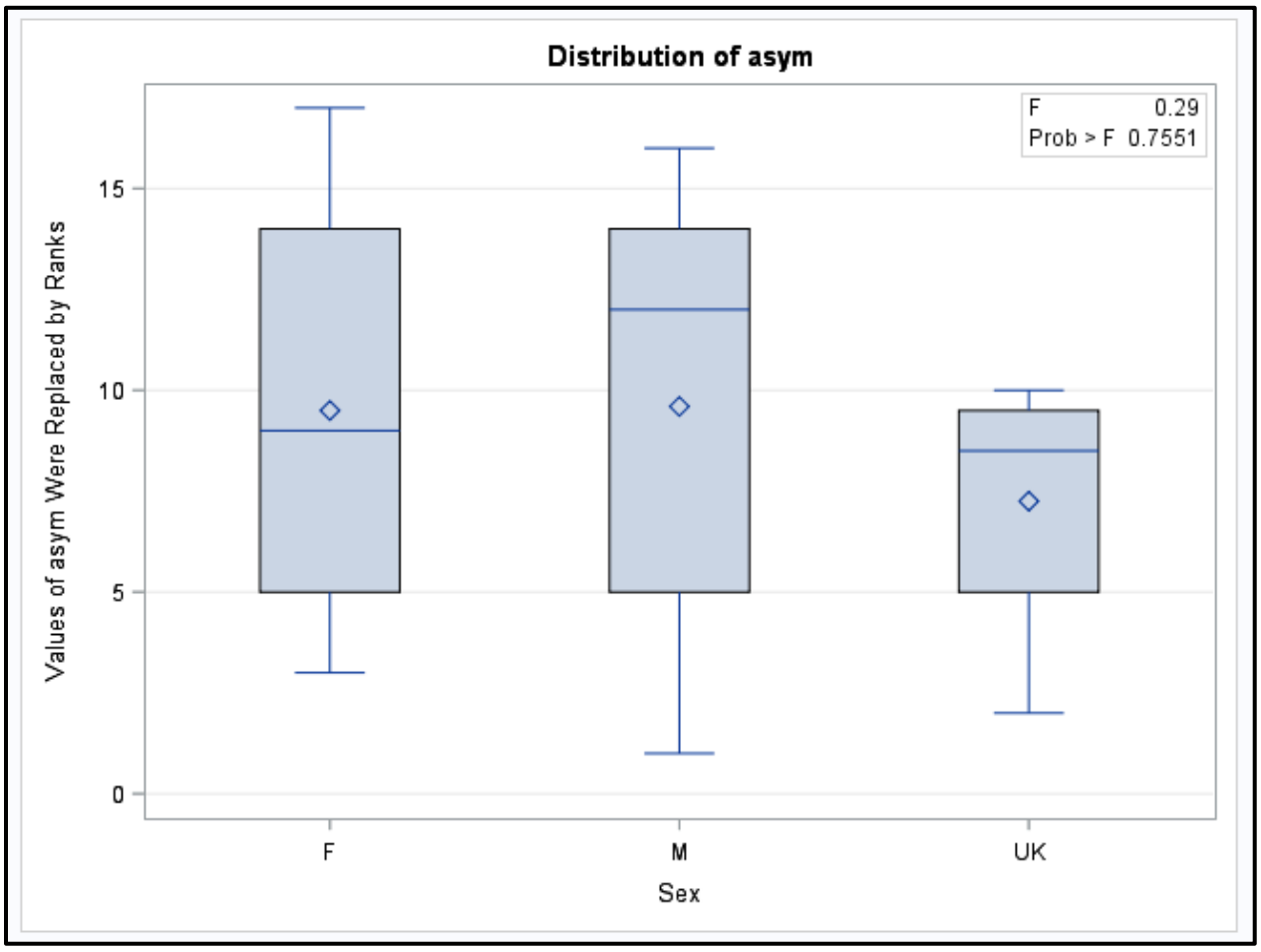

Figure 6. Plot of mean (diamond), median (line) and range (whiskers) from ANOVA comparing male, female and unknown sex ranked asymmetry values.

There was a significant regression of ranked fluctuating asymmetry and 2D:4D (F= 7.19, df=1,15, p=0.0171, significant) with a regression line of 2D:4D = 53.644 - 48.280 x asymmetry with an R-squared of 0.324 or 32.4% of the variance explained by the regression line.

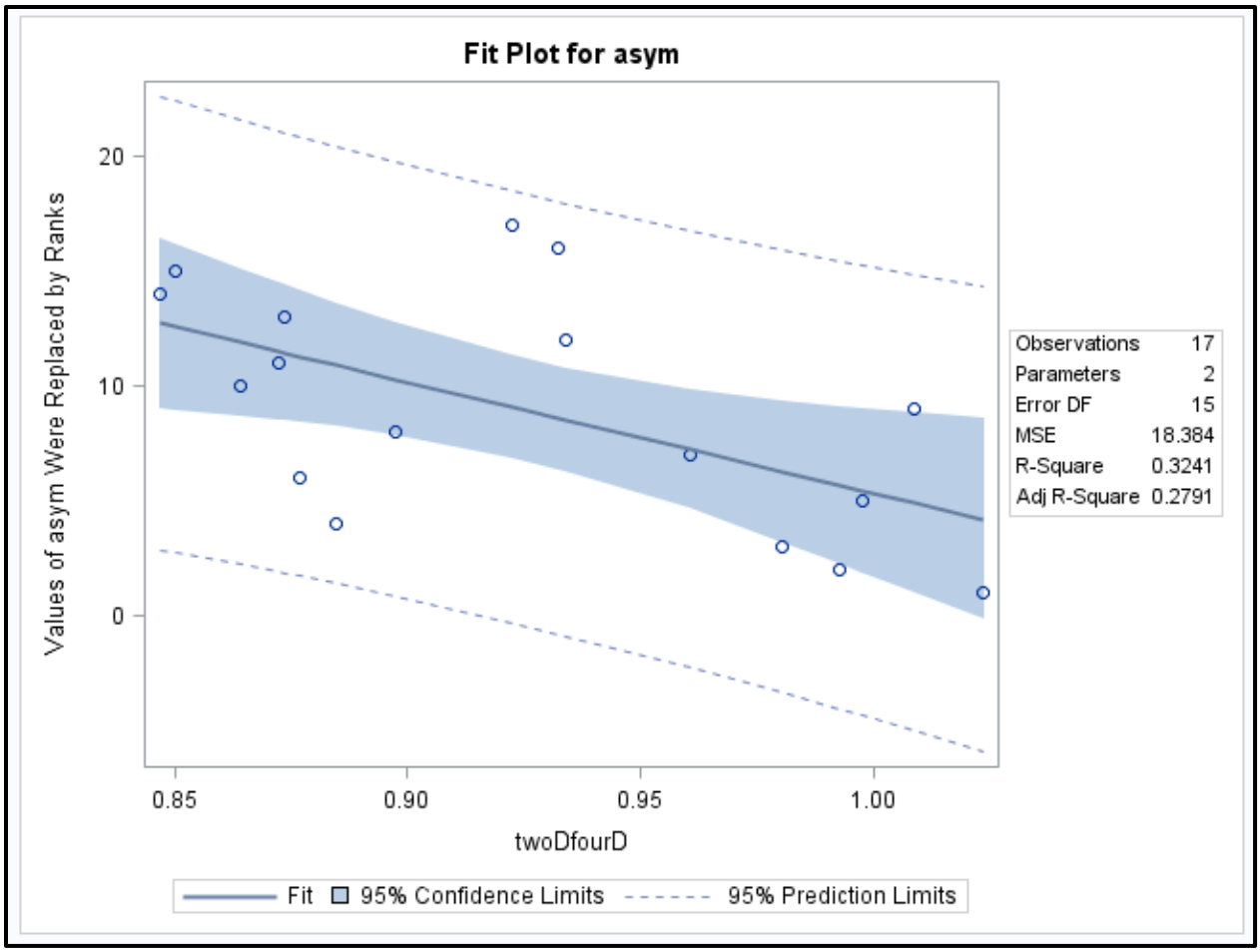

Figure 7. Regression of ranked asymmetry values on 2D:4D ratios showing regression line and 95% confidence limits (dashed) with regression results connected in SAS©.

The non-parametric correlations of mating system ("mating") and body weight ("dimorph") and canine teeth dimorphism ("canine") showed significant correlations of body weight dimorphism with asymmetry ("asym") but not 2D:4D ("twoDfourD") ratio. There was a significant correlation between mating systems and canine dimorphism.

Spearman Correlation Coefficients Prob > |r| under H0: Rho=0 Number of Observations					
	asym	twoDfourD	mating	dimorph	canine
asym	1.00000 17	-0.57353 0.0161 17	0.17988 0.4897 17	-0.48921 0.0463 17	-0.46552 0.0934 14
twoDfourD	-0.57353 0.0161 17	1.00000 17	-0.16337 0.5310 17	0.24831 0.3366 17	0.11360 0.6990 14
mating	0.17988 0.4897 17	-0.16337 0.5310 17	1.00000 17	0.42421 0.0897 17	0.64603 0.0126 14
dimorph	-0.48921 0.0463 17	0.24831 0.3366 17	0.42421 0.0897 17	1.00000 17	0.67946 0.0075 14
canine	-0.46552 0.0934 14	0.11360 0.6990 14	0.64603 0.0126 14	0.67946 0.0075 14	1.00000 14

Table 6. Spearman rank correlation coefficients, significance levels, and sample sizes for ranked asymmetry, 2D:4D ratio, mating system scale (mating), degree of body size dimorphism (dimorph), and canine dimorphism (canine).

Discussion and Limitations

Discussion

This data set shows a significant relationship between the 2D:4D ratio and the asymmetry measures within the individuals studied, where the 2D:4D ratio was found to be a significant driver of cranial asymmetry, independent of species or mating system (see Figure 7). This is particularly interesting in regard to the monogamous species included in this sample, as low competition environments typically lead to minimal prenatal androgen effects (Nelson and Shultz 2010). However, only two specimens included in this study were from typically monogamous species, and a much larger sample size is needed to make any further conclusions. Higher competition environments lead to greater asymmetry, indicating greater stress in the environment (Nelson and Shultz 2010), but it is also significant to note that these prenatal androgen effects also confer benefits to individuals, potentially selecting for increased asymmetry (Howlett 2019). It is notable that Klingenberg (2019) indicated genetic and environmental perturbations alone did not result in a perfectly linear relationship that outputs the observed phenotype of individuals. Some of this selection for increased asymmetry may explain the complex relationship between asymmetry and stress.

There was no significant difference found in either the 2D:4D ratio or the asymmetry of the skull between male, female, and unknown individuals. It is possible that sex-based differences would emerge from a larger sample size, especially given the differences in the importance of prenatal androgens between males and females, particularly testosterone. However, this data set is consistent with the species-by-species trends outlined in Nelson and Shultz (2010), where only a near-significant trend was found in differences in 2D:4D ratios between males and females of polygynous or polygynandrous species and no differences were

found between monogamous males and females. Future work is needed to determine the effect of sex on asymmetry in both polygynous and polygynandrous mating systems and monogamous mating systems. It is possible that the high association between males and females of the same species experiencing similar competition and aggression reduces the sex difference found in their measurements and merits a closer investigation of both within-species and between species measurements. Similarly, prenatal androgens have been found to confer the same benefits to both males and females (Howlett 2019). Comparison between the growth rates of males and females of each species merits further investigation as well, as an increased length of time for development allows more time for perturbations to affect development and may be another factor influencing sex differences beyond the levels of prenatal androgen effects (Hallgrímsson 1998).

It is difficult to assess the competitive stress a primate experiences in regard to the expression of appropriate sex-linked behaviors, as the actual reproductive success and ranks of these individuals within their groups is unknown (Howlett 2019). With greater information regarding relatedness, rank, and reproductive success within an individual's life history, it may be possible to investigate the mechanisms of fluctuating asymmetry across the whole body to a much greater degree than is currently possible. This would provide significant insight about species with highly competitive polygynandrous mating systems, where males and females may sustain different levels and types of asymmetries across their whole body as a result of their rank and stage of development within the larger context of a group. Similarly, specimens used in this study are of relatively unknown origin, and those of the same species were collected at differing times and location from one another. As such, we have a limited understanding of the influence of life-history strategies and patterns on fluctuating asymmetry. Studying individuals from the same groups or regions may prove useful in investigating the efficacy of different buffering

strategies within and between species. The nature of environmental perturbations, in terms of frequency and severity, ranges broadly between sites, groups, and species. The nature of perturbations may remain similar between different individuals but may impact symmetry in significantly different ways depending on rank and stage of development. Primates of all ranks experience resource-related stress, but those of higher rank sustain greater access to resources even in times of general group stress and can continue devoting more energy to maintaining symmetry. The timing of perturbations can also be impactful, affecting individuals differently depending on their age, such as juveniles having more supported buffering strategies due to their more established development than infants.

It is clear that there is a strong and statistically significant relationship between the 2D:4D ratio, fluctuating asymmetry, and stress across the whole body of an individual. However, many questions remain as some of these results are different to previous studies that compared values between species. Possible differences between males and females within the same species could not be addressed in this study due to the small sample size, and the distribution of species of different mating systems was uneven. Of particular note here is the importance of the mating systems with low mating competition seen in monogamous primates like marmosets and tamarins. Future studies would benefit from the inclusion of a higher representation of these monogamous species to better assess the impact of mating systems on fluctuating asymmetry. It may also prove beneficial to gather specimens of each sex, which would allow for a more detailed analysis of sex differences within and between species.

Limitations

The most significant limitation of this study is the specimens available and intact enough to investigate both morphological measures within the same individual. Most of the specimens

from the comparative collection are primates from typically polygynous or polygynandrous social structures. Only two specimens, *Callimico goeldii* and *Hylobates syndactylus*, out of seventeen total specimens were from typically monogamous social structures. These differences are very significant in regard to stress, competition, sexual selection, and aggression, as individuals in polygynandrous environments experience significantly greater stressors than monogamous individuals (Nelson and Shultz 2010). Given the prevalence of macaques in the University of Oregon's Comparative Primate Collection, specimens with the proper elements and intactness of monogamous social structures were limited. Future work expanding the proportion of monogamous species is vital to attaining a fuller view of symmetry and the effects of stress on the development of the whole body.

The utilization of a more robust sample size, with ample representation from monogamous, polygynous, or polygynandrous species, may also prove useful for statistical analysis, as analyses of symmetry in the body are often dependent on large sample sizes (Graham et al. 2010). The greatest limitation of small sample sizes is that there may be insufficient samples to show statistical significance. Statistical significance relies on the chance that a variable measured on one specimen is different to that measured on a different specimen, and as such, a large enough sample is needed to gain sufficient variation. Very small sample sizes may have insufficient variation for statistical tests to show significant differences. Although this is a possible limitation, it does not appear to impact this study as, even though it was not possible to increase the sample size in this study, the particular statistical methods utilized for analysis (Procrustes superimpositions and multivariate regressions) typically perform quite well with reduced sample sizes (Klingenberg 2016) and in this case showed significant effects. While a greater sample size may prove overall useful for comparing within-individual symmetry to

different scales of symmetry, such as the population or species-wide level, a larger sample size is not absolutely necessary given the methods utilized in this study. However, the reduced sample size does not allow for further separation and investigation of the specimens into categories of interest, such as by the mating systems outlined above.

Specimen collection for investigating symmetry in phalanges and skulls is challenging in most collections. Few collections keep phalanges sorted during processing or after disarticulation, which makes assigning each phalange to its digits challenging and time consuming. Given the need in this project for correct ordering of digits, especially the second and fourth digits which are most morphologically similar, the lack of initial curation for digit orders during processing remains a significant setback. Similarly, only specimens with present and assignable epiphyses were utilized in this study, as total phalangeal length was necessary on each specimen for consistent measurements to be made across all available specimens. Many specimens from the collection were excluded from this sample due to missing epiphyses.

Three specimens of unknown sex were included in the final sample, *Callimico goeldii*, *Hylobates syndactylus*, and *Cacajao calvus rubicundus.* In the case of *Cacajao calvus rubicundus*, very little is known about the species (Robinson et al. 1987). While *Cacajao calvus* are expected to be sexually dimorphic due to their polygynous social structure, the extent of the dimorphism remains unclear, making sex identification challenging on skeletal remains (Robinson et al. 1987). *Callimico goeldii* and *Hylobates syndactylus* are monogamous and have minimal sexual dimorphism, as is typical of primates from monogamous social structures (Nelson and Shultz 2010). In the case of these particular specimens, it was not possible to sex these individuals.

Beyond issues with the specimens sampled, studying bilateral symmetry is, by nature, limited. Analyses of symmetry in the body are easier on organisms with more repeated, modular forms, such as plants, as symmetry measures can be taken across many individual leaves (Graham et al. 2010). In primates, symmetry is limited to traits occurring on either side of the body. To ensure accuracy, each skull was landmarked repeatedly, across as many bilaterally occurring traits as possible for each specimen, as outlined in previous studies (Frost et al. 2003; Tallman et al. 2014). In future analyses, continuous line measures would likely improve accuracy in association with bilateral landmarks as well (Tallman et al. 2014). Overall, investigating the subtleties of fluctuating asymmetry is challenging even with an ideal collection from which to develop a substantial sample of specimens.

References

Frost, S. R., L. F. Marcus, F. L. Bookstein, D. P. Reddy, and E. Delson. 2003. “Cranial allometry, phylogeography, and systematics of large-bodied papionins (primates: Cercopithecinae) inferred from geometric morphometric analysis of landmark data.” *The Anatomical Record Part A: Discoveries in Molecular, Cellular, and Evolutionary Biology: An Official Publication of the American Association of Anatomists* 275, no. 2: 1048-1072.

Graham, J. H., S. Raz, H. Hel-Or, E. Nevo. 2010. "Fluctuating asymmetry: methods, theory, and applications." *Symmetry* 2, no. 2: 466-540.

Hallgrímsson, Benedikt. 1998. “Fluctuating asymmetry in the mammalian skeleton: evolutionary and developmental implications.” *Evolutionary Biology* 30: 187-251

Hallgrímsson, B., K. Willmore, and B. K. Hall. "Canalization, developmental stability, and morphological integration in primate limbs." *American Journal of Physical Anthropology: The Official Publication of the American Association of Physical Anthropologists* 119, no. S35: 131-158.

Howlett, C. 2019. *The Expression of the 2D:4D ratio across the Order Primates.* University of Kent.

Klingenberg, C. P., M. Barluenga, and A. Meyer. 2002. "Shape analysis of symmetric structures: quantifying variation among individuals and asymmetry." *Evolution* 56, no.10: 1909-1920.

Klingenberg, C.P. 2011. MorphoJ: an integrated software package for geometric morphometrics. *Molecular Ecology Resources* 11**:** 353-357.

Klingenberg, C. P. 2015. "Analyzing fluctuating asymmetry with geometric morphometrics: concepts, methods, and applications." *Symmetry* 7, no. 2: 843-934.

Klingenberg, C. P. 2016. "Size, shape, and form: concepts of allometry in geometric morphometrics." *Development Genes and Evolution* 226, no. 3: 113-137.

Klingenberg, C. P. 2019. "Phenotypic plasticity, developmental instability, and robustness: The concepts and how they are connected." *Frontiers in Ecology and Evolution* 7.

Little, A. C., B. C. Jones, C. Waitt, B. O. Tiddeman, D. R. Feinberg, D. I. Perrett, C. L. Apicella, and F. W. Marlowe. 2008. "Symmetry is related to sexual dimorphism in faces: data across culture and species." *PloS One* 3, no. 5.

Manning, J. T. 2002. *Digit ratio: A pointer to fertility, behavior, and health*. Rutgers University Press.

McGlothlin, J. W., J. M. Jawor, T. J. Greives, J. M. Casto, J. L. Phillips, and E. D. Ketterson. 2008. Hormones and honest signals: males with larger ornaments elevate testosterone more when challenged. *Journal of Evolutionary Biology* 21, no. 1: 39-48.

Nelson, E., C. L. Hoffman, M. S. Gerald, and S. Shultz. 2010. "Digit ratio (2D:4D) and dominance rank in female rhesus macaques (Macaca mulatta)." *Behavioral Ecology and Sociobiology* 64: 1001-1009.

Nelson, E., C. Rolian, L. Cashmore, and S. Shultz. 2011. "Digit ratios predict polygyny in early apes, Ardipithecus, Neanderthals and early modern humans but not in Australopithecus." *Proceedings of the Royal Society B: Biological Sciences* 278, no. 1711: 1556-1563.

Nelson, E., and S. Shultz. 2010. "Finger length ratios (2D:4D) in anthropoids implicate reduced prenatal androgens in social bonding." *American Journal of Physical Anthropology: The Official Publication of the American Association of Physical Anthropologists* 141, no. 3: 395-405.

Plavcan, J. M. 2004. "Sexual selection, measures of sexual selection, and sexual dimorphism in primates." In *Sexual Selection in Primates: New and Comparative Perspectives*. Kappeler, Peter M., and Carel P. Van Schaik, eds. Cambridge University Press.

Rowe, N., and M. Myers. 2016. *All the World's Primates*. Vol. 777. Charlestown: Pogonias Press.

RStudio Team. 2020. *RStudio: Integrated Development for R*. RStudio, PBC, Boston, MA.

SAS©. 2013. *Statistical Analysis Software*. Users' Guide Statistics Version 9.4. SAS Institute Inc., Cary.

Sokal, R. R., and F.J. Rohlf. 1995. *Biometry*. Macmillan.

Tallman, M., N. Amenta, E. Delson, S. R. Frost, D. Ghosh, Z. S. Klukkert, A. Morrow, and G. J. Sawyer. 2014. “Evaluation of a new method of fossil retrodeformation by algorithmic symmetrization: crania of papionins (Primates, Cercopithecidae) as a test case.” *PloS One* 9, no. 7.

Wang, Qian. 2012. "Dental maturity and the ontogeny of sex-based differences in the dentofacial complex of rhesus macaques from Cayo Santiago." *Bones, genetics, and behavior of rhesus macaques: Macaca mulatta of Cayo Santiago and Beyond*. Springer, 177-194.

Willmore, K. E., C. P. Klingenberg, and B. Hallgrímsson. "The relationship between fluctuating asymmetry and environmental variance in rhesus macaque skulls." *Evolution* 59, no. 4: 898-909.

Appendix 1: Complete 2D:4D Ratio Replicates

Proximal only	2D (mm)	4D (mm)
127-23107	19.61	19.63
Left Hand	19.59	19.79
	19.67	19.64
	19.60	19.62
	19.61	19.61

Proximal only	2D	4D
300-2512	21.79	24.65
Right Hand	21.85	24.71
	21.83	24.66
	21.84	24.69
	21.83	24.67

Proximal only	2D	4D
305-2412	19.94	22.82
Left Hand	19.93	22.80
	19.91	22.79
	19.90	22.81
	19.94	22.79

Proximal only	2D	4D
305-2413	20.67	21.50
Right Hand	20.66	21.52
	20.66	21.50
	20.68	21.50
	20.65	21.53

Proximal only	2D	4D
305-10004	14.33	16.82
Right Hand	14.29	16.81
	14.26	16.83
	14.31	16.81
	14.29	16.80

Proximal only	2D	4D
195-7613	15.84	16.16
Right Hand	15.87	16.2
	15.85	16.17
	15.84	16.15
	15.87	16.16

Proximal only	2D	4D
244-2415	47.95	47.53
Left hand	47.99	47.57
	47.98	47.51
	47.95	47.56
	47.95	47.51

Proximal only	2D	4D
305-10433	23.82	22.98
Left Hand	23.82	22.95
	23.84	22.99
	23.87	22.98
	23.82	22.95

Proximal only	2D	4D
342-2392	19.20	19.14
Left Hand	19.16	19.17
	19.14	19.13
	19.01	19.18
	19.18	19.17

Proximal only	2D	4D
300-673	27.38	26.76
Right Hand	27.46	26.75
	27.4	26.74
	27.35	26.78
	27.37	26.76

Proximal only	2D	4D
137-2112	24.03	25.73
Right Hand	24.00	25.78
	24.02	25.76
	24.08	25.79
	24.01	25.80

Proximal only	2D	4D
170-2414	22.52	26.03
Right Hand	22.49	26.05
	22.51	26.05
	22.47	26.06
	22.58	26.08

Proximal only	2D	4D
195-7337	17.20	19.66
Left Hand	17.2	19.69
	17.29	19.66
	17.38	19.71
	17.19	19.67

Proximal only	2D	4D
079-3924	10.67	11.93
Right Hand	10.66	11.93
	10.67	11.91
	10.72	11.87
	10.69	11.87

Proximal only	2D	4D
291-06069	19.08	20.69
Right Hand	19.02	20.54
	19.01	20.67
	19.04	20.65
	19.04	20.65

Proximal only	2D	4D
343-6000	12.15	13.95
Right Hand	12.12	13.94
	12.17	13.91
	12.15	13.91
	12.13	13.89

Proximal only	2D	4D
127-1791	13.16	15.58
Left Hand	13.13	15.51
	13.18	15.54
	13.18	15.49
	13.14	15.57

Appendix 2: Sorted Disarticulated Phalanges

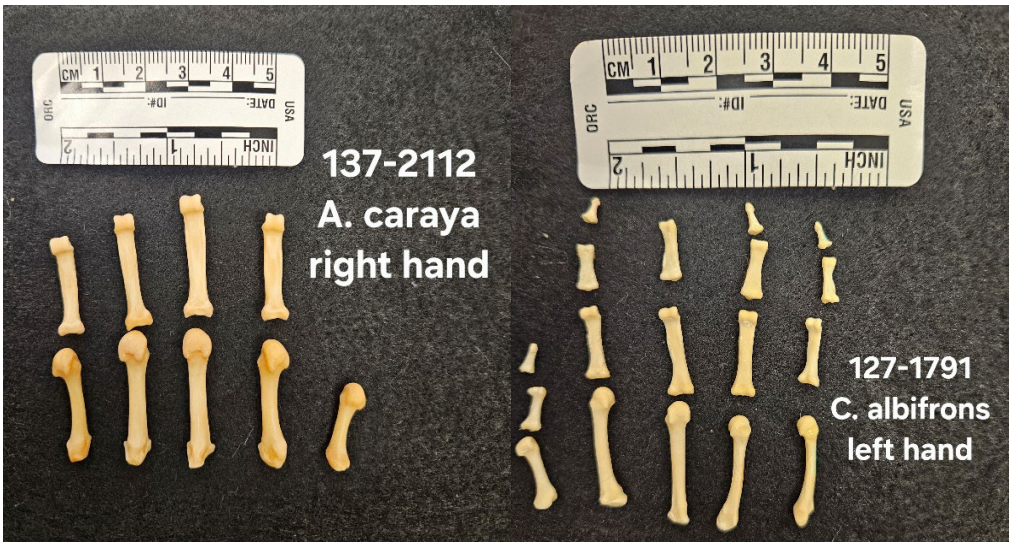


305-2413
M. mulatta
right hand
291-06069
M. fuscata
right hand

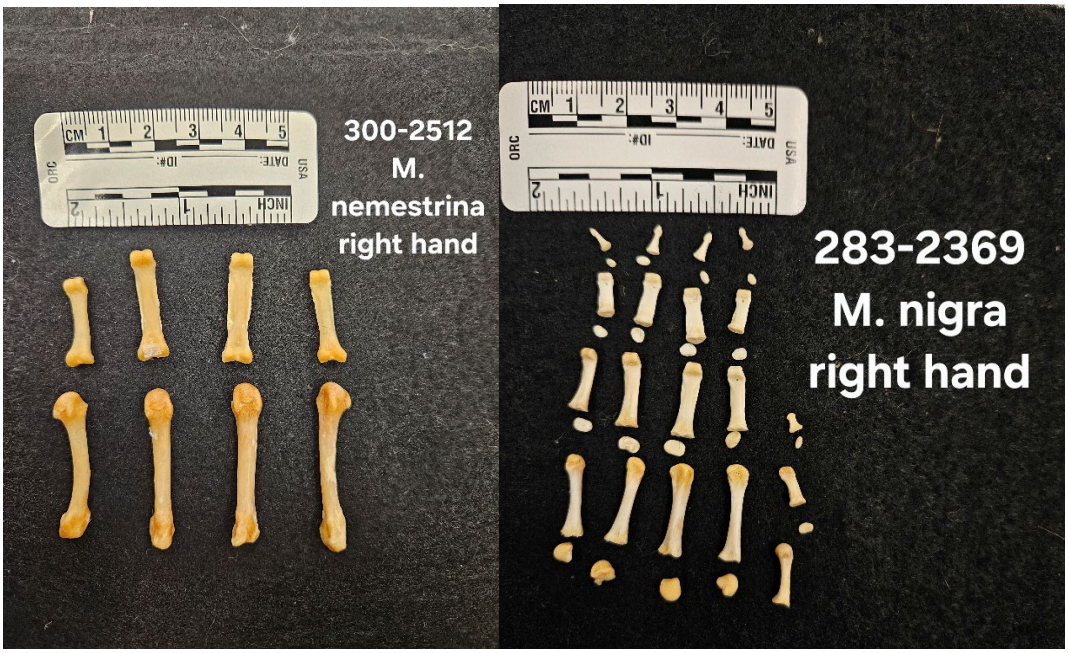
300-2512
M.
nemestrina
right hand
283-2369
M. nigra
right hand


195-7337
M.
fascicularis
left hand
170-2414
C. rubicundus
right hand

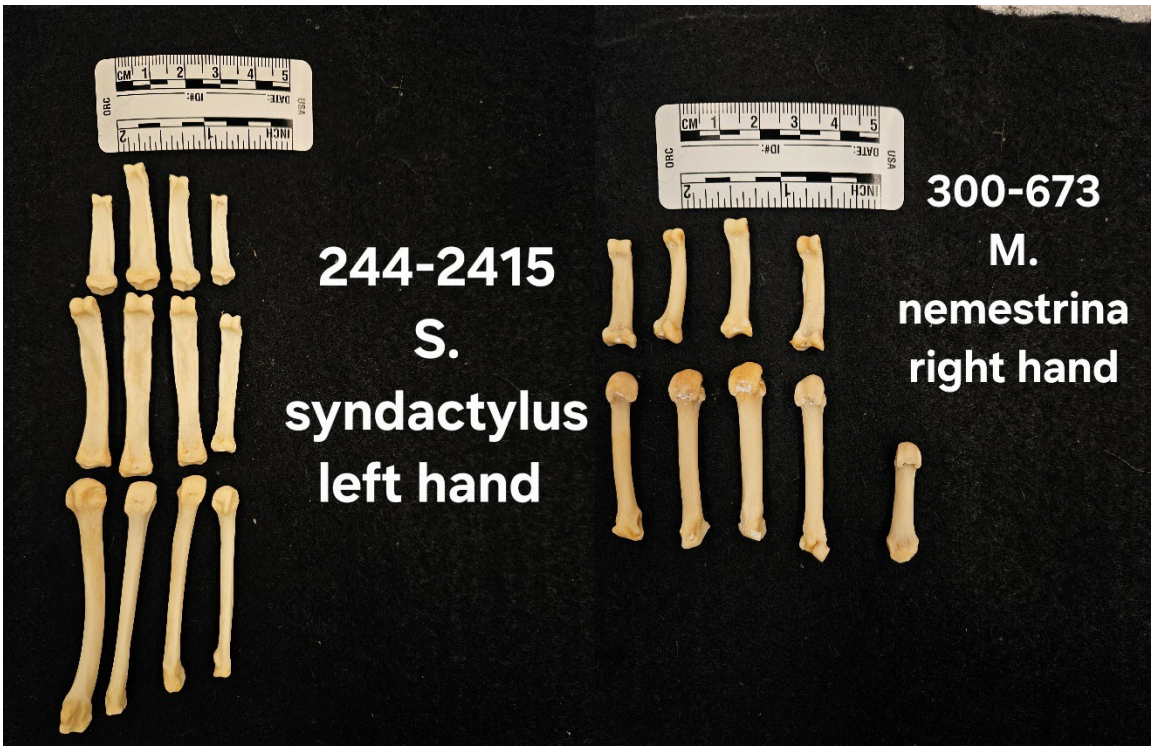
244-2415
S.
syndactylus
left hand
300-673
M.
nemestrina
right hand


305-2412
M. mulatta
left hand
305-10004
M. mulatta
right hand


343-6000
M. talapoin
right hand
305-10433
M. mulatta
right hand


127-23107
C. albifrons
left hand

Appendix 3: Complete Microscribe data for replicate asymmetry measures

342-2392 Scan 1

Landmark	X	Y	Z
Inion			
Bregma			
Glabella	282.2487	-142.7003	78.6332
Nasion	290.4669	-138.2438	66.9827
Rhinion	303.2034	-118.6501	55.4566
Nasospinale	310.4164	-112.91	50.7075
Prosthion	317.169	-104.7901	45.7185
R Prosthion-2	320.1474	-114.6877	44.0817
R Premax-max superior	297.0905	-136.6754	63.1824
R Zygo-max inferior	311.9135	-158.4803	37.7053
R Zygo-max superior	303.2357	-150	60.9046
R Dacryon	290.3534	-143.5988	65.1218
R Mid-torus inferior	291.1676	-146.56	74.3407
R Mid-torus superior	293.0108	-158.0279	82.3007
R Fronto-malare orbitale	305.1656	-159.5659	69.2735
R Fronto-malare temporale	304.0674	-170.3754	67.8479
R Porion	289.0441	-199.7933	34.9629
R Zygo-temp superior	314.8225	-177.2312	46.9994
R Zygo-temp inferior	311.4957	-185.4388	39.1087
L Prosthion-2	305.29	-103.0184	41.2362
L Premax-max superior	290.6169	-132.2628	60.1149
L Zygo-max inferior	271.0344	-127.483	30.2097
L Zygo-max superior	281.0457	-132.66	58.3452
L Dacryon	286.7959	-142.3379	65.4658
L Mid-torus inferior	278.1674	-137.5811	71.9308
L Mid-torus superior	270.9213	-137.1293	81.3539
L Fronto-malare orbitale	264.2506	-131.6552	63.6392
L Fronto-malare temporale	254.4597	-136.6347	60.5145
L Porion	240.004	-168.7456	29.4936
L Zygo-temp superior	248.1304	-135.1766	35.7834
L Zygo-temp inferior	244.9878	-142.6439	29.6105

342-2392 Scan 2

Landmark	X	Y	Z
Inion			
Bregma			
Glabella	287.8013	-142.3042	77.0088
Nasion	292.0873	-136.9865	66.6747
Rhinion	306.2051	-119.0377	55.1731
Nasospinale	312.1266	-110.7021	50.1753
Prosthion	316.6282	-101.9376	44.9489
R Prosthion-2	316.7255	-108.5254	45.9308
R Premax-max superior	296.4961	-131.663	62.3719
R Zygo-max inferior	316.6266	-155.8286	35.7411
R Zygo-max superior	306.7353	-143.9622	60.4724
R Dacryon	294.7661	-144.388	63.461
R Mid-torus inferior	297.3013	-147.4978	74.353
R Mid-torus superior	298.4714	-151.5626	83.52
R Fronto-malare orbitale	310.2175	-158.1169	67.982
R Fronto-malare temporale	311.2869	-168.7497	67.8249
R Porion	297.1554	-199.9152	34.2337
R Zygo-temp superior	322.2403	-174.8595	46.7361
R Zygo-temp inferior	318.6811	-184.496	38.1297
L Prosthion-2	312.4437	-104.2201	45.0661
L Premax-max superior	296.7043	-133.9076	65.4038
L Zygo-max inferior	274.2448	-128.2858	31.3787
L Zygo-max superior	278.2807	-132.9242	55.3114
L Dacryon	290.1321	-142.4362	64.1239
L Mid-torus inferior	282.6589	-138.9052	72.7145
L Mid-torus superior	270.507	-142.868	78.3073
L Fronto-malare orbitale	268.0117	-133.3171	63.3537
L Fronto-malare temporale	257.7519	-140.1466	61.6056
L Porion	245.3345	-173.0394	30.0323
L Zygo-temp superior	250.7921	-137.3368	36.6011
L Zygo-temp inferior	246.7211	-145.842	29.742

342-2392 Scan 3

Landmark	X	Y	Z
Inion			
Bregma			
Glabella	280.6637	-137.3811	78.1886
Nasion	284.9771	-130.8963	66.7247
Rhinion	301.1377	-114.4966	54.8275
Nasospinale	307.1966	-108.3397	50.0381
Prosthion	308.9294	-105.358	43.2818
R Prosthion-2	316.6451	-110.0104	43.4201
R Premax-max superior	293.1466	-133.5676	61.9406
R Zygo-max inferior	309.5261	-149.4172	36.3889
R Zygo-max superior	300.9485	-141.5807	60.8694
R Dacryon	287.0932	-139.4934	63.3121
R Mid-torus inferior	289.991	-142.5549	73.9926
R Mid-torus superior	291.501	-146.6397	83.7137
R Fronto-malare orbitale	302.2637	-153.5536	68.0638
R Fronto-malare temporale	302.5439	-165.0496	68.9031
R Porion	285.66	-196.2637	36.4922
R Zygo-temp superior	309.0052	-172.8929	46.4232
R Zygo-temp inferior	308.7799	-181.4054	37.8669
L Prosthion-2	301.8785	-97.4768	40.0836
L Premax-max superior	286.8538	-127.6032	59.6176
L Zygo-max inferior	267.3353	-121.456	31.8543
L Zygo-max superior	271.5766	-126.4085	55.9935
L Dacryon	283.4499	-137.0813	63.841
L Mid-torus inferior	275.6038	-132.1892	71.8343
L Mid-torus superior	268.2903	-131.8764	81.7725
L Fronto-malare orbitale	262.0613	-126.9159	63.5877
L Fronto-malare temporale	251.0681	-132.2336	61.5072
L Porion	236.9448	-164.4908	29.8191
L Zygo-temp superior	244.6045	-130.5945	36.5108
L Zygo-temp inferior	241.1943	-138.4349	30.8382

342-2392 Scan 4

Landmark	X	Y	Z
Inion			
Bregma			
Glabella	280.6282	-135.859	77.2433
Nasion	284.2347	-131.349	66.672
Rhinion	300.1883	-113.0699	54.7195
Nasospinale	306.8365	-106.6257	50.0177
Prosthion	313.6502	-100.4933	44.4871
R Prosthion-2	316.1149	-109.6378	43.3625
R Premax-max superior	293.1487	-126.1715	62.9448
R Zygo-max inferior	309.0379	-150.0437	35.5849
R Zygo-max superior	299.2231	-138.7946	59.7957
R Dacryon	286.953	-138.3199	64.207
R Mid-torus inferior	289.4642	-141.4037	73.5587
R Mid-torus superior	290.5718	-145.6257	82.9821
R Fronto-malare orbitale	301.9436	-152.9905	66.7869
R Fronto-malare temporale	302.0837	-164.0442	67.8636
R Porion	285.3544	-195.1898	35.5692
R Zygo-temp superior	311.4458	-165.6184	46.5191
R Zygo-temp inferior	307.0045	-180.438	36.9043
L Prosthion-2	301.0993	-98.9313	40.927
L Premax-max superior	286.6839	-127.5986	58.9782
L Zygo-max inferior	266.9099	-119.7498	32.359
L Zygo-max superior	275.7014	-123.4272	56.7003
L Dacryon	282.8486	-136.7676	64.7794
L Mid-torus inferior	275.4275	-131.4708	71.7512
L Mid-torus superior	268.4318	-130.6583	80.9828
L Fronto-malare orbitale	261.6246	-125.3455	63.3052
L Fronto-malare temporale	250.5865	-131.2825	61.0396
L Porion	236.5051	-163.3039	30.0245
L Zygo-temp superior	245.474	-127.5445	36.4679
L Zygo-temp inferior	239.7863	-136.3887	28.8869

342-2392 Scan 5

Landmark	X	Y	Z
Inion			
Bregma			
Glabella	280.1016	-136.4814	77.0432
Nasion	284.9628	-131.448	66.3746
Rhinion	299.6466	-113.0891	54.4226
Nasospinale	307.4033	-105.9663	49.6693
Prosthion	313.9098	-99.3585	44.782
R Prosthion-2	316.5013	-109.8777	43.2357
R Premax-max superior	291.4632	-133.7594	60.7169
R Zygo-max inferior	308.8156	-149.7685	35.2015
R Zygo-max superior	300.0519	-139.421	59.7986
R Dacryon	287.0004	-138.7162	63.3422
R Mid-torus inferior	289.4925	-141.8351	73.0582
R Mid-torus superior	291.1408	-146.3934	83.1072
R Fronto-malare orbitale	301.5341	-153.6862	66.7807
R Fronto-malare temporale	301.4048	-164.7451	67.362
R Porion	284.7377	-195.6534	35.2652
R Zygo-temp superior	312.3736	-170.3331	45.8245
R Zygo-temp inferior	307.5983	-179.8483	37.4939
L Prosthion-2	302.0537	-98.0384	40.1644
L Premax-max superior	284.8679	-126.4026	59.7484
L Zygo-max inferior	267.7802	-121.9064	30.8825
L Zygo-max superior	278.3275	-125.3354	57.2284
L Dacryon	282.9652	-136.4933	63.1841
L Mid-torus inferior	275.1734	-131.715	71.6163
L Mid-torus superior	268.9103	-130.7132	80.6444
L Fronto-malare orbitale	261.4731	-126.4535	63.4266
L Fronto-malare temporale	250.7908	-131.0941	61.8955
L Porion	236.4296	-162.9831	30.0063
L Zygo-temp superior	244.7755	-128.8571	35.7505
L Zygo-temp inferior	239.0776	-137.0917	28.687

343-6000 Scan 1

Landmark	X	Y	Z
Inion	299.8026	-98.3425	25.1858
Bregma	305.4713	-75.7642	44.6002
Glabella	316.7414	-45.7664	36.9797
Nasion	317.5253	-42.1337	30.6081
Rhinion	319.4681	-37.361	25.6899
Nasospinale	320.6223	-34.3334	16.4174
Prosthion	322.3082	-32.711	12.2911
R Prosthion-2	325.2775	-34.7536	12.9419
R Premax-max superior	318.9263	-42.4182	30.121
R Zygo-max inferior	330.8268	-54.1297	13.8894
R Zygo-max superior	329.5409	-48.2792	22.5752
R Dacryon	319.2528	-45.9161	30.0548
R Mid-torus inferior	326.2659	-54.743	37.1409
R Mid-torus superior	325.3627	-56.3098	38.9905
R Fronto-malare orbitale	333.6972	-55.8456	28.2722
R Fronto-malare temporale	334.1948	-60.1963	29.3738
R Porion	327.7643	-81.4697	13.1583
R Zygo-temp superior	334.2091	-62.6608	13.5673
R Zygo-temp inferior	333.6205	-66.6943	11.3802
L Prosthion-2	318.0268	-31.5928	12.3502
L Premax-max superior	317.829	-41.4692	30.369
L Zygo-max inferior	299.0937	-44.8358	13.1686
L Zygo-max superior	305.5459	-40.6523	22.7501
L Dacryon	315.321	-45.8616	30.8428
L Mid-torus inferior	304.667	-47.2929	37.8871
L Mid-torus superior	303.6093	-48.884	39.5278
L Fronto-malare orbitale	298.703	-44.3494	28.7494
L Fronto-malare temporale	294.9648	-46.2187	29.3778
L Porion	287.0439	-67.8376	12.8479
L Zygo-temp superior	294.3531	-48.2718	13.7791
L Zygo-temp inferior	290.8779	-53.1149	11.7518

343-6000 Scan 2

Landmark	X	Y	Z
Inion	295.3644	-100.8121	22.4097
Bregma	301.7346	-77.7113	41.4413
Glabella	313.3993	-48.4538	33.3427
Nasion	313.906	-46.8637	30.6019
Rhinion	316.0822	-40.1946	21.3763
Nasospinale	316.5414	-37.1184	11.9224
Prosthion	317.627	-35.7297	7.045
R Prosthion-2	320.9718	-37.9966	7.5147
R Premax-max superior	315.0582	-44.0661	24.8105
R Zygo-max inferior	326.9383	-56.8415	8.7233
R Zygo-max superior	324.8971	-50.1442	17.3231
R Dacryon	314.8444	-48.1359	25.701
R Mid-torus inferior	322.9059	-55.8471	32.7843
R Mid-torus superior	321.8655	-57.3183	34.3664
R Fronto-malare orbitale	329.6249	-57.8926	23.4906
R Fronto-malare temporale	329.9171	-61.6118	24.4726
R Porion	322.542	-84.3441	9.6019
R Zygo-temp superior	329.5608	-64.4616	8.8697
R Zygo-temp inferior	329.0506	-69.2024	7.4264
L Prosthion-2	313.6146	-35.0343	6.9835
L Premax-max superior	313.7682	-43.1417	25.9034
L Zygo-max inferior	296.7717	-47.3727	9.6734
L Zygo-max superior	300.7813	-41.8526	17.8578
L Dacryon	311.5552	-46.5311	25.8319
L Mid-torus inferior	299.6992	-48.3695	33.5017
L Mid-torus superior	298.9547	-49.9275	35.5655
L Fronto-malare orbitale	294.2553	-46.2484	25.0407
L Fronto-malare temporale	291.0983	-47.9632	26.0769
L Porion	282.5022	-70.0734	10.8549
L Zygo-temp superior	289.8951	-50.4377	10.4437
L Zygo-temp inferior	286.376	-54.4065	9.041

343-6000 Scan 3

Landmark	X	Y	Z
Inion	145.5288	-271.1885	19.9613
Bregma	168.695	-260.1312	41.4829
Glabella	196.1079	-247.7619	30.9927
Nasion	197.7024	-247.4004	28.0762
Rhinion	203.1711	-244.8561	19.6795
Nasospinale	205.8663	-242.999	8.7297
Prosthion	206.6079	-243.2907	3.9273
R Prosthion-2	207.5206	-247.0419	4.3562
R Premax-max superior	200.0082	-246.9277	23.2349
R Zygo-max inferior	198.6985	-264.6272	7.7634
R Zygo-max superior	202.9204	-258.416	15.3334
R Dacryon	197.4592	-248.9335	24.0282
R Mid-torus inferior	196.4498	-256.2846	31.4947
R Mid-torus superior	196.6602	-260.0223	32.6595
R Fronto-malare orbitale	200.4484	-266.7859	23.0211
R Fronto-malare temporale	199.2745	-269.1348	23.6537
R Porion	176.6496	-280.505	10.5198
R Zygo-temp superior	194.1471	-272.0964	8.0654
R Zygo-temp inferior	191.5055	-274.3341	6.8435
L Prosthion-2	204.7777	-240.2203	4.2375
L Premax-max superior	199.7876	-246.2017	23.8691
L Zygo-max inferior	184.4471	-236.5332	7.7221
L Zygo-max superior	191.74	-236.0352	15.2599
L Dacryon	196.2637	-245.7666	23.7027
L Mid-torus inferior	189.7941	-242.4099	31.3847
L Mid-torus superior	187.0967	-238.3004	32.9193
L Fronto-malare orbitale	184.3135	-232.6304	22.6358
L Fronto-malare temporale	181.0211	-232.1638	23.5554
L Porion	158.1215	-242.4621	10.6798
L Zygo-temp superior	177.4927	-233.7267	8.2427
L Zygo-temp inferior	171.8026	-234.7338	6.7603

343-6000 Scan 4

Landmark	X	Y	Z
Inion	237.1208	-183.1796	23.0222
Bregma	248.789	-162.6108	41.5868
Glabella	267.1008	-137.7353	33.4398
Nasion	268.1248	-136.0925	30.4118
Rhinion	271.9519	-130.2681	21.0943
Nasospinale	273.6601	-127.2703	11.5697
Prosthion	274.8557	-126.5127	7.0699
R Prosthion-2	277.1354	-129.5325	7.4939
R Premax-max superior	269.916	-134.1545	25.5045
R Zygo-max inferior	277.8151	-149.3066	9.4754
R Zygo-max superior	278.1137	-142.6049	17.895
R Dacryon	268.8439	-137.8956	25.9775
R Mid-torus inferior	273.9078	-147.3369	33.7581
R Mid-torus superior	272.7913	-148.3843	34.9792
R Fronto-malare orbitale	280.1075	-151.4142	24.4094
R Fronto-malare temporale	280.1425	-154.4073	25.4368
R Porion	267.5894	-174.6708	10.1448
R Zygo-temp superior	278.9491	-157.6842	9.4243
R Zygo-temp inferior	276.822	-161.9812	7.5609
L Prosthion-2	270.6254	-124.921	7.2321
L Premax-max superior	268.7017	-133.2905	26.2762
L Zygo-max inferior	251.746	-132.1542	9.7918
L Zygo-max superior	256.7296	-128.4044	18.0617
L Dacryon	265.9287	-135.6124	25.9738
L Mid-torus inferior	253.4729	-134.8688	33.848
L Mid-torus superior	252.8878	-135.1447	35.2996
L Fronto-malare orbitale	249.3918	-130.9829	24.7174
L Fronto-malare temporale	246.4839	-131.6419	26.2775
L Porion	232.4984	-150.2471	10.677
L Zygo-temp superior	244.3522	-133.654	10.3374
L Zygo-temp inferior	240.1054	-136.888	8.6051

343-6000 Scan 5

Landmark	X	Y	Z
Inion	237.8138	-180.7117	24.228
Bregma	250.612	-160.369	41.976
Glabella	268.9227	-136.248	33.2932
Nasion	270.9432	-132.8972	26.3264
Rhinion	274.0119	-129.2289	20.8531
Nasospinale	275.8348	-126.6734	11.3173
Prosthion	277.5414	-126.1264	6.8829
R Prosthion-2	279.5965	-128.9194	7.0084
R Premax-max superior	272.0072	-133.2039	25.4679
R Zygo-max inferior	280.1054	-149.1565	9.3471
R Zygo-max superior	280.1209	-141.5127	17.4
R Dacryon	270.8181	-136.6957	25.5176
R Mid-torus inferior	275.8566	-146.1918	33.0121
R Mid-torus superior	275.397	-146.5483	34.3969
R Fronto-malare orbitale	282.1038	-150.1304	23.5494
R Fronto-malare temporale	282.4121	-153.4734	24.8758
R Porion	268.4455	-173.3619	10.561
R Zygo-temp superior	280.4011	-156.8663	9.292
R Zygo-temp inferior	278.5376	-160.9708	7.4028
L Prosthion-2	273.7759	-124.0342	6.9538
L Premax-max superior	271.241	-132.3938	25.6027
L Zygo-max inferior	254.0934	-130.7605	9.2808
L Zygo-max superior	259.9084	-127.1938	17.8059
L Dacryon	268.1423	-134.183	26.4893
L Mid-torus inferior	255.0641	-132.7347	33.6073
L Mid-torus superior	255.1847	-133.0001	34.9724
L Fronto-malare orbitale	251.4935	-128.6794	24.3654
L Fronto-malare temporale	248.5844	-129.1215	25.0577
L Porion	234.0708	-148.2676	10.4968
L Zygo-temp superior	246.3896	-131.799	9.5356
L Zygo-temp inferior	241.6017	-135.4773	8.244

195-7337 Scan 1

Landmark	X	Y	Z
Inion	126.3705	-281.3375	18.3934
Bregma	146.0431	-269.7569	49.5112
Glabella	184.1698	-251.2446	48.2422
Nasion	186.1831	-250.2694	42.02
Rhinion	201.1338	-244.1214	26.2397
Nasospinale	208.1214	-240.5824	13.9321
Prosthion	213.4087	-237.9837	9.6303
R Prosthion-2			
R Premax-max superior	191.34	-248.694	32.4714
R Zygo-max inferior	195.1985	-273.8586	11.4864
R Zygo-max superior	194.0088	-256.9707	27.7036
R Dacryon	186.396	-251.9131	36.8188
R Mid-torus inferior	186.1329	-257.1029	43.3722
R Mid-torus superior	188.4595	-262.2849	49.2312
R Fronto-malare orbitale	192.1035	-272.5304	36.5216
R Fronto-malare temporale	191.3565	-276.6985	35.6268
R Porion	159.662	-289.9785	11.4446
R Zygo-temp superior	192.3318	-281.0457	16.0985
R Zygo-temp inferior	183.488	-288.7847	12.2583
L Prosthion-2			
L Premax-max superior	190.8739	-247.5346	32.4632
L Zygo-max inferior	173.5883	-231.1907	9.9806
L Zygo-max superior	185.2048	-239.7177	26.8366
L Dacryon	184.952	-249.1956	36.9519
L Mid-torus inferior	180.921	-246.283	43.7762
L Mid-torus superior	176.7057	-240.6654	48.2971
L Fronto-malare orbitale	171.0247	-231.9489	35.461
L Fronto-malare temporale	167.2347	-230.356	33.5568
L Porion	137.9032	-248.002	11.2428
L Zygo-temp superior	166.0348	-227.9021	13.969
L Zygo-temp inferior	155.0961	-230.0891	10.887

195-7337 Scan 2

Landmark	X	Y	Z
Inion	125.4982	-275.089	20.0212
Bregma	148.0648	-265.7481	50.3235
Glabella	187.458	-251.1016	46.9754
Nasion	188.7056	-250.4295	41.3166
Rhinion	203.502	-244.5756	24.8238
Nasospinale	209.1773	-241.5021	11.6348
Prosthion	215.69	-239.1124	6.8306
R Prosthion-2			
R Premax-max superior	194.2506	-249.0097	31.1304
R Zygo-max inferior	194.3707	-272.9293	9.3728
R Zygo-max superior	195.1274	-257.0314	25.5693
R Dacryon	189.1135	-251.5168	35.8819
R Mid-torus inferior	188.4922	-257.3898	42.3073
R Mid-torus superior	190.085	-262.7444	47.3052
R Fronto-malare orbitale	192.5007	-272.5515	34.0507
R Fronto-malare temporale	191.2345	-276.3475	33.5022
R Porion	157.0846	-286.0437	10.8367
R Zygo-temp superior	190.1627	-280.2025	13.3995
R Zygo-temp inferior	181.1795	-286.2013	9.8502
L Prosthion-2			
L Premax-max superior	193.8627	-247.7319	31.3213
L Zygo-max inferior	176.9906	-228.5993	9.8352
L Zygo-max superior	188.5397	-238.4929	25.8417
L Dacryon	188.7999	-248.0544	35.4596
L Mid-torus inferior	184.4049	-245.4701	42.8352
L Mid-torus superior	181.1927	-239.401	48.0126
L Fronto-malare orbitale	175.2539	-230.4735	35.9371
L Fronto-malare temporale	171.9677	-228.3906	34.7378
L Porion	139.171	-242.5213	13.2325
L Zygo-temp superior	169.5304	-225.1907	14.9192
L Zygo-temp inferior	158.0884	-225.8755	12.3769

195-7337 Scan 3

Landmark	X	Y	Z
Inion	121.7734	-279.4716	19.7569
Bregma	142.0318	-267.553	48.5579
Glabella	182.3475	-253.1394	47.2409
Nasion	183.8511	-252.209	40.9228
Rhinion	198.6425	-246.9323	24.4892
Nasospinale	204.3196	-243.5472	11.6055
Prosthion	210.659	-240.9674	7.052
R Prosthion-2			
R Premax-max superior	188.8373	-250.8737	31.1554
R Zygo-max inferior	190.2599	-276.1331	9.5833
R Zygo-max superior	191.2084	-259.4472	25.7857
R Dacryon	184.5159	-253.5737	35.8516
R Mid-torus inferior	183.8628	-259.3345	42.3622
R Mid-torus superior	185.2016	-264.7468	47.0848
R Fronto-malare orbitale	188.587	-274.7101	34.8988
R Fronto-malare temporale	187.3628	-278.2713	33.6708
R Porion	153.7383	-289.926	10.2252
R Zygo-temp superior	187.0676	-283.2462	13.3123
R Zygo-temp inferior	177.5283	-289.4951	10.4027
L Prosthion-2			
L Premax-max superior	188.429	-250.2907	31.3309
L Zygo-max inferior	171.605	-232.4707	9.2221
L Zygo-max superior	183.6079	-241.7739	25.6867
L Dacryon	182.3552	-250.6229	36.4752
L Mid-torus inferior	178.6534	-248.1105	42.7619
L Mid-torus superior	175.295	-242.1692	47.4665
L Fronto-malare orbitale	169.5204	-233.3368	35.0858
L Fronto-malare temporale	166.0273	-231.1694	33.6379
L Porion	133.9224	-246.7788	12.9505
L Zygo-temp superior	164.1588	-228.3517	13.8313
L Zygo-temp inferior	152.7103	-229.81	11.4477

195-7337 Scan 4

Landmark	X	Y	Z
Inion	116.2447	-285.6457	16.5028
Bregma	134.395	-275.041	47.2464
Glabella	173.4462	-258.0643	49.1878
Nasion	175.4579	-257.0944	43.4433
Rhinion	191.1536	-250.8396	28.2417
Nasospinale	198.6649	-246.9051	16.0562
Prosthion	204.5485	-244.9182	10.8481
R Prosthion-2			
R Premax-max superior	181.3893	-255.6082	33.9477
R Zygo-max inferior	185.3097	-280.0034	12.5514
R Zygo-max superior	183.0919	-263.5905	28.6959
R Dacryon	176.0555	-258.6697	38.1533
R Mid-torus inferior	174.8801	-264.4632	44.3197
R Mid-torus superior	176.9764	-269.2372	50.082
R Fronto-malare orbitale	181.1745	-279.1642	37.0565
R Fronto-malare temporale	180.6266	-283.3693	36.4556
R Porion	148.8421	-296.0768	10.7404
R Zygo-temp superior	182.1751	-288.0928	15.8739
R Zygo-temp inferior	173.0583	-294.4436	12.1036
L Prosthion-2			
L Premax-max superior	181.1185	-254.2978	33.789
L Zygo-max inferior	165.68	-237.4667	11.1397
L Zygo-max superior	176.4318	-246.8367	28.5475
L Dacryon	174.4118	-255.2602	38.8339
L Mid-torus inferior	170.0531	-253.3355	44.7639
L Mid-torus superior	166.21	-247.2753	49.3205
L Fronto-malare orbitale	161.2833	-238.5897	36.4743
L Fronto-malare temporale	157.9429	-236.674	34.769
L Porion	128.1683	-252.5901	11.3434
L Zygo-temp superior	158.0443	-233.799	14.9821
L Zygo-temp inferior	146.64	-235.238	11.2564

195-7337 Scan 5

Landmark	X	Y	Z
Inion	117.6818	-282.5012	16.7232
Bregma	135.8426	-270.4102	47.7162
Glabella	175.9915	-255.127	47.6615
Nasion	177.5516	-254.6221	42.5349
Rhinion	194.1765	-249.4787	27.4657
Nasospinale	201.9218	-245.7781	15.042
Prosthion	205.9733	-243.1181	8.5328
R Prosthion-2			
R Premax-max superior	184.0467	-253.0472	33.1497
R Zygo-max inferior	186.8148	-276.9396	11.7106
R Zygo-max superior	185.098	-261.1739	27.8985
R Dacryon	178.039	-256.3335	37.9332
R Mid-torus inferior	176.9609	-262.1087	43.5761
R Mid-torus superior	178.4652	-268.0977	49.2295
R Fronto-malare orbitale	182.9876	-277.3699	36.819
R Fronto-malare temporale	181.513	-280.9994	35.9404
R Porion	150.3981	-292.8132	11.1931
R Zygo-temp superior	182.9653	-284.9197	15.7997
R Zygo-temp inferior	174.1942	-292.7547	12.2792
L Prosthion-2			
L Premax-max superior	183.1144	-252.9075	33.2502
L Zygo-max inferior	169.3571	-235.5177	10.6334
L Zygo-max superior	178.4869	-244.2906	27.2893
L Dacryon	177.1064	-253.3863	37.785
L Mid-torus inferior	173.0893	-251.1844	43.6474
L Mid-torus superior	169.1278	-244.7672	48.3582
L Fronto-malare orbitale	164.1829	-235.7942	34.7611
L Fronto-malare temporale	161.2461	-234.0176	33.5784
L Porion	130.2979	-250.1382	9.4927
L Zygo-temp superior	160.4576	-231.342	13.583
L Zygo-temp inferior	149.5472	-233.204	9.5513

195-7613 Scan 1

Landmark	X	Y	Z
Inion	170.7335	-250.1143	23.0586
Bregma	190.1152	-237.6938	49.2498
Glabella	227.1749	-213.8159	47.555
Nasion	228.6505	-213.2978	44.2175
Rhinion	242.4877	-205.4619	27.642
Nasospinale	252.8589	-199.6841	17.9284
Prosthion	258.463	-197.3097	11.8872
R Prosthion-2	260.3574	-202.0311	11.2897
R Premax-max superior	240.4358	-210.6097	28.4626
R Zygo-max inferior	241.8949	-233.935	13.5705
R Zygo-max superior	236.639	-220.0871	27.917
R Dacryon	229.2928	-215.1031	36.4753
R Mid-torus inferior	228.7851	-220.3653	44.7301
R Mid-torus superior	230.4298	-228.8328	50.0666
R Fronto-malare orbitale	237.5865	-234.8733	34.5635
R Fronto-malare temporale	235.4299	-240.1829	36.92
R Porion	204.8577	-257.7684	13.6514
R Zygo-temp superior	237.2502	-245.1229	16.7887
R Zygo-temp inferior	230.1951	-253.6286	13.9961
L Prosthion-2	254.5773	-193.2542	10.632
L Premax-max superior	236.5094	-204.4982	28.1805
L Zygo-max inferior	217.2306	-194.6431	11.536
L Zygo-max superior	227.3686	-204.7047	27.3506
L Dacryon	227.4598	-211.5699	36.8897
L Mid-torus inferior	222.1595	-209.6011	43.224
L Mid-torus superior	215.5806	-202.4791	47.5315
L Fronto-malare orbitale	213.8855	-195.9511	32.4177
L Fronto-malare temporale	208.1882	-194.6218	33.3863
L Porion	179.9787	-216.0673	12.505
L Zygo-temp superior	205.1279	-193.295	13.0643
L Zygo-temp inferior	194.9067	-196.515	9.8585

195-7613 Scan 2

Landmark	X	Y	Z
Inion	177.4282	-261.0837	23.9992
Bregma	195.7269	-248.9093	49.5212
Glabella	227.09	-219.2615	50.4376
Nasion	229.0911	-217.3123	44.9409
Rhinion	241.1328	-206.1864	28.929
Nasospinale	249.7776	-198.4857	18.7732
Prosthion	254.6002	-194.2039	12.701
R Prosthion-2	257.6328	-199.3226	12.1078
R Premax-max superior	239.1953	-212.0863	30.2828
R Zygo-max inferior	245.2836	-233.9395	13.57
R Zygo-max superior	238.8516	-220.8363	28.3417
R Dacryon	230.456	-218.0344	35.3236
R Mid-torus inferior	230.7022	-224.1577	44.5751
R Mid-torus superior	233.9485	-231.7533	49.9506
R Fronto-malare orbitale	242.2218	-236.2626	33.881
R Fronto-malare temporale	240.9074	-241.9592	36.0043
R Porion	213.3256	-264.31	12.59
R Zygo-temp superior	243.0417	-246.4685	15.7425
R Zygo-temp inferior	237.2474	-255.7132	13.2595
L Prosthion-2	250.3145	-191.4922	11.3804
L Premax-max superior	234.9288	-206.8317	29.7165
L Zygo-max inferior	214.3425	-199.4765	13.8075
L Zygo-max superior	226.4001	-207.6251	28.8031
L Dacryon	227.6436	-216.2207	36.7967
L Mid-torus inferior	222.4547	-214.9512	44.6785
L Mid-torus superior	216.2171	-210.3969	49.256
L Fronto-malare orbitale	211.6377	-201.9393	34.2185
L Fronto-malare temporale	205.7695	-202.4364	35.191
L Porion	181.6897	-228.7076	11.7339
L Zygo-temp superior	201.7626	-200.0863	15.3419
L Zygo-temp inferior	192.7713	-204.4241	12.2934

195-7613 Scan 3

Landmark	X	Y	Z
Inion	174.2134	-262.8262	18.108
Bregma	193.048	-250.5352	48.8243
Glabella	224.981	-220.875	47.5855
Nasion	226.3396	-219.3637	43.6264
Rhinion	237.3284	-207.31	27.2184
Nasospinale	245.3683	-198.9619	17.9461
Prosthion	250.1427	-194.8266	11.7714
R Prosthion-2	252.7912	-199.0455	10.432
R Premax-max superior	235.2507	-213.4533	28.5626
R Zygo-max inferior	240.0684	-234.1224	10.0977
R Zygo-max superior	234.4448	-222.3783	26.6617
R Dacryon	226.8501	-219.9916	34.7438
R Mid-torus inferior	227.6827	-226.2002	43.238
R Mid-torus superior	231.4299	-235.2291	47.5868
R Fronto-malare orbitale	238.3512	-237.7049	30.8969
R Fronto-malare temporale	237.7191	-243.2801	32.896
R Porion	208.5802	-263.9592	10.0746
R Zygo-temp superior	238.1239	-246.7495	12.2312
R Zygo-temp inferior	232.2264	-255.4263	9.0853
L Prosthion-2	245.6051	-190.8401	11.4702
L Premax-max superior	231.3253	-207.5658	28.7349
L Zygo-max inferior	209.5453	-199.3454	14.7213
L Zygo-max superior	222.757	-208.7298	28.62
L Dacryon	224.5481	-217.1959	37.3108
L Mid-torus inferior	219.3895	-216.6804	43.8815
L Mid-torus superior	212.4942	-211.7313	49.4725
L Fronto-malare orbitale	207.8742	-203.385	35.1672
L Fronto-malare temporale	202.2716	-203.7087	36.8999
L Porion	177.2848	-228.4532	14.0942
L Zygo-temp superior	197.1518	-200.3848	16.8734
L Zygo-temp inferior	187.8177	-204.6629	14.2572

195-7613 Scan 4

Landmark	X	Y	Z
Inion	186.6865	-271.5783	20.5157
Bregma	202.1613	-255.6144	46.7969
Glabella	230.1691	-222.1141	46.0572
Nasion	231.5622	-220.9434	42.4349
Rhinion	242.0605	-208.2494	26.2474
Nasospinale	250.3673	-199.1295	17.0714
Prosthion	255.1795	-195.166	11.2508
R Prosthion-2	258.4697	-199.1152	10.4612
R Premax-max superior	242.3448	-213.6427	27.5327
R Zygo-max inferior	249.8625	-235.6514	11.1036
R Zygo-max superior	241.3559	-223.3979	26.2936
R Dacryon	232.5697	-221.8569	36.0151
R Mid-torus inferior	233.8338	-227.4133	42.214
R Mid-torus superior	237.693	-235.5041	47.7265
R Fronto-malare orbitale	246.9179	-238.0097	31.7325
R Fronto-malare temporale	246.4862	-243.9716	33.8735
R Porion	221.8855	-269.5065	10.4263
R Zygo-temp superior	249.1623	-247.5274	13.7338
R Zygo-temp inferior	244.4794	-257.6687	10.5445
L Prosthion-2	250.147	-192.2188	9.7546
L Premax-max superior	236.6501	-209.2166	27.1372
L Zygo-max inferior	215.4019	-204.4238	11.3285
L Zygo-max superior	228.3341	-211.4859	26.6176
L Dacryon	229.995	-220.0649	36.9055
L Mid-torus inferior	224.2109	-219.2485	41.7432
L Mid-torus superior	216.18	-215.018	46.8119
L Fronto-malare orbitale	212.591	-207.9918	31.6443
L Fronto-malare temporale	206.6743	-209.1893	33.332
L Porion	186.7487	-237.1925	8.6975
L Zygo-temp superior	202.7627	-206.8331	12.5961
L Zygo-temp inferior	194.4758	-212.2921	9.4769

195-7613 Scan 5

Landmark	X	Y	Z
Inion	233.638	-254.9147	51.3147
Bregma			
Glabella	251.0747	-214.2182	49.6184
Nasion	252.006	-212.8126	45.8298
Rhinion	258.9905	-198.2902	29.5325
Nasospinale	264.3423	-187.8015	19.8848
Prosthion	267.3917	-182.2408	13.8813
R Prosthion-2	272.4223	-186.108	13.1597
R Premax-max superior	259.1551	-204.8978	31.3567
R Zygo-max inferior	274.0421	-222.7353	14.9047
R Zygo-max superior	262.2921	-212.6015	29.8729
R Dacryon	253.6292	-213.1595	38.5325
R Mid-torus inferior	256.1719	-218.7541	45.7769
R Mid-torus superior	261.465	-224.5342	51.7551
R Fronto-malare orbitale	271.4851	-225.3371	35.8897
R Fronto-malare temporale	272.6689	-230.8288	38.3053
R Porion	256.4313	-261.9614	14.9
R Zygo-temp superior	276.9467	-233.9115	18.3727
R Zygo-temp inferior	274.9554	-245.4403	15.4279
L Prosthion-2	261.98	-181.2219	12.131
L Premax-max superior	253.2726	-201.7544	30.7178
L Zygo-max inferior	231.7606	-203.2487	13.703
L Zygo-max superior	246.0765	-205.1852	29.4899
L Dacryon	249.9908	-212.3191	39.8957
L Mid-torus inferior	244.5671	-213.1368	45.4657
L Mid-torus superior	235.1229	-211.1089	49.7093
L Fronto-malare orbitale	229.7332	-205.9952	34.6114
L Fronto-malare temporale	224.4926	-207.9477	35.8436
L Porion	213.3158	-242.2829	13.7516
L Zygo-temp superior	220.5981	-208.5424	15.2738
L Zygo-temp inferior	213.7903	-216.157	12.4335

291-06069 Scan 1

Landmark	X	Y	Z
Inion	240.2845	-204.4701	29.1298
Bregma	256.7179	-176.6203	83.2924
Glabella	290.2118	-132.4162	80.522
Nasion	299.3627	-123.9986	63.3076
Rhinion	307.5535	-114.4236	57.1277
Nasospinale	308.4124	-110.8318	43.6126
Prosthion	314.2773	-104.6366	41.1043
R Prosthion-2	319.0201	-109.2901	41.5509
R Premax-max superior	301.2856	-119.7849	62.7334
R Zygo-max inferior	321.6641	-151.5846	37.8248
R Zygo-max superior	308.0661	-135.9548	61.3618
R Dacryon	296.198	-135.4943	67.7147
R Mid-torus inferior	298.5344	-141.6678	76.9448
R Mid-torus superior	299.1126	-141.5235	86.0675
R Fronto-malare orbitale	310.8255	-153.0291	66.952
R Fronto-malare temporale	309.9865	-163.3952	66.2963
R Porion	289.8534	-193.4141	37.7187
R Zygo-temp superior	321.4987	-161.0638	48.5504
R Zygo-temp inferior	317.5512	-173.1138	40.8271
L Prosthion-2	310.4499	-97.5334	35.8204
L Premax-max superior	298.4349	-118.8843	60.4773
L Zygo-max inferior	273.1948	-112.1788	30.6243
L Zygo-max superior	280.3892	-119.681	56.2637
L Dacryon	290.4121	-131.3666	67.8831
L Mid-torus inferior	281.9578	-127.646	74.1735
L Mid-torus superior	277.4093	-125.8739	83.4938
L Fronto-malare orbitale	269.4538	-119.016	59.8262
L Fronto-malare temporale	259.2595	-125.0671	57.5586
L Porion	242.3956	-158.7071	30.0395
L Zygo-temp superior	258.8493	-119.2241	38.0647
L Zygo-temp inferior	253.9602	-126.4446	32.4262

291-06069 Scan 2

Landmark	X	Y	Z
Inion	244.0913	-208.9382	34.3733
Bregma	260.6344	-179.6605	81.451
Glabella	292.4171	-136.0991	85.8773
Nasion	300.3229	-128.0627	69.9955
Rhinion	307.5883	-114.5153	56.9753
Nasospinale	310.4476	-112.3005	43.837
Prosthion	313.6665	-104.0136	40.5894
R Prosthion-2	318.2502	-107.0894	41.2027
R Premax-max superior	300.1067	-121.3771	64.4816
R Zygo-max inferior	324.2572	-149.6233	37.4723
R Zygo-max superior	309.5243	-135.7529	61.2075
R Dacryon	297.4422	-136.612	66.9219
R Mid-torus inferior	300.2584	-142.3761	76.1798
R Mid-torus superior	298.5331	-147.9632	82.8156
R Fronto-malare orbitale	313.4763	-152.8452	66.3081
R Fronto-malare temporale	313.8409	-162.78	65.3933
R Porion	295.9862	-193.0192	35.7651
R Zygo-temp superior	322.1558	-164.4636	46.8517
R Zygo-temp inferior	321.8903	-171.4315	40.1616
L Prosthion-2	308.42	-98.2136	36.2365
L Premax-max superior	295.6008	-121.3281	61.3604
L Zygo-max inferior	273.2632	-114.7661	30.3871
L Zygo-max superior	280.6075	-122.6687	55.8691
L Dacryon	292.6469	-133.0818	67.5752
L Mid-torus inferior	283.0265	-129.6286	73.5708
L Mid-torus superior	279.2081	-127.9842	82.7523
L Fronto-malare orbitale	270.3683	-121.567	59.7337
L Fronto-malare temporale	260.0588	-126.8936	56.454
L Porion	243.8517	-163.2646	29.8196
L Zygo-temp superior	258.8021	-122.9689	37.7182
L Zygo-temp inferior	254.3568	-129.7852	32.2093

291-06069 Scan 3

Landmark	X	Y	Z
Inion	238.9542	-207.9127	42.0159
Bregma	253.1244	-181.3676	80.782
Glabella	285.952	-129.7169	78.6308
Nasion	293.6228	-122.3384	61.4273
Rhinion	300.8788	-112.1304	54.2044
Nasospinale	306.7915	-106.0182	42.2274
Prosthion	311.7388	-99.8805	34.7764
R Prosthion-2	316.4646	-109.2109	34.492
R Premax-max superior	298.0382	-120.1645	62.8916
R Zygo-max inferior	315.8167	-148.3461	34.5
R Zygo-max superior	304.4008	-139.1784	59.6649
R Dacryon	290.8282	-134.0416	66.6098
R Mid-torus inferior	295.504	-139.9662	75.7643
R Mid-torus superior	296.1845	-146.5037	83.9952
R Fronto-malare orbitale	307.2624	-151.0064	65.4123
R Fronto-malare temporale	307.2607	-161.6875	64.8566
R Porion	287.7026	-194.1319	38.5216
R Zygo-temp superior	310.7129	-157.656	47.687
R Zygo-temp inferior	313.5216	-172.7556	39.1762
L Prosthion-2	305.1966	-101.8108	37.8473
L Premax-max superior	292.2714	-118.8498	59.2431
L Zygo-max inferior	265.2229	-114.3828	30.4426
L Zygo-max superior	280.246	-122.8177	58.5263
L Dacryon	285.6915	-129.6764	65.895
L Mid-torus inferior	277.503	-127.4936	73.9162
L Mid-torus superior	274.1445	-124.7445	82.2501
L Fronto-malare orbitale	263.2353	-119.9265	59.6583
L Fronto-malare temporale	253.0206	-125.375	57.3558
L Porion	236.1566	-162.5195	33.2892
L Zygo-temp superior	251.5526	-120.4166	39.767
L Zygo-temp inferior	247.8351	-128.8171	34.0509

291-06069 Scan 4

Landmark	X	Y	Z
Inion	238.5813	-207.4015	31.254
Bregma	250.7076	-180.4287	78.0601
Glabella	286.937	-130.9929	78.3758
Nasion	293.1244	-123.5234	62.4151
Rhinion	302.7817	-113.1071	54.4439
Nasospinale	310.0228	-106.7383	42.5397
Prosthion	314.9381	-100.6543	35.7523
R Prosthion-2	313.0127	-107.2475	37.9946
R Premax-max superior	294.6302	-120.9897	62.9304
R Zygo-max inferior	317.4177	-149.483	35.5174
R Zygo-max superior	304.4935	-140.9055	59.0188
R Dacryon	292.3724	-135.0105	65.72
R Mid-torus inferior	295.7058	-139.6399	75.0556
R Mid-torus superior	300.5466	-144.2539	83.6713
R Fronto-malare orbitale	307.6412	-152.1317	64.749
R Fronto-malare temporale	307.3633	-162.4703	63.882
R Porion	286.6406	-193.0119	35.7178
R Zygo-temp superior	315.3567	-164.802	45.7897
R Zygo-temp inferior	313.8199	-173.5407	38.6492
L Prosthion-2	303.3907	-99.4722	33.5225
L Premax-max superior	292.7207	-119.2448	58.922
L Zygo-max inferior	267.9341	-113.517	29.5039
L Zygo-max superior	275.839	-120.9426	54.8919
L Dacryon	287.5097	-130.7915	66.4855
L Mid-torus inferior	278.1203	-126.6042	72.4264
L Mid-torus superior	275.074	-126.613	82.3045
L Fronto-malare orbitale	265.6143	-119.6706	59.047
L Fronto-malare temporale	255.643	-124.2275	57.0062
L Porion	237.6343	-160.5144	31.7193
L Zygo-temp superior	253.4501	-120.1068	37.8917
L Zygo-temp inferior	247.9709	-128.3619	31.9059

291-06069 Scan 5

Landmark	X	Y	Z
Inion	237.2173	-207.4488	36.5693
Bregma	249.7782	-180.7517	76.7244
Glabella	286.9704	-131.3298	77.0242
Nasion	294.507	-123.3371	60.3224
Rhinion	302.9642	-113.2494	53.6163
Nasospinale	308.6753	-106.4244	41.6287
Prosthion	315.4965	-101.8219	35.197
R Prosthion-2	313.6928	-107.9153	37.0449
R Premax-max superior	294.962	-121.7287	62.1649
R Zygo-max inferior	317.1556	-150.5612	34.3143
R Zygo-max superior	299.0307	-136.884	58.4238
R Dacryon	292.8474	-136.4134	65.7305
R Mid-torus inferior	294.8837	-140.2006	73.683
R Mid-torus superior	297.464	-148.4294	82.8283
R Fronto-malare orbitale	307.3845	-152.0627	64.052
R Fronto-malare temporale	306.9197	-163.6833	64.4665
R Porion	285.9191	-194.0461	35.8576
R Zygo-temp superior	310.9217	-159.3677	46.1292
R Zygo-temp inferior	312.7977	-173.3452	37.807
L Prosthion-2	304.1764	-98.5203	33.092
L Premax-max superior	291.6699	-120.1353	58.886
L Zygo-max inferior	268.3861	-113.9388	29.4095
L Zygo-max superior	278.0621	-118.3015	55.0764
L Dacryon	287.8036	-131.8425	65.7306
L Mid-torus inferior	278.425	-127.3903	71.8073
L Mid-torus superior	275.1628	-124.8326	80.4681
L Fronto-malare orbitale	265.507	-118.9837	58.4315
L Fronto-malare temporale	254.7045	-124.3113	55.6898
L Porion	237.6309	-159.9315	30.9086
L Zygo-temp superior	253.5527	-118.9068	38.4561
L Zygo-temp inferior	249.3167	-126.9277	31.9453

305-2413 Scan 1

Landmark	X	Y	Z
Inion	120.8258	-279.1082	24.8257
Bregma	143.2536	-271.6029	49.1758
Glabella	186.0102	-252.0434	46.6034
Nasion	189.0201	-250.8557	37.5144
Rhinion	201.7818	-244.9118	23.0785
Nasospinale	208.5113	-241.4453	11.65
Prosthion	212.2334	-239.9722	6.6807
R Prosthion-2	214.0932	-245.027	3.7594
R Premax-max superior	193.5451	-249.2911	29.5704
R Zygo-max inferior	190.3069	-274.2916	7.617
R Zygo-max superior	194.0311	-260.3648	23.8263
R Dacryon	188.7313	-252.0897	32.7818
R Mid-torus inferior	187.5051	-259.3669	42.8326
R Mid-torus superior	189.6181	-265.6354	47.3877
R Fronto-malare orbitale	191.6232	-274.5081	34.2438
R Fronto-malare temporale	189.3869	-278.5457	34.6342
R Porion	154.3999	-295.757	16.2345
R Zygo-temp superior	188.473	-282.1168	12.4514
R Zygo-temp inferior	179.8655	-289.3799	10.2569
L Prosthion-2	207.7212	-235.3235	5.4742
L Premax-max superior	193.6232	-248.6391	29.4812
L Zygo-max inferior	173.2172	-232.3185	8.5671
L Zygo-max superior	185.5336	-238.957	23.9595
L Dacryon	187.4492	-249.4506	34.8151
L Mid-torus inferior	181.9411	-245.3063	42.9613
L Mid-torus superior	178.0642	-240.0176	47.7768
L Fronto-malare orbitale	173.552	-232.0604	33.3673
L Fronto-malare temporale	168.386	-229.9023	33.8142
L Porion	134.2373	-242.9934	16.9396
L Zygo-temp superior	165.7114	-227.8575	13.0912
L Zygo-temp inferior	153.9043	-228.9898	11.0448

305-2413 Scan 2

Landmark	X	Y	Z
Inion	117.7708	-282.7003	21.0534
Bregma	138.0752	-275.1345	47.2831
Glabella	180.8397	-254.4554	48.1813
Nasion	183.6504	-253.2431	41.0154
Rhinion	197.91	-246.8023	25.5576
Nasospinale	205.0391	-242.9322	15.094
Prosthion	209.6033	-241.061	9.7871
R Prosthion-2	211.6884	-247.0558	8.6023
R Premax-max superior	189.6423	-251.5618	31.6472
R Zygo-max inferior	189.3358	-276.1965	10.0027
R Zygo-max superior	191.2344	-261.6331	26.0989
R Dacryon	183.5178	-254.3414	37.8552
R Mid-torus inferior	182.8598	-262.0026	45.1573
R Mid-torus superior	185.2568	-266.5149	49.1797
R Fronto-malare orbitale	187.9078	-276.7075	35.5898
R Fronto-malare temporale	185.4452	-280.6047	36.655
R Porion	152.3544	-298.556	14.8237
R Zygo-temp superior	186.1608	-285.0621	13.5322
R Zygo-temp inferior	177.8539	-291.7329	11.3528
L Prosthion-2	204.6474	-236.5089	8.4324
L Premax-max superior	189.5392	-250.2593	31.4368
L Zygo-max inferior	170.5922	-234.5443	9.8281
L Zygo-max superior	181.4474	-241.1181	25.7257
L Dacryon	182.8954	-252.0765	36.4337
L Mid-torus inferior	177.0228	-248.1237	44.7812
L Mid-torus superior	172.2678	-241.4695	48.7117
L Fronto-malare orbitale	168.9364	-235.0977	34.2652
L Fronto-malare temporale	163.683	-232.7596	34.904
L Porion	131.2887	-246.5242	13.9906
L Zygo-temp superior	162.6697	-231	13.5115
L Zygo-temp inferior	150.7224	-231.7774	10.4686

305-2413 Scan 3

Landmark	X	Y	Z
Inion	313.5523	25.216	20.536
Bregma	314.561	51.0808	47.2493
Glabella	309.1826	95.9882	45.7645
Nasion	308.5021	98.0452	40.9821
Rhinion	306.2903	114.3994	23.3995
Nasospinale	305.408	122.0056	13.1523
Prosthion	304.2031	126.7595	8.2813
R Prosthion-2	311.03	125.4082	7.5377
R Premax-max superior	308.4369	105.1467	29.2298
R Zygo-max inferior	330.436	96.5687	7.3452
R Zygo-max superior	318.7174	101.2991	23.6063
R Dacryon	310.0097	98.5812	31.9756
R Mid-torus inferior	316.4514	94.9463	42.2653
R Mid-torus superior	318.8883	93.6944	47.3681
R Fronto-malare orbitale	331.4146	94.3999	32.3897
R Fronto-malare temporale	334.2877	89.0377	34.4857
R Porion	339.2295	52.0033	12.6751
R Zygo-temp superior	337.5149	89.5709	10.8367
R Zygo-temp inferior	342.2339	77.7685	8.7857
L Prosthion-2	298.0905	123.1153	6.8788
L Premax-max superior	306.5589	105.2701	29.3232
L Zygo-max inferior	284.4062	92.7645	8.9458
L Zygo-max superior	295.459	99.8427	24.6261
L Dacryon	305.8586	99.3116	32.0098
L Mid-torus inferior	300.7009	93.9608	42.6076
L Mid-torus superior	299.9323	93.0859	48.0118
L Fronto-malare orbitale	285.4672	90.6319	34.3635
L Fronto-malare temporale	282.4871	85.2933	35.6237
L Porion	282.6992	49.8659	14.217
L Zygo-temp superior	278.4883	85.3625	13.2181
L Zygo-temp inferior	275.6476	73.7895	10.1077

305-2413 Scan 4

Landmark	X	Y	Z
Inion	310.5613	48.9713	20.0079
Bregma	305.6012	71.5397	49.258
Glabella	296.319	115.9705	51.0504
Nasion	295.3926	117.8806	47.0869
Rhinion	292.6459	135.8285	29.902
Nasospinale	290.4498	143.2824	19.8596
Prosthion	289.9209	148.9602	15.6245
R Prosthion-2	297.8971	147.6684	14.6504
R Premax-max superior	295.5196	126.6596	35.0967
R Zygo-max inferior	318.842	121.2089	13.2994
R Zygo-max superior	306.73	124.6146	29.9206
R Dacryon	297.2478	119.7302	36.7012
R Mid-torus inferior	304.0296	116.5207	48.006
R Mid-torus superior	306.1565	115.2831	52.8744
R Fronto-malare orbitale	319.4269	118.3088	38.6367
R Fronto-malare temporale	323.4955	114.0428	39.7049
R Porion	333.3174	78.8787	15.925
R Zygo-temp superior	327.6504	115.0364	17.2609
R Zygo-temp inferior	333.2598	104.5425	14.1741
L Prosthion-2	284.545	145.6364	13.7419
L Premax-max superior	293.6241	126.3437	35.0758
L Zygo-max inferior	274.9049	112.731	12.4772
L Zygo-max superior	283.2274	119.81	29.2413
L Dacryon	293.584	119.844	36.9114
L Mid-torus inferior	288.8771	113.2936	47.3754
L Mid-torus superior	286.5886	111.6986	52.6262
L Fronto-malare orbitale	273.9967	109.4819	36.8078
L Fronto-malare temporale	270.9269	104.0297	36.438
L Porion	277.1652	70.0735	14.898
L Zygo-temp superior	268.6619	104.1417	15.9564
L Zygo-temp inferior	267.3954	93.7945	12.2955

305-2413 Scan 5

Landmark	X	Y	Z
Inion	320.1512	-21.5943	23.5138
Bregma	323.5501	3.1102	50.6687
Glabella	322.2041	48.2229	50.6534
Nasion	321.9852	50.1174	46.4021
Rhinion	321.5855	67.5284	28.3754
Nasospinale	321.0493	75.7185	18.3291
Prosthion	320.8249	80.4356	13.6892
R Prosthion-2	327.6505	77.9646	11.9939
R Premax-max superior	322.79	57.889	33.8899
R Zygo-max inferior	342.496	47.0345	10.8375
R Zygo-max superior	332.8372	53.8526	28.3127
R Dacryon	323.1556	51.5519	35.0977
R Mid-torus inferior	329.9042	46.9005	46.99
R Mid-torus superior	331.9995	44.7883	52.0948
R Fronto-malare orbitale	344.6259	44.854	36.8187
R Fronto-malare temporale	347.3649	39.9612	37.6465
R Porion	348.5381	2.8853	15.3588
R Zygo-temp superior	350.3734	39.9134	15.0269
R Zygo-temp inferior	353.5606	31.369	11.9257
L Prosthion-2	314.0475	77.647	12.0677
L Premax-max superior	320.976	57.5977	33.9883
L Zygo-max inferior	298.2043	48.2776	13.6285
L Zygo-max superior	309.0887	54.0015	29.4315
L Dacryon	319.8401	52.1534	36.0728
L Mid-torus inferior	314.5493	47.243	47.3359
L Mid-torus superior	311.4002	46.1661	52.7874
L Fronto-malare orbitale	298.6157	46.0253	37.635
L Fronto-malare temporale	294.3087	41.3265	38.0392
L Porion	291.5202	6.1505	18.428
L Zygo-temp superior	290.6268	41.019	17.7858
L Zygo-temp inferior	287.0303	32.0159	14.1618

305-2412 Scan 1

Landmark	X	Y	Z
Inion	59.6501	-480.9713	-39.2403
Bregma	15.0519	-493.5874	-27.7304
Glabella	4.6177	-518.9982	12.4324
Nasion	8.3692	-519.3588	15.1193
Rhinion	17.4614	-528.6952	32.5823
Nasospinale	27.5215	-534.3926	45.8621
Prosthion	30.8011	-537.4591	51.8027
R Prosthion-2	32.6497	-541.6419	49.317
R Premax-max superior	20.4903	-531.145	28.9918
R Zygo-max inferior	44.1702	-542.1876	13.077
R Zygo-max superior	25.4812	-533.4504	18.3885
R Dacryon	15.0782	-522.0056	16.7916
R Mid-torus inferior	9.2936	-526.2168	6.7804
R Mid-torus superior	4.8143	-526.1497	4.8562
R Fronto-malare orbitale	21.0937	-539.012	0.3577
R Fronto-malare temporale	22.9546	-539.1712	-6.6789
R Porion	57.722	-519.8334	-33.0805
R Zygo-temp superior	43.1992	-544.0396	0.4585
R Zygo-temp inferior	51.7552	-539.7164	-12.7195
L Prosthion-2	30.7822	-531.3774	54.0372
L Premax-max superior	19.7911	-521.4908	34.7079
L Zygo-max inferior	39.2631	-498.348	38.5591
L Zygo-max superior	22.996	-509.2185	30.7878
L Dacryon	17.6642	-516.4583	20.3248
L Mid-torus inferior	7.6618	-508.6713	17.322
L Mid-torus superior	3.3354	-506.0515	16.1576
L Fronto-malare orbitale	15.6954	-492.9584	25.5299
L Fronto-malare temporale	16.2146	-487.59	21.1225
L Porion	52.7477	-466.6669	-3.7548
L Zygo-temp superior	36.2056	-484.8293	33.051
L Zygo-temp inferior	43.9844	-476.0782	24.1079

305-2412 Scan 2

Landmark	X	Y	Z
Inion	61.0313	-479.6614	-41.3647
Bregma	16.9219	-492.9195	-30.4393
Glabella	7.0206	-520.3038	9.5358
Nasion	10.1515	-521.1663	11.4609
Rhinion	19.1018	-531.1041	28.8995
Nasospinale	29.4484	-536.644	41.3596
Prosthion	32.7092	-540.423	47.3575
R Prosthion-2	34.7915	-544.1954	43.7487
R Premax-max superior	23.0949	-532.9328	23.2702
R Zygo-max inferior	46.1105	-543.899	7.7661
R Zygo-max superior	27.7527	-534.7335	13.1713
R Dacryon	16.2691	-522.429	11.8676
R Mid-torus inferior	11.6857	-526.8843	2.3887
R Mid-torus superior	7.6609	-528.0861	0.6233
R Fronto-malare orbitale	23.6964	-539.8188	-4.7847
R Fronto-malare temporale	22.0895	-537.5991	-13.1145
R Porion	57.9151	-517.8079	-36.2483
R Zygo-temp superior	45.9842	-544.9796	-4.349
R Zygo-temp inferior	52.5628	-539.7241	-17.9442
L Prosthion-2	33.6762	-534.595	49.4719
L Premax-max superior	21.5613	-523.9796	30.5809
L Zygo-max inferior	41.2713	-500.3413	35.1602
L Zygo-max superior	24.8909	-510.94	27.406
L Dacryon	20.0966	-517.9156	16.3888
L Mid-torus inferior	9.4915	-510.731	13.5916
L Mid-torus superior	5.0762	-508.4975	12.3656
L Fronto-malare orbitale	16.8324	-495.1704	22.3475
L Fronto-malare temporale	17.2227	-488.7629	18.6945
L Porion	53.2218	-467.2102	-5.0299
L Zygo-temp superior	37.1913	-487.4058	29.085
L Zygo-temp inferior	44.8188	-476.5111	21.2033

305-2412 Scan 3

Landmark	X	Y	Z
Inion	61.1577	-480.1587	-38.4874
Bregma	16.1508	-491.6338	-31.0891
Glabella	0.8799	-516.7511	8.1998
Nasion	4.3541	-517.5009	11.2402
Rhinion	11.9149	-526.9254	29.8097
Nasospinale	20.4398	-532.4681	43.382
Prosthion	22.0584	-535.7538	49.6144
R Prosthion-2	24.8223	-539.7077	46.292
R Premax-max superior	15.5604	-529.4196	25.5433
R Zygo-max inferior	40.7413	-540.6716	11.2845
R Zygo-max superior	21.0516	-531.738	14.9106
R Dacryon	10.8348	-519.5098	12.8327
R Mid-torus inferior	7.1318	-524.0421	2.0006
R Mid-torus superior	2.8531	-524.3433	0.3793
R Fronto-malare orbitale	18.1226	-537.1968	-3.0345
R Fronto-malare temporale	20.5827	-537.2705	-9.7937
R Porion	57.3926	-518.0161	-31.2193
R Zygo-temp superior	41.3928	-543.559	-1.0031
R Zygo-temp inferior	48.707	-537.836	-13.3275
L Prosthion-2	22.8149	-529.4106	51.8313
L Premax-max superior	14.2572	-519.2451	31.4683
L Zygo-max inferior	34.0768	-496.5054	36.6727
L Zygo-max superior	18.2257	-507.0575	27.7408
L Dacryon	13.3977	-514.3899	16.5234
L Mid-torus inferior	4.0272	-506.7758	11.9556
L Mid-torus superior	-0.0206	-504.7248	10.6545
L Fronto-malare orbitale	11.2204	-491.653	21.3931
L Fronto-malare temporale	12.1362	-485.2885	16.7562
L Porion	51.3809	-465.696	-2.9865
L Zygo-temp superior	31.039	-483.295	30.1807
L Zygo-temp inferior	40.0946	-473.8691	22.2085

305-2412 Scan 4

Landmark	X	Y	Z
Inion	55.3276	-471.4028	-37.4472
Bregma	11.8965	-486.0072	-25.7707
Glabella	2.8945	-513.688	13.2259
Nasion	6.6004	-514.5039	15.725
Rhinion	16.4419	-524.2905	33.0495
Nasospinale	27.2451	-529.7832	46.1468
Prosthion	29.7482	-533.054	51.1733
R Prosthion-2	32.5872	-537.1686	46.3334
R Premax-max superior	22.3089	-528.0765	28.6957
R Zygo-max inferior	44.3588	-535.6952	10.4657
R Zygo-max superior	25.2054	-527.1771	16.0701
R Dacryon	14.3795	-515.971	16.1693
R Mid-torus inferior	9.3943	-520.0719	5.8666
R Mid-torus superior	4.874	-521.4523	4.3179
R Fronto-malare orbitale	20.9558	-532.5577	-1.0755
R Fronto-malare temporale	22.425	-532.1179	-8.6599
R Porion	55.5882	-510.3305	-32.8981
R Zygo-temp superior	43.0962	-538.0746	-1.2827
R Zygo-temp inferior	48.9514	-530.5607	-15.6958
L Prosthion-2	31.4848	-527.4116	52.9951
L Premax-max superior	19.4507	-517.0923	34.1245
L Zygo-max inferior	38.1297	-493.0576	38.7454
L Zygo-max superior	22.1026	-504.5976	30.6503
L Dacryon	17.2496	-511.111	20.2637
L Mid-torus inferior	6.3119	-504.123	17.3338
L Mid-torus superior	2.0931	-501.7353	16.3288
L Fronto-malare orbitale	14.9572	-488.2955	25.7685
L Fronto-malare temporale	14.1054	-481.5459	22.2553
L Porion	49.4103	-459.3671	-1.3257
L Zygo-temp superior	34.1186	-479.9456	33.934
L Zygo-temp inferior	42.0472	-469.3824	25.012

305-2412 Scan 5

Landmark	X	Y	Z
Inion	63.1355	-487.8476	-50.25
Bregma	18.8469	-499.3667	-38.9658
Glabella	7.4047	-524.3645	1.5695
Nasion	10.7705	-524.6614	4.0433
Rhinion	19.4586	-533.8434	22.1795
Nasospinale	29.4933	-539.3116	35.4259
Prosthion	33.0672	-542.8931	41.7106
R Prosthion-2	35.2026	-546.4238	38.068
R Premax-max superior	23.4503	-536.6571	17.2405
R Zygo-max inferior	47.3691	-548.0376	2.2346
R Zygo-max superior	28.075	-538.6251	7.0052
R Dacryon	17.2257	-526.142	5.1404
R Mid-torus inferior	12.3739	-531.6851	-4.8695
R Mid-torus superior	8.4286	-531.6351	-6.2909
R Fronto-malare orbitale	23.5476	-544.1964	-11.3027
R Fronto-malare temporale	24.8367	-543.991	-18.6814
R Porion	59.8255	-525.2159	-43.0989
R Zygo-temp superior	45.9796	-550.1525	-10.0102
R Zygo-temp inferior	55.153	-545.6938	-23.4216
L Prosthion-2	34.3773	-536.5715	43.52
L Premax-max superior	22.5543	-526.5264	22.9624
L Zygo-max inferior	42.4932	-503.5096	26.8764
L Zygo-max superior	25.8623	-514.3184	19.3511
L Dacryon	21.5432	-521.6299	9.3726
L Mid-torus inferior	11.0694	-514.2086	5.5036
L Mid-torus superior	6.2801	-511.0697	3.749
L Fronto-malare orbitale	19.4841	-498.6417	13.5175
L Fronto-malare temporale	18.9534	-491.9507	9.4126
L Porion	56.2598	-472.4251	-15.0052
L Zygo-temp superior	38.9771	-490.7142	20.5457
L Zygo-temp inferior	47.2941	-481.3065	12.7805

305-10004 Scan 1

Landmark	X	Y	Z
Inion	51.792	-488.3439	-30.4214
Bregma	14.1843	-500.1978	-16.2177
Glabella	11.857	-524.8384	22.5544
Nasion	14.9098	-525.5629	24.8616
Rhinion	25.6366	-528.8287	33.8609
Nasospinale	34.6348	-531.1505	41.3642
Prosthion	37.9992	-532.5251	43.7884
R Prosthion-2	40.0392	-536.178	41.3218
R Premax-max superior	26.541	-531.8576	30.8155
R Zygo-max inferior	44.6032	-540.3137	16.5312
R Zygo-max superior	30.5481	-535.1107	24.2489
R Dacryon	20.449	-526.4642	24.6471
R Mid-torus inferior			
R Mid-torus superior			
R Fronto-malare orbitale	25.1086	-540.9111	9.911
R Fronto-malare temporale	24.0268	-538.8337	4.3344
R Porion	52.6558	-526.8081	-16.8607
R Zygo-temp superior	42.5038	-543.4478	8.6768
R Zygo-temp inferior	45.5304	-540.3895	-1.0248
L Prosthion-2	39.2087	-528.308	46.2525
L Premax-max superior	25.7717	-524.8301	34.9173
L Zygo-max inferior	40.3615	-505.9489	37.6272
L Zygo-max superior	28.7234	-515.6686	35.5826
L Dacryon	22.7147	-523.1931	28.6447
L Mid-torus inferior			
L Mid-torus superior			
L Fronto-malare orbitale	21.1257	-503.4873	31.7839
L Fronto-malare temporale	21.3689	-498.5267	29.9012
L Porion	48.46	-482.156	11.5817
L Zygo-temp superior	37.5957	-495.6771	34.6672
L Zygo-temp inferior	42.1261	-488.4578	29.6836

305-10004 Scan 2

Landmark	X	Y	Z
Inion	54.3398	-486.8161	-33.5404
Bregma	16.4733	-499.6418	-19.6085
Glabella	15.151	-525.3892	17.6895
Nasion	18.3125	-526.2623	19.9664
Rhinion	29.0263	-529.6551	28.9397
Nasospinale	38.2195	-532.277	36.0262
Prosthion	41.6884	-533.6019	38.3724
R Prosthion-2	43.4517	-537.4388	35.674
R Premax-max superior	29.9553	-532.444	26.1731
R Zygo-max inferior	47.2978	-540.8761	10.8955
R Zygo-max superior	33.6174	-534.9992	19.0703
R Dacryon	22.6858	-526.4993	19.8739
R Mid-torus inferior			
R Mid-torus superior			
R Fronto-malare orbitale	27.706	-540.7194	4.5516
R Fronto-malare temporale	29.207	-539.724	-0.6575
R Porion	52.5571	-525.3702	-22.402
R Zygo-temp superior	45.6675	-542.9341	3.116
R Zygo-temp inferior	46.9993	-539.3802	-7.1856
L Prosthion-2	42.8126	-529.153	41.1688
L Premax-max superior	28.9665	-525.8106	30.0762
L Zygo-max inferior	43.314	-507.0301	33.1851
L Zygo-max superior	31.6136	-516.6594	30.9216
L Dacryon	25.3515	-524.1057	23.8932
L Mid-torus inferior			
L Mid-torus superior			
L Fronto-malare orbitale	23.829	-504.6267	28.0421
L Fronto-malare temporale	23.6157	-499.5724	26.2328
L Porion	50.6092	-481.7838	7.7644
L Zygo-temp superior	39.8977	-496.6923	30.876
L Zygo-temp inferior	44.4263	-489.0204	26.5061

305-10004 Scan 3

Landmark	X	Y	Z
Inion	179.8461	-216.7395	27.9387
Bregma	199.2679	-194.31	55.0902
Glabella	231.6921	-164.1115	41.1355
Nasion	232.4024	-163.0261	37.2521
Rhinion	234.9714	-158.4716	24.405
Nasospinale	236.6466	-154.8026	12.9195
Prosthion	237.3539	-153.5156	9.6381
R Prosthion-2	240.2838	-157.4533	7.3254
R Premax-max superior	237.0583	-162.1838	24.108
R Zygo-max inferior	239.8325	-183.2915	10.6477
R Zygo-max superior	238.75	-170.5435	22.0199
R Dacryon	232.4164	-164.8722	30.4806
R Mid-torus inferior			
R Mid-torus superior			
R Fronto-malare orbitale	242.9918	-183.0986	30.7035
R Fronto-malare temporale	241.3817	-187.6614	31.9809
R Porion	220.0428	-211.1349	12.8026
R Zygo-temp superior	240.9517	-190.8214	14.6236
R Zygo-temp inferior	236.7378	-199.6119	12.8811
L Prosthion-2	233.4074	-150.8574	8.2091
L Premax-max superior	230.5989	-156.704	24.4702
L Zygo-max inferior	208.8244	-154.8143	12.694
L Zygo-max superior	222.1167	-155.1426	22.8809
L Dacryon	228.8546	-162.491	31.7345
L Mid-torus inferior			
L Mid-torus superior			
L Fronto-malare orbitale	211.0218	-153.5032	31.4532
L Fronto-malare temporale	206.1919	-153.0058	32.9592
L Porion	183.0675	-175.0903	17.7386
L Zygo-temp superior	201.3427	-154.1373	17.5549
L Zygo-temp inferior	191.7847	-158.3809	16.1328

305-10004 Scan 4

Landmark	X	Y	Z
Inion	50.6392	-481.0654	-24.381
Bregma	12.0857	-495.8983	-10.1713
Glabella	13.2083	-520.674	28.4244
Nasion	15.9652	-521.1776	30.4462
Rhinion	26.779	-523.6398	39.0594
Nasospinale	36.4733	-525.7159	46.1648
Prosthion	39.9489	-526.6862	48.7821
R Prosthion-2	42.4795	-529.9372	46.1064
R Premax-max superior	28.0816	-526.5602	35.7734
R Zygo-max inferior	44.977	-534.5757	21.2091
R Zygo-max superior	32.0145	-529.7216	29.129
R Dacryon	21.7404	-521.4662	30.1822
R Mid-torus inferior			
R Mid-torus superior			
R Fronto-malare orbitale	26.208	-535.9899	14.7917
R Fronto-malare temporale	27.5688	-534.9797	9.9634
R Porion	52.5515	-519.174	-12.5718
R Zygo-temp superior	44.8567	-537.2711	12.6392
R Zygo-temp inferior	48.0345	-533.3665	3.3275
L Prosthion-2	41.4877	-522.1282	50.8849
L Premax-max superior	27.3563	-519.687	39.9085
L Zygo-max inferior	40.7892	-499.998	42.4346
L Zygo-max superior	29.7742	-510.3721	40.3998
L Dacryon	23.6292	-518.0147	34.0228
L Mid-torus inferior			
L Mid-torus superior			
L Fronto-malare orbitale	21.4567	-498.6147	37.345
L Fronto-malare temporale	20.9083	-493.4593	35.5972
L Porion	46.9573	-475.4313	16.0513
L Zygo-temp superior	37.3113	-490.1855	39.8725
L Zygo-temp inferior	41.7135	-482.3732	34.8227

305-10004 Scan 5

Landmark	X	Y	Z
Inion	56.9944	-490.2707	-39.8064
Bregma	18.3979	-500.619	-24.9307
Glabella	16.4642	-525.9903	13.8469
Nasion	19.4345	-526.8062	15.9551
Rhinion	29.8244	-530.2965	24.8014
Nasospinale	39.3491	-532.6265	32.0841
Prosthion	42.8448	-534.0141	34.7179
R Prosthion-2	44.7633	-537.7018	32.068
R Premax-max superior	31.1336	-533.3572	21.9395
R Zygo-max inferior	45.6877	-540.9245	6.8547
R Zygo-max superior	34.819	-536.5507	15.0602
R Dacryon	25.5498	-527.1803	15.9531
R Mid-torus inferior			
R Mid-torus superior			
R Fronto-malare orbitale	28.8312	-542.0626	0.7205
R Fronto-malare temporale	27.4352	-539.5157	-4.6615
R Porion	54.3223	-528.7592	-26.4585
R Zygo-temp superior	46.3872	-545.1605	-1.3626
R Zygo-temp inferior	48.2767	-541.3577	-10.6356
L Prosthion-2	43.7589	-529.9059	37.0426
L Premax-max superior	30.0716	-526.0594	25.4996
L Zygo-max inferior	45.493	-507.5791	28.3705
L Zygo-max superior	33.5304	-516.8903	26.478
L Dacryon	27.3853	-524.1543	19.9977
L Mid-torus inferior			
L Mid-torus superior			
L Fronto-malare orbitale	25.9122	-504.7437	22.7963
L Fronto-malare temporale	25.6824	-499.9001	20.6675
L Porion	53.7018	-483.5802	1.4867
L Zygo-temp superior	42.4658	-497.1133	25.6057
L Zygo-temp inferior	46.6721	-490.4968	21.0408

305-10433 Scan 1

Landmark	X	Y	Z
Inion	238.3066	-213.7735	37.7368
Bregma	254.1049	-188.3536	82.2588
Glabella	282.9657	-136.1012	89.8875
Nasion	291.0667	-127.804	76.8306
Rhinion	309.8123	-110.7934	63.7854
Nasospinale	321.4869	-98.5272	51.059
Prosthion	327.9846	-89.9709	40.4864
R Prosthion-2			
R Premax-max superior	298.1395	-121.6786	69.9157
R Zygo-max inferior	324.8237	-152.3027	41.95
R Zygo-max superior	305.6577	-138.4309	68.0582
R Dacryon	294.0762	-138.3177	76.9791
R Mid-torus inferior	295.1256	-143.9641	84.5025
R Mid-torus superior	298.9064	-151.7498	95.1103
R Fronto-malare orbitale	311.6181	-156.6716	75.8687
R Fronto-malare temporale	312.4553	-169.398	75.6898
R Porion	287.9319	-206.5605	42.0422
R Zygo-temp superior	324.8378	-171.8457	50.8715
R Zygo-temp inferior	323.0598	-182.4388	46.6801
L Prosthion-2			
L Premax-max superior	296.0912	-118.758	66.8195
L Zygo-max inferior	269.4247	-111.503	34.7391
L Zygo-max superior	275.4176	-123.2627	63.1274
L Dacryon	287.6297	-133.6774	75.9446
L Mid-torus inferior	279.1837	-131.7194	80.9186
L Mid-torus superior	270.4617	-130.0351	92.5955
L Fronto-malare orbitale	261.4557	-122.5604	71.9848
L Fronto-malare temporale	250.4965	-129.2292	67.5953
L Porion	232.7622	-168.8642	31.6547
L Zygo-temp superior	248.943	-120.2825	40.2758
L Zygo-temp inferior	244.1267	-127.5089	36.0615

305-10433 Scan 2

Landmark	X	Y	Z
Inion	238.4057	-214.19	37.0147
Bregma	255.5266	-190.6297	82.7981
Glabella	285.4282	-137.8236	89.8478
Nasion	311.1869	-112.1686	63.5423
Rhinion	311.0793	-111.1888	63.2196
Nasospinale	321.7613	-99.1372	50.3685
Prosthion	329.3404	-91.0316	40.0847
R Prosthion-2	333.12	-100.5483	40.5081
R Premax-max superior	304.1014	-122.6585	71.4385
R Zygo-max inferior	325.539	-154.1054	40.7998
R Zygo-max superior	311.3864	-141.0717	67.8611
R Dacryon	295.3824	-139.6731	76.2212
R Mid-torus inferior	297.3373	-147.0168	84.0282
R Mid-torus superior	296.4577	-154.5043	93.532
R Fronto-malare orbitale	313.0684	-158.6002	74.5231
R Fronto-malare temporale	313.6883	-171.666	74.6915
R Porion	288.0879	-207.8601	39.1842
R Zygo-temp superior	328.4039	-170.3083	50.7943
R Zygo-temp inferior	324.1924	-182.7209	45.1362
L Prosthion-2	319.3048	-85.7369	39.2305
L Premax-max superior	296.8006	-120.0472	66.8603
L Zygo-max inferior	270.2517	-111.7325	35.6938
L Zygo-max superior	281.5541	-120.6357	65.6
L Dacryon	289.3545	-134.8607	75.1552
L Mid-torus inferior	281.0016	-133.4488	81.6054
L Mid-torus superior	270.1158	-136.5194	89.5974
L Fronto-malare orbitale	263.3713	-124.3174	72.7847
L Fronto-malare temporale	251.7519	-130.6358	68.0147
L Porion	231.4342	-168.4522	32.696
L Zygo-temp superior	250.2951	-120.3239	43.4534
L Zygo-temp inferior	241.1175	-127.7668	35.3665

305-10433 Scan 3

Landmark	X	Y	Z
Inion	225.8	-220.9877	38.5991
Bregma	245.4599	-198.2501	84.7538
Glabella	275.063	-144.4191	89.5631
Nasion	282.7752	-135.6039	74.8097
Rhinion	298.7449	-118.5141	62.2952
Nasospinale	305.4509	-110.7335	46.9582
Prosthion	316.3928	-97.6102	38.8886
R Prosthion-2	320.5369	-105.6633	39.1364
R Premax-max superior	291.599	-128.9962	70.987
R Zygo-max inferior	312.6628	-160.1581	39.9344
R Zygo-max superior	299.3867	-150.1851	67.3854
R Dacryon	283.3134	-147.9006	75.0182
R Mid-torus inferior	284.5757	-151.9722	83.4372
R Mid-torus superior	288.2768	-160.5936	94.3153
R Fronto-malare orbitale	301.1066	-165.0775	74.3421
R Fronto-malare temporale	301.6599	-177.4965	74.6433
R Porion	275.4571	-214.6655	39.6961
R Zygo-temp superior	311.9572	-180.0322	48.6777
R Zygo-temp inferior	311.4692	-189.9676	44.7697
L Prosthion-2	306.6242	-92.545	37.7746
L Premax-max superior	285.5006	-125.5973	66.5339
L Zygo-max inferior	257.658	-118.7333	35.8061
L Zygo-max superior	266.5389	-127.9616	64.8187
L Dacryon	278.2704	-143.2663	76.5817
L Mid-torus inferior	269.0003	-139.1237	81.0924
L Mid-torus superior	261.5569	-137.4044	92.6482
L Fronto-malare orbitale	251.0051	-130.7508	72.8784
L Fronto-malare temporale	239.6072	-137.3328	69.0113
L Porion	217.6025	-176.1174	32.8366
L Zygo-temp superior	237.1504	-126.5799	43.3277
L Zygo-temp inferior	228.1907	-136.5157	35.7788

305-10433 Scan 4

Landmark	X	Y	Z
Inion	225.6643	-221.6199	38.135
Bregma	244.8606	-198.3556	84.4619
Glabella	276.8808	-144.608	87.8917
Nasion	284.1515	-136.727	73.9502
Rhinion	298.5172	-118.3611	62.1854
Nasospinale	304.5442	-110.0083	46.6392
Prosthion	310.5173	-99.8767	43.3237
R Prosthion-2	320.5	-107.1689	39.252
R Premax-max superior	291.3969	-135.8886	69.4292
R Zygo-max inferior	313.3911	-159.8733	39.4621
R Zygo-max superior	298.8272	-152.4532	66.7758
R Dacryon	283.247	-146.4586	75.6113
R Mid-torus inferior	285.5368	-152.1724	83.2782
R Mid-torus superior	286.5618	-154.1617	94.1266
R Fronto-malare orbitale	301.5498	-165.0273	73.8445
R Fronto-malare temporale	301.9629	-178.0689	74.232
R Porion	276.1255	-214.1808	39.4291
R Zygo-temp superior	314.1935	-178.6435	50.7081
R Zygo-temp inferior	311.7542	-190.1381	44.4124
L Prosthion-2	306.4839	-92.4391	37.6811
L Premax-max superior	286.4537	-124.9749	66.4042
L Zygo-max inferior	257.7437	-119.4915	35.7911
L Zygo-max superior	269.1598	-127.6248	65.3603
L Dacryon	277.9213	-142.4527	75.2157
L Mid-torus inferior	269.2385	-139.665	80.857
L Mid-torus superior	261.2325	-137.767	92.4175
L Fronto-malare orbitale	251.7915	-132.0801	72.8365
L Fronto-malare temporale	239.9862	-137.6778	68.9685
L Porion	218.5722	-176.8277	32.8806
L Zygo-temp superior	237.2446	-126.47	43.3351
L Zygo-temp inferior	230.3662	-136.2504	37.012

305-10433 Scan 5

Landmark	X	Y	Z
Inion	227.8056	-222.0435	38.1223
Bregma	245.8487	-198.2699	84.3311
Glabella	276.4296	-144.9191	88.861
Nasion	284.0546	-136.5203	74.0867
Rhinion	299.4255	-117.5204	61.9466
Nasospinale	304.807	-110.0283	47.094
Prosthion	316.6514	-97.2092	39.0882
R Prosthion-2	315.425	-104.3071	42.5665
R Premax-max superior	290.364	-128.8126	70.5205
R Zygo-max inferior	314.2603	-159.3491	39.5699
R Zygo-max superior	301.0165	-148.6581	66.6274
R Dacryon	284.6832	-147.5886	75.7598
R Mid-torus inferior	286.4452	-152.2548	83.4883
R Mid-torus superior	290.3885	-161.174	94.4321
R Fronto-malare orbitale	302.328	-164.8473	73.6153
R Fronto-malare temporale	302.8808	-178.0833	74.8375
R Porion	277.5605	-214.3531	39.5143
R Zygo-temp superior	316.503	-177.5357	50.6788
R Zygo-temp inferior	312.1451	-189.6218	44.1744
L Prosthion-2	305.6504	-93.1019	38.6324
L Premax-max superior	285.6312	-125.6064	66.6555
L Zygo-max inferior	258.6725	-119.7084	35.8433
L Zygo-max superior	272.0055	-130.1258	65.9845
L Dacryon	278.4813	-142.0531	75.7983
L Mid-torus inferior	268.929	-139.4252	80.6495
L Mid-torus superior	262.405	-139.342	92.7853
L Fronto-malare orbitale	251.502	-131.5361	72.7068
L Fronto-malare temporale	239.9387	-137.7473	68.4038
L Porion	219.1342	-176.8314	33.5021
L Zygo-temp superior	239.7466	-124.2739	43.6988
L Zygo-temp inferior	230.5061	-136.1314	36.8309

300-673 Scan 1

Landmark	X	Y	Z
Inion	148.4413	-227.2282	36.8833
Bregma	175.8135	-204.6992	68.1
Glabella	220.949	-174.9294	68.7738
Nasion	228.0247	-171.5244	56.8815
Rhinion	252.4687	-155.5267	42.7551
Nasospinale	270.7073	-145.2782	20.801
Prosthion			
R Prosthion-2			
R Premax-max superior	252.5895	-164.998	42.0651
R Zygo-max inferior	251.9515	-203.7755	22.6856
R Zygo-max superior	242.8295	-184.7656	43.6947
R Dacryon	226.097	-178.0348	52.1328
R Mid-torus inferior	228.1269	-185.9412	65.0124
R Mid-torus superior	227.3838	-192.099	73.0804
R Fronto-malare orbitale	237.9602	-204.9501	53.8999
R Fronto-malare temporale	231.9025	-214.7349	58.8191
R Porion	197.9795	-241.9672	24.0855
R Zygo-temp superior	245.7733	-224.4102	26.2983
R Zygo-temp inferior	235.1299	-233.0823	16.971
L Prosthion-2			
L Premax-max superior	244.3194	-153.1068	41.0292
L Zygo-max inferior	209.7007	-142.271	16.633
L Zygo-max superior	221.2163	-155.4501	40.2686
L Dacryon	221.5636	-170.9086	51.2194
L Mid-torus inferior	213.4037	-166.3308	61.6508
L Mid-torus superior	206.9322	-160.4297	67.8961
L Fronto-malare orbitale	201.1477	-150.6931	46.8885
L Fronto-malare temporale	189.2154	-151.1334	50.6038
L Porion	152.5165	-178.537	18.2205
L Zygo-temp superior	186.1761	-140.4174	17.7726
L Zygo-temp inferior	176.6693	-146.3938	9.3793

300-673 Scan 2

Landmark	X	Y	Z
Inion	147.2155	-234.9373	36.0193
Bregma	175.3236	-214.1602	66.7929
Glabella	219.2717	-183.3295	68.9739
Nasion	226.6677	-179.3215	56.7474
Rhinion	250.3508	-162.0912	43.0027
Nasospinale	267.9301	-150.0397	20.9217
Prosthion			
R Prosthion-2			
R Premax-max superior	250.311	-171.0331	41.1721
R Zygo-max inferior	249.7429	-208.3225	19.8241
R Zygo-max superior	240.8355	-191.4053	42.0319
R Dacryon	224.6431	-185.3772	51.2919
R Mid-torus inferior	227.417	-194.2615	63.7084
R Mid-torus superior	227.3801	-202.6248	70.3331
R Fronto-malare orbitale	236.8846	-211.905	51.3663
R Fronto-malare temporale	231.7742	-222.2177	55.4032
R Porion	197.2296	-248.7007	21.0307
R Zygo-temp superior	244.0051	-230.1865	22.6652
R Zygo-temp inferior	233.3363	-238.9813	13.4028
L Prosthion-2			
L Premax-max superior	241.5981	-159.7424	41.1134
L Zygo-max inferior	206.9294	-147.9922	19.458
L Zygo-max superior	218.9722	-161.5215	41.2752
L Dacryon	220.0071	-178.3019	50.9217
L Mid-torus inferior	212.2719	-173.0502	62.1528
L Mid-torus superior	202.1424	-167.4686	67.7286
L Fronto-malare orbitale	198.6978	-158.2863	49.1752
L Fronto-malare temporale	187.0902	-159.1875	52.7489
L Porion	150.5903	-184.5051	20.8447
L Zygo-temp superior	183.6513	-145.8316	20.407
L Zygo-temp inferior	175.616	-151.1909	10.9694

300-673 Scan 3

Landmark	X	Y	Z
Inion	164.9004	-231.6122	29.5327
Bregma	189.6646	-212.4592	62.8214
Glabella	231.8974	-181.1998	70.4213
Nasion	240.5262	-175.8431	58.6715
Rhinion	264.3045	-156.873	48.1118
Nasospinale	283.5997	-142.8181	28.4197
Prosthion			
R Prosthion-2			
R Premax-max superior	266.003	-164.9899	45.6927
R Zygo-max inferior	265.5109	-202.4536	21.0281
R Zygo-max superior	255.6272	-186.4445	44.7241
R Dacryon	238.7655	-181.6015	53.003
R Mid-torus inferior	240.1165	-191.2345	64.7539
R Mid-torus superior	239.8734	-195.8878	72.2392
R Fronto-malare orbitale	251.9039	-207.353	52.1945
R Fronto-malare temporale	246.8637	-217.9777	55.6633
R Porion	215.5414	-241.9816	13.2823
R Zygo-temp superior	262.7657	-222.265	23.0885
R Zygo-temp inferior	253.3916	-231.9202	13.0339
L Prosthion-2			
L Premax-max superior	256.9279	-153.9977	46.6064
L Zygo-max inferior	221.9602	-143.8353	21.0961
L Zygo-max superior	233.4692	-156.8977	43.8877
L Dacryon	233.4039	-174.8924	53.0795
L Mid-torus inferior	225.3369	-171.0211	63.91
L Mid-torus superior	219.708	-168.6897	70.374
L Fronto-malare orbitale	211.5502	-155.3197	50.9141
L Fronto-malare temporale	200.3552	-157.4518	55.6123
L Porion	167.9302	-181.028	11.8961
L Zygo-temp superior	199.0737	-140.7824	21.0999
L Zygo-temp inferior	189.6909	-147.3482	11.6035

300-673 Scan 4

Landmark	X	Y	Z
Inion	169.2267	-232.3862	29.6658
Bregma	191.9653	-210.5165	63.4173
Glabella	231.6838	-175.1244	70.2678
Nasion	239.0208	-169.3666	59.2126
Rhinion	261.1486	-148.4891	48.288
Nasospinale	278.5802	-132.9457	28.418
Prosthion			
R Prosthion-2			
R Premax-max superior	262.903	-157.0453	46.0057
R Zygo-max inferior	267.8155	-193.9788	22.3223
R Zygo-max superior	255.6199	-178.417	45.4141
R Dacryon	237.7899	-175.2956	53.6938
R Mid-torus inferior	240.0475	-184.6969	65.5266
R Mid-torus superior	241.0851	-188.805	72.3017
R Fronto-malare orbitale	253.6571	-199.6488	53.1109
R Fronto-malare temporale	249.4232	-210.7774	57.4944
R Porion	220.4773	-239.155	14.0755
R Zygo-temp superior	266.0792	-214.3068	24.4155
R Zygo-temp inferior	257.3647	-223.914	13.4757
L Prosthion-2			
L Premax-max superior	253.1985	-147.1098	46.3438
L Zygo-max inferior	217.9386	-139.3228	20.7762
L Zygo-max superior	231.0811	-151.8502	44.2332
L Dacryon	231.8997	-169.7772	53.6565
L Mid-torus inferior	223.4	-166.4581	63.7118
L Mid-torus superior	218.77	-163.6214	70.1932
L Fronto-malare orbitale	208.8517	-152.1354	50.9528
L Fronto-malare temporale	197.974	-155.0446	55.8994
L Porion	168.135	-181.8122	12.9111
L Zygo-temp superior	195.1866	-139.358	20.8505
L Zygo-temp inferior	188.4032	-145.0501	11.4265

300-673 Scan 5

Landmark	X	Y	Z
Inion	153.706	-213.0849	28.4516
Bregma	182.0881	-200.5642	62.3552
Glabella	229.8439	-177.5961	69.2937
Nasion	239.119	-174.3338	57.7735
Rhinion	266.0181	-160.8077	46.3097
Nasospinale	287.1827	-149.9621	26.8353
Prosthion			
R Prosthion-2			
R Premax-max superior			
R Zygo-max inferior	259.7471	-205.8116	20.834
R Zygo-max superior	252.4111	-187.8178	43.7784
R Dacryon	236.5132	-179.6943	52.0745
R Mid-torus inferior	235.8519	-189.5923	63.9443
R Mid-torus superior	235.5926	-193.9174	71.2238
R Fronto-malare orbitale	244.6964	-207.4922	51.6082
R Fronto-malare temporale	237.3092	-216.753	56.2583
R Porion	201.547	-235.8117	12.8191
R Zygo-temp superior	252.0263	-224.9003	22.9033
R Zygo-temp inferior	241.067	-232.0323	11.9532
L Prosthion-2			
L Premax-max superior			
L Zygo-max inferior	226.3956	-139.6304	19.5341
L Zygo-max superior	235.8233	-154.9639	42.9118
L Dacryon	232.1451	-172.3077	52.2099
L Mid-torus inferior	224.7113	-166.5445	62.3815
L Mid-torus superior	221.3475	-163.0534	68.8576
L Fronto-malare orbitale	214.6638	-149.3186	49.6543
L Fronto-malare temporale	203.0618	-149.2059	53.9181
L Porion	166.6152	-166.8802	10.734
L Zygo-temp superior	204.6907	-132.8805	19.6311
L Zygo-temp inferior	195.3131	-137.5274	9.2756

300-2512 Scan 1

Landmark	X	Y	Z
Inion	171.1802	-266.3208	22.3103
Bregma	191.2636	-245.7727	54.3278
Glabella	233.013	-218.3694	55.7676
Nasion	238.3045	-215.41	46.0537
Rhinion	256.843	-203.4787	32.0454
Nasospinale	266.7535	-198.1023	13.7386
Prosthion	270.7198	-196.406	6.7596
R Prosthion-2	272.6832	-201.684	6.6925
R Premax-max superior	253.2448	-210.8512	32.8295
R Zygo-max inferior	252.4417	-244.0005	14.8614
R Zygo-max superior	248.9963	-228.383	33.0687
R Dacryon	238.2555	-218.7446	43.4359
R Mid-torus inferior	236.1908	-227.6489	52.9262
R Mid-torus superior	237.3945	-233.3321	57.8762
R Fronto-malare orbitale	243.1959	-244.6737	44.439
R Fronto-malare temporale	239.7778	-250.0397	45.3987
R Porion	213.8172	-270.5465	17.3142
R Zygo-temp superior	249.505	-254.8722	20.2555
R Zygo-temp inferior	244.2017	-261.8446	16.9055
L Prosthion-2	265.4037	-192.0037	5.6077
L Premax-max superior	249.0399	-203.5084	32.3728
L Zygo-max inferior	220.014	-195.1829	11.4154
L Zygo-max superior	228.9583	-200.3584	31.4438
L Dacryon	235.0042	-214.8683	44.1897
L Mid-torus inferior	225.2289	-212.3042	51.6973
L Mid-torus superior	218.194	-209.5983	56.3978
L Fronto-malare orbitale	212.8538	-199.5724	41.0982
L Fronto-malare temporale	205.7237	-202.1552	39.1294
L Porion	178.8038	-220.9641	14.8771
L Zygo-temp superior	205.6058	-192.8276	15.3486
L Zygo-temp inferior	198.9893	-195.4558	12.9529

300-2512 Scan 2

Landmark	X	Y	Z
Inion	162.346	-265.6457	25.7634
Bregma	185.248	-248.5025	57.1326
Glabella	225.4505	-219.3775	57.1656
Nasion	228.9838	-215.5209	47.8518
Rhinion	246.0207	-201.5229	32.995
Nasospinale	254.6378	-194.345	14.7721
Prosthion	257.5732	-191.5424	6.9208
R Prosthion-2	259.9443	-197.3333	6.9372
R Premax-max superior	243.515	-208.7963	33.8608
R Zygo-max inferior	242.9579	-240.9825	14.1169
R Zygo-max superior	239.5726	-226.0092	33.1437
R Dacryon	229.5783	-218.3358	42.0319
R Mid-torus inferior	228.9785	-228.5932	53.567
R Mid-torus superior	230.8323	-233.7173	57.9616
R Fronto-malare orbitale	235.9875	-243.979	44.2896
R Fronto-malare temporale	232.6139	-249.4456	43.9427
R Porion	205.8855	-270.5961	16.789
R Zygo-temp superior	240.5125	-252.3213	17.8187
R Zygo-temp inferior	235.8527	-259.1555	14.8041
L Prosthion-2	252.5697	-187.8451	6.9857
L Premax-max superior	238.9172	-201.9199	33.7447
L Zygo-max inferior	207.0567	-193.6069	15.7522
L Zygo-max superior	218.6992	-199.7793	34.2311
L Dacryon	225.3607	-214.8527	44.185
L Mid-torus inferior	217.1919	-213.1603	53.8898
L Mid-torus superior	214.209	-210.2888	58.872
L Fronto-malare orbitale	203.0953	-200.466	45.2183
L Fronto-malare temporale	196.2976	-203.6713	44.4138
L Porion	168.818	-222.0998	19.1393
L Zygo-temp superior	194.3096	-192.1167	20.3561
L Zygo-temp inferior	187.3433	-196.3526	17.3019

300-2512 Scan 3

Landmark	X	Y	Z
Inion	174.6877	-270.274	21.3447
Bregma	194.015	-251.0404	54.7845
Glabella	234.0168	-222.2224	58.0099
Nasion	238.7434	-218.4729	49.0817
Rhinion	257.0719	-204.2096	35.8614
Nasospinale	266.7864	-197.0526	18.0989
Prosthion	270.489	-194.2725	10.9997
R Prosthion-2	272.9181	-200.4499	10.8928
R Premax-max superior	254.2096	-211.9895	36.2256
R Zygo-max inferior	254.6465	-243.5892	15.4421
R Zygo-max superior	250.3306	-229.1342	34.8857
R Dacryon	239.3291	-221.156	45.6528
R Mid-torus inferior	238.5766	-231.0309	54.9572
R Mid-torus superior	239.6221	-236.1082	59.3213
R Fronto-malare orbitale	245.9103	-246.5157	45.0597
R Fronto-malare temporale	242.0093	-252.5734	44.5767
R Porion	217.2442	-273.1503	16.1431
R Zygo-temp superior	252.4791	-254.6879	20.1617
R Zygo-temp inferior	247.532	-262.0598	16.6562
L Prosthion-2	265.1859	-190.5399	10.501
L Premax-max superior	249.5456	-204.8231	36.0752
L Zygo-max inferior	220.1744	-196.5113	15.5629
L Zygo-max superior	229.0953	-202.5434	35.0745
L Dacryon	235.5161	-217.7128	46.6602
L Mid-torus inferior	226.2431	-215.8934	54.6605
L Mid-torus superior	221.1155	-213.7072	59.4494
L Fronto-malare orbitale	212.9671	-203.1455	44.857
L Fronto-malare temporale	205.8912	-205.5079	42.3253
L Porion	179.6016	-224.0906	16.5164
L Zygo-temp superior	206.0817	-194.9596	19.8925
L Zygo-temp inferior	199.1781	-197.7333	16.1901

300-2512 Scan 4

Landmark	X	Y	Z
Inion	200.4376	-279.1224	19.7906
Bregma	216.5704	-258.601	53.1602
Glabella	250.2567	-222.4434	57.25
Nasion	254.0414	-217.5809	48.5403
Rhinion	269.4758	-200.4727	36.0056
Nasospinale	277.5819	-190.9521	18.6054
Prosthion	280.9907	-187.492	11.296
R Prosthion-2	284.6509	-192.9607	10.893
R Premax-max superior	268.2907	-208.3983	36.169
R Zygo-max inferior	274.475	-238.3268	14.7288
R Zygo-max superior	267.7897	-225.8408	34.4735
R Dacryon	255.2943	-220.5791	45.4778
R Mid-torus inferior	255.8681	-230.5081	54.1614
R Mid-torus superior	258.2776	-235.4577	58.4492
R Fronto-malare orbitale	266.8188	-244.1609	44.4986
R Fronto-malare temporale	263.8261	-250.4668	44.8524
R Porion	243.5292	-275.0161	14.0537
R Zygo-temp superior	274.7219	-250.3994	18.9082
R Zygo-temp inferior	271.4739	-258.1588	15.286
L Prosthion-2	274.9105	-184.0477	10.95
L Premax-max superior	262.3531	-201.6763	36.0748
L Zygo-max inferior	232.1134	-198.5866	15.7001
L Zygo-max superior	242.045	-203.4677	35.1058
L Dacryon	251.1958	-217.2345	46.1939
L Mid-torus inferior	241.6591	-217.9866	54.1455
L Mid-torus superior	235.4065	-215.6486	58.9292
L Fronto-malare orbitale	226.1772	-207.5896	44.5549
L Fronto-malare temporale	219.4613	-210.4593	41.6812
L Porion	197.8316	-233.8327	15.319
L Zygo-temp superior	217.8164	-200.3723	19.9235
L Zygo-temp inferior	211.4692	-204.4194	16.5936

300-2512 Scan 5

Landmark	X	Y	Z
Inion	201.2373	-280.6245	19.6881
Bregma	216.0525	-258.2612	53.4319
Glabella	248.6514	-221.0982	57.0184
Nasion	252.0282	-216.3851	48.536
Rhinion	266.8654	-198.7866	35.5403
Nasospinale	274.9869	-189.2184	17.8783
Prosthion	278.3226	-185.9356	10.853
R Prosthion-2	282.0245	-191.2047	10.4028
R Premax-max superior	266.0483	-206.8695	35.8236
R Zygo-max inferior	273.334	-237.6239	14.5373
R Zygo-max superior	266.0683	-224.1642	34.2075
R Dacryon	253.6176	-219.2771	45.2674
R Mid-torus inferior	254.3342	-229.2448	53.7622
R Mid-torus superior	256.8136	-233.7717	58.3688
R Fronto-malare orbitale	265.4409	-242.487	44.3839
R Fronto-malare temporale	263.3138	-248.8549	43.8239
R Porion	243.4971	-273.6973	14.3911
R Zygo-temp superior	273.3915	-249.1897	19.1617
R Zygo-temp inferior	270.2579	-256.7809	14.9465
L Prosthion-2	272.1253	-182.6581	10.3223
L Premax-max superior	259.7085	-200.3895	35.5189
L Zygo-max inferior	229.6961	-198.2401	15.589
L Zygo-max superior	248.989	-216.2885	46.0204
L Dacryon	249.087	-216.1719	46.0359
L Mid-torus inferior	239.3705	-217.0384	53.896
L Mid-torus superior	234.3641	-214.7415	58.6773
L Fronto-malare orbitale	223.7217	-207.3587	44.2957
L Fronto-malare temporale	217.328	-210.264	42.114
L Porion	197.0203	-234.1536	15.8109
L Zygo-temp superior	215.4527	-200.3998	19.5597
L Zygo-temp inferior	209.1428	-204.5913	15.9584

244-2415 Scan 1

Landmark	X	Y	Z
Inion	311.3018	15.5062	31.7275
Bregma	309.2526	59.0536	63.1026
Glabella	304.967	104.5729	48.7565
Nasion	305.4357	107.2822	45.9245
Rhinion	304.8427	119.0158	36.8177
Nasospinale	303.9709	133.7575	20.1851
Prosthion	304.2418	140.1504	15.3466
R Prosthion-2	309.3501	139.6178	15.1067
R Premax-max superior	308.6888	116.8216	38.0047
R Zygo-max inferior	339.2118	100.2115	12.7805
R Zygo-max superior	330.0355	109.8271	30.5836
R Dacryon	311.3411	107.74	41.5069
R Mid-torus inferior	319.9824	103.8516	51.4817
R Mid-torus superior	321.4211	102.1689	54.7792
R Fronto-malare orbitale	337.0822	101.228	41.6835
R Fronto-malare temporale	339.4111	95.0354	40.3375
R Porion	341.6748	49.9044	9.8017
R Zygo-temp superior	344.5155	90.0541	17.4724
R Zygo-temp inferior	347.6272	81.1743	11.877
L Prosthion-2	298.0346	139.067	14.8695
L Premax-max superior	299.6546	116.5611	37.4614
L Zygo-max inferior	271.4857	96.9512	12.23
L Zygo-max superior	276.7025	104.9366	29.1913
L Dacryon	298.404	106.6713	41.1507
L Mid-torus inferior	290.5849	102.6015	51.0448
L Mid-torus superior	290.133	101.1167	54.0782
L Fronto-malare orbitale	273.3698	98.482	40.4491
L Fronto-malare temporale	271.7158	91.348	40.7892
L Porion	275.4022	44.5027	9.4204
L Zygo-temp superior	267.4202	85.8567	16.8367
L Zygo-temp inferior	265.6217	76.6893	10.6097

244-2415 Scan 2

Landmark	X	Y	Z
Inion	317.8299	38.9663	35.644
Bregma	311.3966	65.1208	61.4183
Glabella	296.7617	125.421	51.518
Nasion	296.3223	127.3666	49.2826
Rhinion	293.6428	139.1164	40.4714
Nasospinale	290.3318	154.9639	24.7161
Prosthion	289.7819	160.3061	17.937
R Prosthion-2	294.6913	160.5439	19.2138
R Premax-max superior	298.573	137.0207	41.7605
R Zygo-max inferior	330.9189	126.3964	16.2118
R Zygo-max superior	319.9954	134.0446	34.2968
R Dacryon	302.0463	128.8169	44.8077
R Mid-torus inferior	312.0766	126.8524	55.3629
R Mid-torus superior	313.7062	124.7197	58.082
R Fronto-malare orbitale	328.9637	126.4304	45.0772
R Fronto-malare temporale	332.0095	120.9977	45.4341
R Porion	341.155	77.4667	11.9386
R Zygo-temp superior	338.2603	117.1265	20.3729
R Zygo-temp inferior	341.7532	110.0356	14.1121
L Prosthion-2	284.5082	158.6608	18.7577
L Premax-max superior	289.4255	135.9873	41.1543
L Zygo-max inferior	264.5392	112.5746	15.6995
L Zygo-max superior	267.5218	121.1536	32.8955
L Dacryon	289.7442	125.6992	44.2981
L Mid-torus inferior	279.1363	119.2434	54.1195
L Mid-torus superior	278.7969	117.0977	57.4517
L Fronto-malare orbitale	266.5091	113.8654	43.6792
L Fronto-malare temporale	265.6734	106.4852	40.9844
L Porion	275.7637	62.1821	12.3854
L Zygo-temp superior	262.2732	100.5426	19.7348
L Zygo-temp inferior	262.0591	91.7816	13.6807

244-2415 Scan 3

Landmark	X	Y	Z
Inion	329.0669	-34.4942	35.4326
Bregma	327.3692	-7.2189	63.5424
Glabella	323.3221	55.0061	53.1409
Nasion	322.7427	56.9728	50.928
Rhinion	322.4184	69.1016	41.7437
Nasospinale	322.5767	84.7531	26.4913
Prosthion	323.1065	90.4727	21.0801
R Prosthion-2	327.6208	89.6247	21.1441
R Premax-max superior	327.2909	66.382	43.4974
R Zygo-max inferior	357.6763	49.7043	18.1295
R Zygo-max superior	348.249	59.6465	36.6171
R Dacryon	329.1208	57.1833	46.6972
R Mid-torus inferior	340.0929	53.3402	57.7387
R Mid-torus superior	340.0563	51.5672	60.4061
R Fronto-malare orbitale	354.9221	50.6502	47.6247
R Fronto-malare temporale	357.2263	45.1217	48.2597
R Porion	360.5401	0.5771	16.0332
R Zygo-temp superior	362.8793	39.8663	23.4488
R Zygo-temp inferior	365.9587	32.4547	17.4771
L Prosthion-2	317.5236	89.3071	20.22
L Premax-max superior	317.1962	66.3363	42.5186
L Zygo-max inferior	290.6414	47.5906	15.6576
L Zygo-max superior	293.6448	55.3776	34.1794
L Dacryon	316.1086	56.6048	46.124
L Mid-torus inferior	304.8636	51.6367	55.8915
L Mid-torus superior	303.8654	50.2427	58.565
L Fronto-malare orbitale	291.4276	48.1829	44.4803
L Fronto-malare temporale	289.3445	41.5722	43.3386
L Porion	292.2603	-3.7358	13.2231
L Zygo-temp superior	285.2751	36.5903	20.6236
L Zygo-temp inferior	283.841	27.4898	14.9037

244-2415 Scan 4

Landmark	X	Y	Z
Inion	324.2418	-28.5969	31.7364
Bregma	326.1498	-0.3579	59.421
Glabella	324.8166	60.6326	48.791
Nasion	324.9019	63.4232	45.6324
Rhinion	324.4745	74.9952	37.132
Nasospinale	323.7425	91.1403	20.5533
Prosthion	325.3101	95.8415	14.8478
R Prosthion-2	329.9149	95.3361	14.9733
R Premax-max superior	329.2997	72.1851	37.9612
R Zygo-max inferior	357.2918	54.0371	11.7356
R Zygo-max superior	348.8962	64.1354	30.1813
R Dacryon	330.781	63.2906	40.8358
R Mid-torus inferior	341.5028	58.51	51.1626
R Mid-torus superior	342.0828	57.3465	54.4531
R Fronto-malare orbitale	356.3839	55.0507	40.9123
R Fronto-malare temporale	357.9377	49.0634	41.5332
R Porion	357.0433	4.4714	9.3252
R Zygo-temp superior	362.6557	43.6608	16.5389
R Zygo-temp inferior	364.5136	36.0915	10.5496
L Prosthion-2	319.1472	95.6277	14.8169
L Premax-max superior	319.3952	72.7509	37.6
L Zygo-max inferior	289.4652	55.0106	13.3474
L Zygo-max superior	294.7215	63.0692	30.6185
L Dacryon	317.5275	62.9778	41.0894
L Mid-torus inferior	307.0042	58.9719	51.8889
L Mid-torus superior	307.0062	57.5611	54.853
L Fronto-malare orbitale	292.6133	56.2992	41.162
L Fronto-malare temporale	290.0196	49.4553	40.0344
L Porion	289.113	3.7592	11.4836
L Zygo-temp superior	285.2533	43.9836	18.3006
L Zygo-temp inferior	282.7243	35.4244	12.4994

244-2415 Scan 5

Landmark	X	Y	Z
Inion	315.1942	-34.737	29.236
Bregma	314.9091	-7.4167	58.9251
Glabella	312.2559	54.2534	50.2434
Nasion	312.3221	56.7228	47.6894
Rhinion	311.9632	68.7285	39.2187
Nasospinale	311.7465	84.3879	23.3733
Prosthion	312.4628	90.4815	18.4216
R Prosthion-2	317.0741	89.9917	18.123
R Premax-max superior	316.4423	66.192	40.2944
R Zygo-max inferior	345.5371	49.5229	13.5779
R Zygo-max superior	337.0627	58.5428	32.5067
R Dacryon	318.5316	56.9267	43.1583
R Mid-torus inferior	329.6388	52.2041	53.1057
R Mid-torus superior	328.6348	50.3707	56.6071
R Fronto-malare orbitale	343.8082	49.2809	42.6002
R Fronto-malare temporale	346.205	43.6565	43.0063
R Porion	346.9011	-0.0777	9.9118
R Zygo-temp superior	350.644	39.1735	18.1327
R Zygo-temp inferior	352.78	31.2862	11.369
L Prosthion-2	306.3846	89.7555	17.8836
L Premax-max superior	306.9278	66.243	39.7993
L Zygo-max inferior	278.2498	48.7434	13.8883
L Zygo-max superior	282.6557	56.7938	32.1888
L Dacryon	305.2638	56.3154	42.3169
L Mid-torus inferior	294.5024	51.3522	51.8709
L Mid-torus superior	293.8871	50.5065	55.9336
L Fronto-malare orbitale	280.2669	49.4585	42.1956
L Fronto-malare temporale	277.8601	42.6315	40.6032
L Porion	278.4363	-1.701	10.9154
L Zygo-temp superior	272.6915	37.1944	18.6966
L Zygo-temp inferior	271.1217	29.1634	12.6153

137-2112 Scan 1

Landmark	X	Y	Z
Inion	168.3115	-264.6326	33.4461
Bregma	198.5462	-242.5914	51.7486
Glabella	234.6754	-221.1416	45.9663
Nasion	238.5604	-219.0885	41.1764
Rhinion	252.2233	-210.5427	35.6447
Nasospinale	266.3571	-203.1599	25.2925
Prosthion	270.7256	-201.6578	23.2742
R Prosthion-2	271.7524	-205.0242	22.6702
R Premax-max superior	250.0523	-217.384	33.8154
R Zygo-max inferior	253.6193	-240.826	12.4549
R Zygo-max superior	248.6376	-230.6076	29.527
R Dacryon	238.0924	-224.3931	38.4596
R Mid-torus inferior	235.1393	-236.5358	47.0657
R Mid-torus superior	232.6304	-237.1903	50.1241
R Fronto-malare orbitale	242.4786	-245.8874	40.5421
R Fronto-malare temporale	243.0357	-248.911	38.8586
R Porion	200.6955	-270.1143	15.8319
R Zygo-temp superior	246.6306	-256.7253	18.6158
R Zygo-temp inferior	235.7148	-266.6354	11.3281
L Prosthion-2	267.455	-198.1931	23.4556
L Premax-max superior	245.5899	-207.5947	33.8523
L Zygo-max inferior	225.9755	-196.3349	11.0903
L Zygo-max superior	232.2562	-205.0823	28.2785
L Dacryon	234.8096	-214.1936	37.6175
L Mid-torus inferior	221.7523	-215.2103	45.7508
L Mid-torus superior	216.3226	-214.4725	48.8601
L Fronto-malare orbitale	213.7933	-204.7359	39.5738
L Fronto-malare temporale	212.1992	-202.2364	39.6254
L Porion	174.1966	-229.4332	16.5791
L Zygo-temp superior	206.5502	-195.6308	17.0024
L Zygo-temp inferior	187.9315	-206.1605	9.9495

137-2112 Scan 2

Landmark	X	Y	Z
Inion	172.5336	-272.4017	30.6878
Bregma	201.1478	-247.6699	50.8957
Glabella	230.9288	-220.3895	45.6589
Nasion	233.5271	-218.0475	41.7404
Rhinion	246.6254	-206.5605	35.5903
Nasospinale	259.651	-196.5928	25.2693
Prosthion	262.6295	-193.4803	22.6274
R Prosthion-2	264.4066	-196.8364	21.8841
R Premax-max superior	246.2303	-213.2622	33.3963
R Zygo-max inferior	253.0452	-236.0504	9.9553
R Zygo-max superior	245.4616	-224.6707	28.7256
R Dacryon	235.4555	-222.5395	37.7353
R Mid-torus inferior	234.4901	-235.1836	45.439
R Mid-torus superior	233.3595	-238.1517	47.9712
R Fronto-malare orbitale	244.0703	-243.3698	37.2966
R Fronto-malare temporale	242.947	-246.1707	36.9637
R Porion	203.6384	-271.3203	10.149
R Zygo-temp superior	248.4711	-252.3841	14.807
R Zygo-temp inferior	238.9044	-262.4144	7.2679
L Prosthion-2	259.8493	-191.0126	22.6297
L Premax-max superior	240.3087	-205.2888	34.305
L Zygo-max inferior	217.42	-195.2726	12.2602
L Zygo-max superior	228.4013	-204.4461	29.4755
L Dacryon	228.0593	-216.1221	39.5474
L Mid-torus inferior	214.4992	-214.8925	46.3343
L Mid-torus superior	211.8538	-215.0121	48.1913
L Fronto-malare orbitale	208.2423	-205.9301	40.0602
L Fronto-malare temporale	205.93	-204.9752	40.621
L Porion	173.5213	-238.8045	15.0397
L Zygo-temp superior	198.3699	-198.6758	18.9857
L Zygo-temp inferior	185.7446	-206.2422	10.8434

137-2112 Scan 3

Landmark	X	Y	Z
Inion	164.6042	-267.5155	30.8084
Bregma	193.4893	-243.6113	50.8297
Glabella	227.191	-217.4411	44.5123
Nasion	231.0805	-213.9909	39.6254
Rhinion	242.5798	-205.5695	36.0123
Nasospinale	256.4118	-196.9648	25.8912
Prosthion	260.2475	-194.1424	23.0877
R Prosthion-2	261.6433	-197.816	22.7639
R Premax-max superior	242.4215	-212.6008	33.7585
R Zygo-max inferior	247.6036	-235.662	11.3635
R Zygo-max superior	240.0431	-222.798	30.2047
R Dacryon	230.5461	-220.9936	38.3076
R Mid-torus inferior	228.9061	-233.1441	46.5972
R Mid-torus superior	226.9665	-236.3374	49.5806
R Fronto-malare orbitale	237.8631	-242.3466	39.6569
R Fronto-malare temporale	236.9313	-244.8298	39.4499
R Porion	198.9197	-270.7921	15.8109
R Zygo-temp superior	242.4592	-251.7731	17.4482
R Zygo-temp inferior	233.0002	-261.9561	9.3787
L Prosthion-2	257.3204	-191.455	22.8206
L Premax-max superior	236.3522	-203.6682	34.3168
L Zygo-max inferior	215.3045	-193.9465	11.2557
L Zygo-max superior	223.3456	-202.5098	28.892
L Dacryon	224.7758	-212.779	37.0804
L Mid-torus inferior	213.3618	-213.3828	46.2816
L Mid-torus superior	208.8042	-213.3942	48.8716
L Fronto-malare orbitale	204.2903	-202.7413	39.4073
L Fronto-malare temporale	201.6255	-202.4282	39.2649
L Porion	167.8171	-235.1014	14.2132
L Zygo-temp superior	195.8571	-195.5076	17.5647
L Zygo-temp inferior	182.0504	-204.298	9.3443

137-2112 Scan 4

Landmark	X	Y	Z
Inion	170.8118	-271.3627	31.2362
Bregma	198.9816	-246.6882	50.1256
Glabella	229.4794	-220.0206	44.6469
Nasion	232.3019	-218.0132	41.0737
Rhinion	245.8847	-206.5839	34.1153
Nasospinale	259.6153	-197.67	24.4817
Prosthion	262.818	-194.688	21.3092
R Prosthion-2	264.2923	-198.1684	20.8517
R Premax-max superior	245.864	-213.9301	32.2825
R Zygo-max inferior	252.6022	-237.1534	9.9858
R Zygo-max superior	244.5227	-225.0815	28.3559
R Dacryon	234.6335	-222.4302	36.9518
R Mid-torus inferior	233.0599	-234.8461	45.0039
R Mid-torus superior	231.3142	-238.2529	48.2328
R Fronto-malare orbitale	242.2964	-243.5308	38.1727
R Fronto-malare temporale	241.9568	-246.2142	37.7021
R Porion	204.3723	-272.9059	14.5323
R Zygo-temp superior	247.4851	-252.5118	15.877
R Zygo-temp inferior	238.2639	-264.0593	8.2964
L Prosthion-2	259.8813	-191.8255	21.1932
L Premax-max superior	239.5961	-204.8268	32.709
L Zygo-max inferior	218.0246	-195.2679	10.9807
L Zygo-max superior	226.6925	-204.3452	27.717
L Dacryon	226.7683	-215.3386	35.5232
L Mid-torus inferior	216.6063	-215.5996	44.8893
L Mid-torus superior	212.853	-215.7319	47.4053
L Fronto-malare orbitale	207.322	-205.5656	38.3196
L Fronto-malare temporale	205.1245	-204.4235	38.4903
L Porion	171.5537	-238.0779	13.5335
L Zygo-temp superior	198.918	-198.3407	16.5427
L Zygo-temp inferior	185.8098	-207.0482	7.9681

137-2112 Scan 5

Landmark	X	Y	Z
Inion	204.4689	-280.8884	31.8789
Bregma	223.7099	-249.2237	50.8914
Glabella	248.3089	-216.0353	45.6084
Nasion	250.7699	-213.1703	41.7066
Rhinion	261.2427	-199.2257	35.5064
Nasospinale	272.5851	-187.319	25.673
Prosthion	275.1378	-183.8997	23.131
R Prosthion-2	277.51	-186.8323	22.4045
R Premax-max superior	263.2204	-206.53	33.5524
R Zygo-max inferior	276.0832	-227.9338	12.5299
R Zygo-max superior	263.825	-217.0121	30.2347
R Dacryon	254.0936	-217.6343	37.912
R Mid-torus inferior	255.4039	-229.603	46.6867
R Mid-torus superior	254.2471	-231.7118	49.5155
R Fronto-malare orbitale	266.2622	-235.9087	40.3847
R Fronto-malare temporale	266.7865	-238.4932	39.8953
R Porion	237.6153	-274.4304	15.8421
R Zygo-temp superior	274.3871	-243.6322	18.7997
R Zygo-temp inferior	269.086	-256.8194	10.6782
L Prosthion-2	271.708	-181.9949	22.4176
L Premax-max superior	254.4522	-199.2773	33.5021
L Zygo-max inferior	232.3169	-195.807	10.7434
L Zygo-max superior	241.8509	-201.9742	27.8766
L Dacryon	245.1857	-212.1176	36.2244
L Mid-torus inferior	234.7214	-214.8848	45.3832
L Mid-torus superior	230.8861	-215.7724	47.6094
L Fronto-malare orbitale	222.887	-207.1568	38.293
L Fronto-malare temporale	220.7435	-207.2225	37.8385
L Porion	198.1945	-247.7703	14.193
L Zygo-temp superior	214.8771	-202.7793	16.0121
L Zygo-temp inferior	203.5424	-213.9616	7.832

170-2414 Scan 1

Landmark	X	Y	Z
Inion	309.0877	21.4233	27.6886
Bregma	307.9861	54.4323	50.5722
Glabella	306.2907	87.9548	39.7668
Nasion	305.471	92.4329	34.0122
Rhinion	304.9203	105.6974	24.851
Nasospinale	304.0756	108.1887	11.7607
Prosthion	304.4023	114.3001	8.941
R Prosthion-2	308.4261	112.8208	7.6269
R Premax-max superior	309.1696	101.2274	24.748
R Zygo-max inferior	324.2902	86.5808	4.4167
R Zygo-max superior	319.8015	94.8196	17.267
R Dacryon	308.5146	91.7674	28.3475
R Mid-torus inferior	313.9697	85.5401	38.7438
R Mid-torus superior	315.1357	83.1329	43.5973
R Fronto-malare orbitale	325.5353	85.4648	30.9336
R Fronto-malare temporale	327.0891	84.4669	30.6104
R Porion	327.1125	45.9576	8.4332
R Zygo-temp superior	332.9636	78.299	10.1703
R Zygo-temp inferior	337.2233	68.3581	9.6576
L Prosthion-2	300.4076	113.0085	7.9133
L Premax-max superior	301.6949	100.6209	25.6872
L Zygo-max inferior	286.5473	86.7438	5.9259
L Zygo-max superior	290.0457	93.7104	18.7958
L Dacryon	302.8648	91.8629	29.294
L Mid-torus inferior	296.7813	83.0714	39.1028
L Mid-torus superior	298.6711	81.2485	44.6581
L Fronto-malare orbitale	287.6566	82.888	33.5126
L Fronto-malare temporale	286.767	81.813	34.3438
L Porion	285.9353	44.6981	12.1297
L Zygo-temp superior	278.701	76.7579	12.8604
L Zygo-temp inferior	276.0202	64.7706	12.0785

170-2414 Scan 2

Landmark	X	Y	Z
Inion	308.9776	55.4599	25.4724
Bregma	301.5165	84.1789	52.1593
Glabella	296.3935	117.9145	46.0034
Nasion	294.6399	123.4258	40.2227
Rhinion	292.4142	137.3894	32.8229
Nasospinale	292.0964	141.868	20.439
Prosthion	291.1392	147.6467	18.2408
R Prosthion-2	295.6105	147.2136	16.9977
R Premax-max superior	296.6259	132.9179	33.3381
R Zygo-max inferior	315.1626	123.3757	10.927
R Zygo-max superior	309.4323	129.947	25.4025
R Dacryon	297.6047	124.2212	35.0869
R Mid-torus inferior	305.7021	116.4874	45.2876
R Mid-torus superior	304.5749	114.3207	49.4414
R Fronto-malare orbitale	315.3179	119.3889	38.6545
R Fronto-malare temporale	316.3382	119.2992	38.8324
R Porion	324.4926	84.624	11.9648
R Zygo-temp superior	325.5247	116.3334	16.7625
R Zygo-temp inferior	329.8857	107.2079	15.1669
L Prosthion-2	287.4626	145.8944	17.6084
L Premax-max superior	289.5563	131.8405	32.831
L Zygo-max inferior	277.8554	118.4424	11.1257
L Zygo-max superior	279.5221	123.9341	24.6102
L Dacryon	292.0682	123.1355	35.6672
L Mid-torus inferior	290.0907	114.869	44.1183
L Mid-torus superior	288.5096	110.6596	49.3639
L Fronto-malare orbitale	277.8137	111.5513	38.0498
L Fronto-malare temporale	276.6432	110.6355	37.9621
L Porion	282.8443	76.5678	10.9562
L Zygo-temp superior	270.8923	107.4693	15.6591
L Zygo-temp inferior	269.3852	95.142	13.5424

170-2414 Scan 3

Landmark	X	Y	Z
Inion	321.9362	48.4272	27.7239
Bregma	313.6919	76.4553	52.3713
Glabella	304.5663	109.7307	46.2836
Nasion	302.7386	115.3233	40.769
Rhinion	298.76	128.6583	33.6167
Nasospinale	297.2153	132.6333	21.0497
Prosthion	295.6091	138.7342	18.4547
R Prosthion-2	299.9103	138.8141	17.3006
R Premax-max superior	303.7931	116.8012	38.3517
R Zygo-max inferior	322.5657	117.9938	12.278
R Zygo-max superior	316.5861	122.6732	25.1862
R Dacryon	305.4048	116.0225	35.2255
R Mid-torus inferior	313.0404	108.8465	46.8131
R Mid-torus superior	313.6517	106.3882	49.6264
R Fronto-malare orbitale	323.1516	112.4737	38.3332
R Fronto-malare temporale	324.5377	112.6386	38.3224
R Porion	335.2043	78.9275	11.4491
R Zygo-temp superior			
R Zygo-temp inferior	338.7299	101.9356	14.6853
L Prosthion-2	292.1335	136.1579	17.7316
L Premax-max superior	301.2408	116.0001	39.2939
L Zygo-max inferior	285.3213	108.7589	11.591
L Zygo-max superior	286.9304	113.9018	25.7503
L Dacryon	300.2194	114.6748	35.9946
L Mid-torus inferior	298.9961	105.8148	45.0266
L Mid-torus superior	300.1761	103.7082	49.4943
L Fronto-malare orbitale	287.0315	101.6629	38.7256
L Fronto-malare temporale	286.0806	100.0939	38.7114
L Porion	294.1698	67.0908	11.7476
L Zygo-temp superior			
L Zygo-temp inferior	279.8118	84.2801	15.112

170-2414 Scan 4

Landmark	X	Y	Z
Inion	330.709	-9.8773	29.0114
Bregma	330.7982	20.6846	49.8845
Glabella	329.1788	54.2195	41.1527
Nasion	328.6434	59.8227	34.9368
Rhinion	327.5156	73.1382	26.5137
Nasospinale	325.7628	76.2671	14.0408
Prosthion	325.9258	82.5461	11.5308
R Prosthion-2	330.0048	81.17	10.0684
R Premax-max superior	329.7177	60.9312	32.7151
R Zygo-max inferior	345.7729	55.5386	4.3793
R Zygo-max superior	341.9559	62.8783	18.4316
R Dacryon	330.7776	58.6008	28.8994
R Mid-torus inferior	336.137	52.605	39.3085
R Mid-torus superior	336.0687	51.5141	43.7389
R Fronto-malare orbitale	347.8915	52.2549	31.19
R Fronto-malare temporale	349.6153	52.009	30.3202
R Porion	348.3228	14.1027	6.7643
R Zygo-temp superior	354.9507	45.5098	9.5434
R Zygo-temp inferior	357.7473	35.8504	7.8768
L Prosthion-2	321.7573	80.7208	10.2068
L Premax-max superior	326.9046	60.9852	33.3231
L Zygo-max inferior	307.2238	55.0449	8.0701
L Zygo-max superior	311.4237	60.9421	21.0609
L Dacryon	325.3829	57.5955	31.3301
L Mid-torus inferior	323.0309	52.0585	40.2139
L Mid-torus superior	322.3397	49.619	45.4573
L Fronto-malare orbitale	309.8889	50.2559	35.0223
L Fronto-malare temporale	308.7123	49.3596	35.6623
L Porion	306.9567	13.0056	11.7928
L Zygo-temp superior	298.9519	43.9408	14.3272
L Zygo-temp inferior	297.2413	33.4586	13.9319

170-2414 Scan 5

Landmark	X	Y	Z
Inion	317.7989	-13.4782	27.1201
Bregma	314.4225	17.8023	51.1602
Glabella	314.4228	51.3399	42.0383
Nasion	313.2838	56.4503	36.198
Rhinion	312.6261	70.0932	27.3382
Nasospinale	312.2922	73.4888	14.9613
Prosthion	312.3203	79.3078	12.8626
R Prosthion-2	316.4639	78.0568	11.4263
R Premax-max superior	314.7827	57.8438	33.4274
R Zygo-max inferior	333.2012	52.2419	7.134
R Zygo-max superior	328.4466	60.0099	20.3358
R Dacryon	316.3488	56.2313	30.802
R Mid-torus inferior	320.4758	50.0619	40.0361
R Mid-torus superior	320.4095	47.6277	45.7585
R Fronto-malare orbitale	332.5771	49.4898	33.4856
R Fronto-malare temporale	334.6779	49.3036	33.0784
R Porion	336.216	11.5298	9.8272
R Zygo-temp superior	341.7612	43.2888	12.7208
R Zygo-temp inferior	345.4279	33.4481	11.5271
L Prosthion-2	308.2956	77.2254	10.9958
L Premax-max superior	312.3917	57.9532	34.3227
L Zygo-max inferior	294.3247	50.2676	7.3393
L Zygo-max superior	297.7895	58.1414	21.2811
L Dacryon	311.3022	55.7921	33.4426
L Mid-torus inferior	307.8802	48.8097	41.003
L Mid-torus superior	308.383	48.1496	45.2546
L Fronto-malare orbitale	294.9192	46.9725	35.0545
L Fronto-malare temporale	294.2709	45.5065	35.3316
L Porion	294.3742	10.242	10.9139
L Zygo-temp superior	286.493	41.2295	14.24
L Zygo-temp inferior	283.7153	30.533	13.1946

079-3924 Scan 1

Landmark	X	Y	Z
Inion	187.7558	-200.0107	20.8481
Bregma	204.1724	-189.2289	29.3222
Glabella	221.6134	-179.5423	19.7372
Nasion	222.0427	-179.0799	18.5419
Rhinion			
Nasospinale	223.6843	-179.2436	6.615
Prosthion	224.3677	-179.0134	4.5422
R Prosthion-2	224.3353	-180.9928	4.6395
R Premax-max superior	224.2119	-179.8879	13.3899
R Zygo-max inferior	219.8188	-193.9627	7.9821
R Zygo-max superior	223.006	-190.1752	12.7892
R Dacryon	221.5919	-181.5483	15.7161
R Mid-torus inferior	222.0435	-184.0724	20.6823
R Mid-torus superior	221.8088	-184.4521	22.2571
R Fronto-malare orbitale	222.5586	-191.2416	18.9219
R Fronto-malare temporale	222.0211	-191.4538	19.8122
R Porion	203.079	-202.4245	11.3
R Zygo-temp superior	218.7256	-197.5025	10.4149
R Zygo-temp inferior	215.1644	-200.4265	9.8681
L Prosthion-2	222.5552	-177.1456	4.5786
L Premax-max superior	222.9092	-177.0618	12.6986
L Zygo-max inferior	208.11	-175.8616	5.883
L Zygo-max superior	212.9659	-174.3692	11.2619
L Dacryon	219.8275	-177.8367	15.3579
L Mid-torus inferior	217.1718	-176.0347	20.0818
L Mid-torus superior	216.5663	-175.9203	21.6982
L Fronto-malare orbitale	211.5175	-173.0379	16.8496
L Fronto-malare temporale	210.6819	-171.8819	17.8213
L Porion	191.3554	-185.8663	8.935
L Zygo-temp superior	203.7393	-173.7848	7.8136
L Zygo-temp inferior	200.6399	-175.7028	7.3609

079-3924 Scan 2

Landmark	X	Y	Z
Inion	331.4524	22.0872	12.3069
Bregma	330.5335	39.5993	24.1863
Glabella	329.6364	62.2752	19.2223
Nasion	329.6071	62.7403	18.4299
Rhinion			
Nasospinale	329.4799	66.3944	7.2382
Prosthion	329.0993	67.5314	5.8274
R Prosthion-2	331.2045	67.0478	5.5623
R Premax-max superior	330.6816	64.6735	14.0871
R Zygo-max inferior	340.3053	55.8826	5.2255
R Zygo-max superior	339.2284	59.2278	11.4648
R Dacryon	331.5808	61.7605	14.8753
R Mid-torus inferior	334.797	59.5233	20.1856
R Mid-torus superior	334.9861	58.4527	21.5603
R Fronto-malare orbitale	340.9206	57.4143	17.0213
R Fronto-malare temporale	340.9353	56.4902	17.7189
R Porion	343.7532	33.4677	7.2701
R Zygo-temp superior	344.3216	52.5019	6.914
R Zygo-temp inferior	344.2673	48.6014	5.9127
L Prosthion-2	327.1586	66.6604	5.9213
L Premax-max superior	327.9814	65.1882	14.0204
L Zygo-max inferior	319.1684	54.9297	5.1346
L Zygo-max superior	319.6137	58.5129	11.9421
L Dacryon	327.6396	61.6279	15.0555
L Mid-torus inferior	324.6803	58.9341	20.3188
L Mid-torus superior	324.7514	58.6401	21.5499
L Fronto-malare orbitale	319.0243	56.4672	16.96
L Fronto-malare temporale	318.3513	55.9651	17.4244
L Porion	317.86	31.7986	8.1352
L Zygo-temp superior	316.0387	51.0801	6.7936
L Zygo-temp inferior	315.9229	46.7605	5.7352

079-3924 Scan 3

Landmark	X	Y	Z
Inion	299.7735	43.6667	12.8965
Bregma	298.1316	61.3984	25.2101
Glabella	296.6315	83.8428	19.8543
Nasion	296.658	84.3298	19.1609
Rhinion			
Nasospinale	296.4963	88.1319	7.7894
Prosthion	295.6214	89.1125	5.8973
R Prosthion-2	298.2906	88.3952	6.0384
R Premax-max superior	297.6854	86.6119	14.8145
R Zygo-max inferior	307.458	78.0673	6.2966
R Zygo-max superior	306.1261	80.7168	11.5822
R Dacryon	299.0576	83.8194	15.2505
R Mid-torus inferior	302.0409	81.104	20.3918
R Mid-torus superior	302.2404	80.2259	21.7093
R Fronto-malare orbitale	308.2491	79.22	17.6299
R Fronto-malare temporale	308.8819	78.5578	17.8035
R Porion	311.6454	54.8995	8.1842
R Zygo-temp superior	311.0132	74.3771	7.2899
R Zygo-temp inferior	311.8376	70.5455	6.5309
L Prosthion-2	294.2129	88.1825	6.4538
L Premax-max superior	295.1681	86.8459	14.4911
L Zygo-max inferior	286.5551	76.2731	6.4856
L Zygo-max superior	287.094	79.8911	12.8766
L Dacryon	294.9718	83.2729	15.4085
L Mid-torus inferior	291.9229	80.3625	21.2682
L Mid-torus superior	291.42	79.4527	21.9844
L Fronto-malare orbitale	286.4315	77.7472	17.69
L Fronto-malare temporale	286.6417	76.6506	18.8903
L Porion	286.3438	52.712	9.4232
L Zygo-temp superior	283.3666	72.0959	7.4118
L Zygo-temp inferior	283.4207	67.8139	6.5747

079-3924 Scan 4

Landmark	X	Y	Z
Inion	323.5391	44.4729	11.4744
Bregma	318.6922	61.4829	23.6966
Glabella	313.1643	83.1849	18.1105
Nasion	312.712	83.4123	17.5552
Rhinion			
Nasospinale	311.4957	86.9842	5.7543
Prosthion	311.0996	88.081	4.2436
R Prosthion-2	313.8732	87.891	4.2669
R Premax-max superior	313.6577	86.1024	12.8338
R Zygo-max inferior	324.9551	79.1659	4.3858
R Zygo-max superior	322.7661	82.4156	10.2868
R Dacryon	314.9004	83.1639	13.7321
R Mid-torus inferior	318.6049	81.6313	19.0405
R Mid-torus superior	318.7324	80.7145	20.1131
R Fronto-malare orbitale	325.0045	81.07	15.9687
R Fronto-malare temporale	325.4478	80.1485	16.6481
R Porion	333.3841	57.3942	7.6164
R Zygo-temp superior	329.1028	76.6783	6.4306
R Zygo-temp inferior	330.5001	73.085	4.8295
L Prosthion-2	309.8449	86.9631	4.4902
L Premax-max superior	310.8022	85.677	12.8001
L Zygo-max inferior	304.7	73.7711	4.3711
L Zygo-max superior	304.6202	77.2342	11.1199
L Dacryon	311.5627	82.1839	14.0879
L Mid-torus inferior	309.4374	78.3059	19.1504
L Mid-torus superior	308.6966	78.0704	20.0243
L Fronto-malare orbitale	304.1808	75.1842	15.9781
L Fronto-malare temporale	303.8748	73.8514	16.7133
L Porion	308.5157	50.4635	7.1625
L Zygo-temp superior	302.3883	69.1072	5.6265
L Zygo-temp inferior	303.1088	66.0711	4.7323

079-3924 Scan 5

Landmark	X	Y	Z
Inion	316.3243	49.2418	22.9022
Bregma	312.7378	66.0723	35.2132
Glabella	308.6902	88.6572	30.5576
Nasion	308.7388	88.9779	29.9506
Rhinion			
Nasospinale	308.4286	92.9822	18.9903
Prosthion	308.1254	93.7989	17.6322
R Prosthion-2	310.1955	93.2858	17.173
R Premax-max superior	309.8691	91.3374	25.7445
R Zygo-max inferior	320.5683	83.9343	16.7913
R Zygo-max superior	318.8169	87.5139	22.8112
R Dacryon	310.8076	88.7386	26.4626
R Mid-torus inferior	314.2777	86.3627	32.008
R Mid-torus superior	314.4776	85.0845	32.7574
R Fronto-malare orbitale	320.631	85.1309	28.4392
R Fronto-malare temporale	321.3016	84.1735	29.2542
R Porion	327.3703	61.6439	19.1564
R Zygo-temp superior	324.7638	80.7708	18.3623
R Zygo-temp inferior	326.1321	77.2237	17.718
L Prosthion-2	306.069	92.671	17.3365
L Premax-max superior	307.0683	91.1492	25.426
L Zygo-max inferior	299.9045	80.577	16.2045
L Zygo-max superior	299.6553	83.4289	22.4689
L Dacryon	307.0659	87.5589	26.7809
L Mid-torus inferior	304.9632	84.3121	31.6491
L Mid-torus superior	304.7639	83.7385	32.6398
L Fronto-malare orbitale	299.221	81.1278	28.1672
L Fronto-malare temporale	298.946	80.0827	28.861
L Porion	302.2782	56.2862	18.8504
L Zygo-temp superior	297.4925	75.4448	17.6373
L Zygo-temp inferior	297.8677	71.0602	16.4994

127-1791 Scan 1

Landmark	X	Y	Z
Inion	133.8828	-277.9958	24.6317
Bregma	151.2718	-272.598	50.6029
Glabella	196.5957	-246.3015	35.646
Nasion	197.1838	-245.425	33.8748
Rhinion	202.971	-243.2073	21.9119
Nasospinale	205.9374	-242.4674	8.7699
Prosthion			
R Prosthion-2			
R Premax-max superior	198.5866	-247.1613	29.4732
R Zygo-max inferior	201.1612	-266.5463	8.7266
R Zygo-max superior	203.0978	-259.7201	16.5782
R Dacryon	197.4938	-247.3089	27.3337
R Mid-torus inferior	197.778	-256.8986	37.0471
R Mid-torus superior	197.6995	-258.9055	38.3282
R Fronto-malare orbitale	200.6529	-267.1098	31.1871
R Fronto-malare temporale	200.0575	-269.6043	33.2547
R Porion	167.3847	-283.4077	11.1214
R Zygo-temp superior	196.4936	-275.7347	10.5117
R Zygo-temp inferior	191.3708	-280.0821	9.7631
L Prosthion-2			
L Premax-max superior	195.7143	-244.048	30.8446
L Zygo-max inferior	180.804	-231.1379	7.5412
L Zygo-max superior	190.2896	-233.0953	16.3554
L Dacryon	192.9485	-245.1552	30.2904
L Mid-torus inferior	189.5343	-239.2133	36.2879
L Mid-torus superior	186.2014	-235.2908	37.9146
L Fronto-malare orbitale	182.3089	-230.2067	30.4834
L Fronto-malare temporale	180.484	-229.2852	33.3701
L Porion	148.5015	-246.8041	9.9938
L Zygo-temp superior	175.9244	-229.0911	9.9555
L Zygo-temp inferior	166.7126	-230.5343	9.1289

127-1791 Scan 2

Landmark	X	Y	Z
Inion	419.8969	-99.9386	123.3886
Bregma	419.8723	-82.0902	150.3368
Glabella	413.3334	-29.7987	138.1506
Nasion	412.7357	-29.5502	136.9559
Rhinion	412.4974	-22.1722	124.5557
Nasospinale	412.4252	-18.2696	111.9648
Prosthion			
R Prosthion-2			
R Premax-max superior	414.5869	-23.9275	125.3836
R Zygo-max inferior	434.6068	-32.8736	111.3154
R Zygo-max superior	428.0789	-28.6388	119.2159
R Dacryon	414.8752	-29.3207	128.0952
R Mid-torus inferior	424.2976	-33.2396	139.2836
R Mid-torus superior	425.3348	-34.1365	140.7381
R Fronto-malare orbitale	433.4756	-34.1646	133.4866
R Fronto-malare temporale	436.2029	-36.1867	135.7776
R Porion	442.0275	-76.8114	114.9651
R Zygo-temp superior	440.6332	-39.4616	111.6329
R Zygo-temp inferior	443.0034	-46.304	109.9861
L Prosthion-2			
L Premax-max superior	410.2802	-23.4958	124.8629
L Zygo-max inferior	391.1447	-38.3896	109.6997
L Zygo-max superior	398.2019	-30.6339	118.8342
L Dacryon	410.604	-29.5897	127.6865
L Mid-torus inferior	402.4204	-35.0056	138.9454
L Mid-torus superior	400.1841	-35.7679	140.7833
L Fronto-malare orbitale	392.5088	-37.3755	132.6231
L Fronto-malare temporale	390.5776	-40.1568	135.6885
L Porion	391.804	-80.2933	114.168
L Zygo-temp superior	388.9988	-42.687	112.4662
L Zygo-temp inferior	386.3065	-50.7031	111.4105

127-1791 Scan 3

Landmark	X	Y	Z
Inion	125.5649	-279.0587	24.7596
Bregma	142.7688	-272.0775	50.0946
Glabella	189.263	-250.6913	37.1364
Nasion	190.2937	-250.3705	34.8554
Rhinion	196.631	-248.4626	22.7358
Nasospinale	199.2263	-248.4913	9.4188
Prosthion			
R Prosthion-2			
R Premax-max superior	192.0807	-251.3515	28.4346
R Zygo-max inferior	193.1973	-270.9721	9.7334
R Zygo-max superior	195.9252	-265.1061	17.7459
R Dacryon	190.4795	-252.1483	28.4756
R Mid-torus inferior	189.8382	-260.6203	37.7098
R Mid-torus superior	189.5684	-264.1165	39.3993
R Fronto-malare orbitale	192.5345	-271.6718	32.4467
R Fronto-malare temporale	192.0059	-273.9512	34.823
R Porion	159.4939	-287.2279	11.0717
R Zygo-temp superior	188.8452	-280.7114	11.823
R Zygo-temp inferior	183.4145	-285.0883	11.1486
L Prosthion-2			
L Premax-max superior	190.5169	-248.6405	28.9629
L Zygo-max inferior	177.8359	-238.15	7.4896
L Zygo-max superior	184.1271	-237.7591	16.6255
L Dacryon	188.6542	-249.4818	30.104
L Mid-torus inferior	182.885	-242.9849	36.7862
L Mid-torus superior	181.0188	-239.8903	38.3844
L Fronto-malare orbitale	176.6161	-233.5658	30.2075
L Fronto-malare temporale	175.1402	-232.7346	32.7973
L Porion	143.291	-250.2815	9.5099
L Zygo-temp superior	169.9715	-233.1093	10.4721
L Zygo-temp inferior	161.4229	-234.1971	9.1421

127-1791 Scan 4

Landmark	X	Y	Z
Inion	409.643	-92.6323	127.6378
Bregma	409.2031	-75.8279	148.2426
Glabella	401.4396	-23.5571	140.2678
Nasion	400.8039	-22.0427	137.6795
Rhinion	400.7143	-14.0501	125.8441
Nasospinale	400.5557	-10.4047	113.2591
Prosthion			
R Prosthion-2			
R Premax-max superior	402.9257	-15.7094	126.4829
R Zygo-max inferior	421.032	-23.3034	112.5681
R Zygo-max superior	416.0653	-19.4006	120.7348
R Dacryon	403.0367	-21.3628	128.2859
R Mid-torus inferior	412.0472	-25.1397	140.6533
R Mid-torus superior	412.6266	-26.4789	142.1053
R Fronto-malare orbitale	421.753	-25.7127	134.8647
R Fronto-malare temporale	424.1586	-27.9419	137.2143
R Porion	433.0827	-67.3519	114.5774
R Zygo-temp superior	430.2036	-29.5892	113.5403
R Zygo-temp inferior	432.9817	-36.328	112.4091
L Prosthion-2			
L Premax-max superior	397.8879	-16.1786	125.4278
L Zygo-max inferior	381.2305	-30.5377	109.473
L Zygo-max superior	386.5331	-23.1837	119.3658
L Dacryon	398.8661	-21.9705	127.5992
L Mid-torus inferior	390.9496	-27.9383	138.9659
L Mid-torus superior	389.9361	-29.1686	140.4657
L Fronto-malare orbitale	381.6386	-31.0902	132.8856
L Fronto-malare temporale	380.0213	-33.352	135.0977
L Porion	382.7737	-72.9942	112.7015
L Zygo-temp superior	378.1132	-35.7759	111.3507
L Zygo-temp inferior	376.8052	-44.1197	110.27

127-1791 Scan 5

Landmark	X	Y	Z
Inion	335.0612	6.8778	25.6114
Bregma	332.9343	24.4462	45.6204
Glabella	325.52	78.4415	34.4368
Nasion	325.4422	79.0824	33.0236
Rhinion	325.9616	86.6851	21.3961
Nasospinale	326.702	89.273	8.9723
Prosthion			
R Prosthion-2			
R Premax-max superior	328.3376	84.3948	21.8919
R Zygo-max inferior	349.722	75.8322	8.7491
R Zygo-max superior	341.8246	80.7019	16.7592
R Dacryon	328.2964	79.122	23.6583
R Mid-torus inferior	336.9861	75.2442	36.357
R Mid-torus superior	337.3025	74.2408	38.0782
R Fronto-malare orbitale	347.3434	74.7135	31.0958
R Fronto-malare temporale	348.6026	72.3325	34.1228
R Porion	357.5262	31.8991	12.7923
R Zygo-temp superior	355.4011	69.0267	10.5527
R Zygo-temp inferior	357.9762	62.2989	9.0756
L Prosthion-2			
L Premax-max superior	323.0909	84.4232	21.7506
L Zygo-max inferior	306.7762	70.0492	5.3036
L Zygo-max superior	311.4213	77.5096	14.9186
L Dacryon	323.9538	78.49	23.951
L Mid-torus inferior	314.997	73.0482	34.9993
L Mid-torus superior	313.5122	71.8148	36.9813
L Fronto-malare orbitale	306.3036	70.3994	28.3884
L Fronto-malare temporale	304.601	67.507	31.077
L Porion	307.2933	26.8869	10.18
L Zygo-temp superior	303.682	63.9749	7.6872
L Zygo-temp inferior	301.7345	55.86	6.4077

127-23107 Scan 1

Landmark	X	Y	Z
Inion	406.4753	-93.8675	124.39
Bregma	405.2331	-70.4582	150.7738
Glabella	404.345	-25.2235	137.1316
Nasion	404.3967	-24.7118	133.8721
Rhinion	403.9841	-16.5416	122.4124
Nasospinale	403.982	-15.9812	111.0938
Prosthion	403.9601	-13.7311	108.3748
R Prosthion-2	407.9713	-14.0637	108.6259
R Premax-max superior	406.6081	-21.6317	123.9915
R Zygo-max inferior			
R Zygo-max superior			
R Dacryon	406.2734	-24.1659	124.8087
R Mid-torus inferior	412.4285	-29.7034	137.2144
R Mid-torus superior	412.3955	-30.5274	139.1912
R Fronto-malare orbitale	422.592	-30.6782	132.2611
R Fronto-malare temporale	423.514	-33.7741	134.3129
R Porion	429.4493	-67.6243	114.745
R Zygo-temp superior			
R Zygo-temp inferior			
L Prosthion-2	399.8294	-14.8848	107.3164
L Premax-max superior	400.1894	-20.4263	122.9657
L Zygo-max inferior			
L Zygo-max superior			
L Dacryon	401.4678	-25.1937	126.5161
L Mid-torus inferior	396.1289	-29.9174	137.1113
L Mid-torus superior	396.0167	-31.2347	138.8406
L Fronto-malare orbitale	386.004	-32.3537	130.196
L Fronto-malare temporale	385.0469	-34.2962	133.1506
L Porion	383.0457	-70.1106	112.8254
L Zygo-temp superior			
L Zygo-temp inferior			

127-23107 Scan 2

Landmark	X	Y	Z
Inion	311.8914	32.0316	27.5519
Bregma	310.5648	50.9858	56.4341
Glabella	308.4461	99.5341	46.5108
Nasion	307.753	99.7	45.4029
Rhinion	307.5415	108.9487	31.5844
Nasospinale	307.6219	109.6529	21.417
Prosthion	306.6088	112.6068	17.8941
R Prosthion-2	310.837	111.9183	17.2131
R Premax-max superior	310.8853	104.9503	32.4547
R Zygo-max inferior			
R Zygo-max superior			
R Dacryon	310.0533	100.8068	34.9638
R Mid-torus inferior	316.2043	96.1419	46.5901
R Mid-torus superior	316.1284	94.5126	48.329
R Fronto-malare orbitale	326.5714	95.4583	40.5762
R Fronto-malare temporale	327.9429	92.4645	42.3853
R Porion	333.5209	58.8486	20.4131
R Zygo-temp superior			
R Zygo-temp inferior			
L Prosthion-2	302.7026	111.4181	17.6405
L Premax-max superior	302.8267	105.2113	32.022
L Zygo-max inferior			
L Zygo-max superior			
L Dacryon	305.7159	100.3753	35.69
L Mid-torus inferior	300.2705	95.1392	46.3733
L Mid-torus superior	299.8651	93.8347	48.6305
L Fronto-malare orbitale	289.8806	93.3624	39.8774
L Fronto-malare temporale	288.8639	90.2818	41.6324
L Porion	287.3794	56.08	21.2435
L Zygo-temp superior			
L Zygo-temp inferior			

127-23107 Scan 3

Landmark	X	Y	Z
Inion	311.3132	32.7733	34.7866
Bregma	311.4795	54.924	56.7379
Glabella	307.172	101.2632	42.5459
Nasion	307.3453	102.2851	40.5192
Rhinion	306.3664	110.0362	26.2455
Nasospinale	305.5101	109.2581	15.3464
Prosthion	305.8103	112.3489	12.1584
R Prosthion-2	309.8222	111.943	12.1372
R Premax-max superior	310.1888	106.1317	27.8253
R Zygo-max inferior			
R Zygo-max superior			
R Dacryon	309.3445	102.6927	29.6901
R Mid-torus inferior	315.2708	97.9506	42.1531
R Mid-torus superior	316.3104	97.1839	44.1199
R Fronto-malare orbitale	325.8038	97.8431	35.7359
R Fronto-malare temporale	327.6554	95.4078	37.9468
R Porion	334.4691	60.3297	20.8078
R Zygo-temp superior			
R Zygo-temp inferior			
L Prosthion-2	301.2936	110.9037	11.4932
L Premax-max superior	302.1752	106.5594	27.046
L Zygo-max inferior			
L Zygo-max superior			
L Dacryon	304.8328	101.0452	31.3999
L Mid-torus inferior	299.2062	96.9011	41.4899
L Mid-torus superior	299.0061	96.1926	44.1415
L Fronto-malare orbitale	288.9895	94.9739	35.3764
L Fronto-malare temporale	288.3333	91.1113	37.5739
L Porion	287.6652	56.0022	20.3861
L Zygo-temp superior			
L Zygo-temp inferior			

127-23107 Scan 4

Landmark	X	Y	Z
Inion	78.9557	-263.0467	31.5724
Bregma	100.8824	-259.4652	54.6266
Glabella	147.0196	-251.6352	38.6775
Nasion	147.5273	-251.9947	35.7353
Rhinion	154.6632	-250.6947	24.0863
Nasospinale	154.6005	-250.9389	13.0308
Prosthion	156.6576	-250.5609	9.6651
R Prosthion-2	157.1729	-255.003	9.6335
R Premax-max superior	151.6625	-254.7618	24.9883
R Zygo-max inferior			
R Zygo-max superior			
R Dacryon	147.2943	-254.1765	31.7484
R Mid-torus inferior	143.4664	-261.9451	39.2763
R Mid-torus superior	143.2367	-262.6629	41.4333
R Fronto-malare orbitale	144.4047	-272.1951	33.2573
R Fronto-malare temporale	141.836	-271.9836	36.7138
R Porion	111.7906	-274.807	14.2567
R Zygo-temp superior			
R Zygo-temp inferior			
L Prosthion-2	155.6986	-246.9195	9.6847
L Premax-max superior	150.2318	-247.789	25.1407
L Zygo-max inferior			
L Zygo-max superior			
L Dacryon	146.9155	-250.1444	33.0354
L Mid-torus inferior	141.3625	-244.2498	39.3549
L Mid-torus superior	139.6194	-242.4762	41.3741
L Fronto-malare orbitale	138.4707	-234.9854	34.1855
L Fronto-malare temporale	135.0392	-233.8858	34.6703
L Porion	104.646	-239.0483	13.502
L Zygo-temp superior			
L Zygo-temp inferior			

127-23107 Scan 5

Landmark	X	Y	Z
Inion	285.4482	56.0328	26.1887
Bregma	281.7827	77.5901	53.723
Glabella	278.3957	124.6441	38.7056
Nasion	277.9931	124.9562	37.2326
Rhinion	278.4489	132.9447	22.7085
Nasospinale	279.054	132.3731	12.3246
Prosthion	278.268	134.8655	8.4278
R Prosthion-2	282.7116	134.6021	8.444
R Premax-max superior	281.6777	128.8918	24.2217
R Zygo-max inferior			
R Zygo-max superior			
R Dacryon	281.078	125.69	26.4094
R Mid-torus inferior	286.8089	122.0062	39.0921
R Mid-torus superior	286.6718	120.6964	41.1947
R Fronto-malare orbitale	297.174	121.1374	33.6881
R Fronto-malare temporale	298.8125	118.6503	35.985
R Porion	306.4102	82.8701	19.207
R Zygo-temp superior			
R Zygo-temp inferior			
L Prosthion-2	274.2799	134.0089	8.7338
L Premax-max superior	274.1622	128.322	23.8119
L Zygo-max inferior			
L Zygo-max superior			
L Dacryon	276.2845	124.747	27.1937
L Mid-torus inferior	269.9117	120.3838	39.3468
L Mid-torus superior	269.9164	119.6152	40.755
L Fronto-malare orbitale	260.911	117.8366	31.852
L Fronto-malare temporale	259.4203	114.7412	33.6443
L Porion	259.5806	78.5989	17.1104
L Zygo-temp superior			
L Zygo-temp inferior			